GENE EXPRESSION PROFILING OF SCRAPIE INFECTED MOUSE SPLEEN

BY

EWAN A. GIBB

A Thesis
Submitted to the Faculty of Graduate Studies
In Partial Fulfillment of the Requirements for the Degree of

MASTER OF SCIENCE

Department of Medical Microbiology
University of Manitoba
Winnipeg, Manitoba

THE UNIVERSITY OF MANITOBA

FACULTY OF GRADUATE STUDIES

*****

COPYRIGHT PERMISSION

GENE EXPRESSION PROFILING OF SCRAPIE INFECTED MOUSE SPLEEN

BY

EWAN A. GIBB

A Thesis/Practicum submitted to the Faculty of Graduate Studies of The University of Manitoba in partial fulfillment of the requirement of the degree

Of

MASTER OF SCIENCE

Table of Contents

Abstract

Prion (PrP^{Sc}) accumulation occurs in spleen and other secondary lymphoid tissues, despite the fact that no antibodies to infective prion are produced, nor is a conspicuous inflammatory response elicited. Splenectomy does, however, severely delay the onset of prion disease in the CNS after intraperitoneal and oral infection. Additionally, PrP^{Sc} builds up in secondary lymphoid tissue even after intracerebral inoculation. The spleen is both a reservoir for infectivity and a site of prion replication and is therefore a candidate tissue for investigating the molecular mechanisms of prion replication. In addition the lack of an antemortem test for prions in accessible tissues or body fluids makes the spleen a target tissue for the identification of surrogate markers to identify prion infection. In this study we used microarray analysis to identify differentially expressed genes in scrapie-infected mouse spleens at early (21dpi), preclinical (100dpi) and clinical (148dpi) stages of the prion disease for two different strains of mouse-adapted scrapie. These genes may have a role directly in the replication of the prion agent or may have potential as surrogate markers of infection. In a scrapie mouse model, we hypothesized that there will be fewer differentially expressed genes found by microarray analysis in the spleen during scrapie infection when compared to the brain due to the neurological nature of the prion disease. We expected differential gene expression profiles to parallel the accumulation of PrP^{Sc} deposits at the pre-clinical (100dpi) and clinical (148dpi) time points. These differentially expressed genes were more likely to reflect a direct response to the prion agent due to the lack of extensive tissue damage within the tissues.

Acknowledgements

I would like to extend my sincere graditude to my supervisor, Dr. Stephanie Booth, for her support and guidance throughout this graduate experience. Without her expertise on prion diseases and microarrays the work presented in this thesis would not have been possible.

I would also like to thank my committee; Dr. Heinz Feldmann, Dr. Aaron Marshall, Dr. Christopher Bowman, and Richard Baumgartner for their comments and expertise.

Many thanks to my fellow graduate student and good friend Reuben Saba for comments on the thesis and his friendship throughout this experience. Thanks also to graduate student Mike Stobart for being himself and for coming for beers on Fridays.

Thank you to Cathy Robertson for her technical advice on histology and immunohistochemistry matters, and helping me get the mouse spleens to 'stick'.

I must also express my appreciation for the love and support of my fiancée, Christina, who endured my absentmindedness through this degree.

I would also like to thank all the members of HGPD for making my graduate experience at the NML a good one.

List of Tables

List of Figures

List of Abbreviations

aRNA	amplified RNA
BMAP	Brain Molecular Anatomy Project
BSE	bovine spongiform encephalopathy
CJD	Creutzfeldt-Jakob disease
dpi	days post infection
ESTs	expressed sequence tags
FDCs	follicular dendritic cells
FDR	false discovery rate
FFI	fatal familial insomnia
gDNA	genomic DNA
GPI	glycosyl-phosphatidylinositol-anchor
GSS	Gerstmann-Sträussler-Scheinker syndrome
i.c.	intracerebral
I.D.	infectious dose
i.p.	intraperitoneal
kDa	kilodalton
LT	lymphotoxins
mRNA	messenger RNA
MSV	Mouse Sequence Verified
NMR	nuclear magnetic resonance
nt	nucleotide
PBS	phosphate buffered saline
PCR	polymerase chain reaction
PK	Proteinase-K
qRT-PCR	quantitative real-time PCR
RER	rough endoplasmic reticulum
SAM	Significance Analysis for Microarrays
S.D.	Standard deviation
sCJD	sporadic Creutzfeldt-Jakob disease
Tg	transgenic
TNF	tumour necrosis factor
TSEs	transmissible spongiform encephalopathies
vCJD	variant Creutzfeldt-Jakob disease

Introduction

1.1 Transmissible spongiform encephalopathies

Transmissible spongiform encephalopathies (TSEs) or prion diseases are rare invariably fatal neurodegenerative disorders that affect numerous mammalian species, including humans (Wickner et al., 2004). Examples of animal prion diseases include scrapie of sheep and goats, bovine spongiform encephalopathy (BSE) of cattle, and chronic wasting disease (CWD) of elk and deer (Aguzzi and Sigurdson, 2004). In humans, the prion diseases are Creutzfeldt-Jacob disease (CJD), Gerstmann-Sträussler-Sheinker (GSS) disease, and Kuru. A summary of some of the TSEs and their respective host animals can be found in **Table 1**.

All TSEs are characterized by the accumulation of a protease-resistant isomer (PrP^{Sc}) of the normal host prion protein (PrP^{C}) in the brain of infected individuals. The accumulation of the PrP^{Sc} isomer in the brain is associated with vacuolation, gliosis and neuronal cell death; which gives the tissue a characteristic spongiform appearance (DeArmond et al., 1985). PrP^{C} is almost ubiquitously expressed in all tissues and cell types, but is highly expressed in the central nervous system and lymphoid tissues (Ford et al., 2002) where prion infectivity is strongly localized. Consequently, prion infectivity appears to be strongly localized to these tissues (Bendheim et al., 1992; Ford et al., 2002; Fournier, 2001; Horiuchi et al., 1995; Moudjou et al., 2001).

Human TSEs can be divided into three groups based on detailed clinical, pathological and molecular data. The three forms include infectious, sporadic and familial forms (Collinge, 2001).

Table 1: Transmissible spongiform encephalopathies in animals and humans

Disease	**Host**
Scrapie	Sheep
Bovine Spongiform Encephalopathy (BSE)	Cattle
Transmissible Mink Encephalopathy (TME)	Mink
Chronic Wasting Disease (CWD)	Deer, Elk
Feline Spongiform Encephalopathy	Cats
Kuru	Humans
Variant Creutzfeldt-Jakob Disease (vCJD)	Humans
Sporadic Creutzfeldt-Jakob Disease (sCJD)	Humans
Familial Creutzfeldt-Jakob Disease (fCJD)	Humans
Gerstmann-Sträussler-Scheinker disease (GSS)	Humans
Fatal Familial Insomnia (FFI)	Humans

The infectious forms of human TSEs include kuru, Creutzfeldt-Jakob disease (CJD) and variant CJD (vCJD) (Chesebro, 2003). Human prion diseases are transmissible through CNS contact with prion contaminated surgical instruments, prion contaminated dural matter or by ingestion of prion infected brain material (Brown, 1998; Guiroy et al., 1991). Bovine tissues designated as high risk for BSE transmission to humans include the brain, spinal cord, tonsil, thymus, spleen, and intestine. Contact of meat destined for consumption with these materials could lead to contaminated foodstuffs entering the human food chain, creating a risk of transmission of BSE to humans resulting in vCJD. Humans contracting vCJD after consuming BSE contaminated meat is an example of cross-species prion transmission and is the most compelling evidence that vCJD is the human derived form of BSE (Will et al., 1996).

Most cases of human TSEs are caused by spontaneous mutational event that leads to sporadic CJD (sCJD) (Chesebro, 2003). For sCJD, the origin of the prion disease has yet been determined and there is no association with a mutant prion gene allele. The world-wide incidence of people affected by sCJD is 1 in $2x10^6$ (Harries-Jones et al., 1988; Will, 1993).

The third types of human TSEs are termed familial; these include familial CJD, Gerstmann-Sträussler-Scheinker syndrome (GSS) and fatal familial insomnia (FFI). Unlike sCJD, the familial TSEs are associated with an autosomal dominant genetic mutation of the PrP gene that causes the prion protein to fold abnormally, leading to the prion disease state (Doh-ura et al., 1989; Hsiao et al., 1989).

1.2 Causative agent of prion diseases: the protein-only hypothesis

The term prion (**pro**teinaceous and **in**fectious) was coined by Stanely Prusiner (1982) to describe unusual data that implied that scrapie in sheep was associated with a protein macromolecule. He showed that reagents that denatured proteins removed the infectivity from scrapie infected brain samples, while reagents that denatured nucleic acids did not affect the infectivity (Prusiner, 1982). The data obtained from these experiments gave rise to the protein-only hypothesis, which suggested that prion diseases were not of viral or bacterial origin, but were caused by an infectious protein (Prusiner, 1982). Further studies showed that prion disease progression involves the conversion of a protease sensitive PrP^{C} host-derived isomer to a protease resistant PrP^{Sc} isomer associated with infectivity (Pan et al., 1993; reviewed in Prusiner, 1998). Studies using PrP^{C} null mice ($PRNP^{0/0}$) showed that expression of the PrP^{C} host protein was absolutely required for disease progression, as these mice were completely resistant to prion infection (Büeler et al., 1993; Malluci et al., 2003; Prusiner et al., 1993).

The exact identity of the infectious agent is unknown, but the PrP^{Sc} isomer is a strong candidate (reviewed in Prusiner, 1998). Scrapie infectivity and PrP^{Sc} co-purify and the levels of expressed PrP^{Sc} are directly proportional to prion titres (Prusiner, 1998). The accumulation of PrP^{Sc} is associated with the pathology of the diseases and mutations in the PRNP gene are linked to inherited prion diseases in humans (Pruisiner, 1998). However, PrP^{Sc} may not be the sole component of the prion agent and other factors may still be involved in the disease (Prusiner, 1998).

1.3 Prion biochemistry and structure

The prion gene has been identified in numerous mammalian species including mice, humans, rats, cattle, sheep and goats (reviewed in Prusiner, 1998). It is also found in non-mammalian species including fish (Rivera-Milla et al., 2003) and fungi (Coustou et al., 1997; Derkatch et al., 2001). Although prion-like characteristics have only been noted in the latter.

The prion protein in mice is encoded on chromosome 2 within a single open reading frame (ORF) (Chesebro et al., 1985; Oesch et al., 1985). The mouse prion is transcribed as a 933 nucleotide (nt) long polyadenylated messenger RNA (mRNA), which is translated and subsequently modified into a 30-35 kilodalton (kDa) glycoprotein on route to the plasma membrane (Bendheim et al., 1992; Stahl et al., 1987). The prion mRNA is expressed in equal levels in infected and uninfected mouse brains (Chesebro et al., 1985). The structure of mouse PrP^C, as determined by nuclear magnetic resonance (NMR), contains three a-helices and a two-stranded antiparallel beta-sheet stabilized by a disulphide bond between residues 179 and 214 (Riek et al., 1996).

Mouse PrP^C has a glycosyl-phosphatidylinositol-anchor (GPI) at the carboxy-terminal Ser 231 (Stahl and Prusiner, 1991). Additionally there are two Asn-glycosylation sites at Asn 181 and Asn 197 (Riek et al., 1996). The PrP^C protein is always isolated as a mixture of three forms; unglycosylated, monoglycosylated, and di-glycosylated (Riesner, 2003). PrP^{Sc} is often less glycosylated at the two Asn-glycosylation sites than the host PrP^C (Hill et al., 1997; Kascsak et al., 1985; Somerville et al., 1997a).

Infectivity in prion diseases is associated with PrP^{Sc}, a β-sheet-rich conformational isomer of the normal cellular form (Bolton et al., 1982; Prusiner et al., 1982). PrP^{C} is composed of 42% α-helix and 3% β-sheet, while PrP^{Sc} is composed of 30% α-helix and 43% β-sheet (Daude, 2004; Pan et al., 1993; Prusiner, 1998) (**Figure 1**). The amino acid sequence of the PrP^{C} and PrP^{Sc} are the same whether derived from the genomic DNA sequence or directly by peptide sequencing (Riesner, 2003). As well as being resistant to Proteinase K (Oesch et al., 1985), the PrP^{Sc} isomer is detergent insoluble (Naslavsky et al., 1997), resistant to heat, formaldehyde (Gordon, 1946), ionizing radiation and ultraviolet light (Alper et al., 1966). These properties of the PrP^{Sc} are used for prion detection; but also make prion decontamination a very difficult procedure. Effective decontaminants are 10% bleach, 2N NaOH and autoclaving at 132°C.

The protein-only hypothesis states that normal host PrP^{C} glycoprotein provides the template for the structural change to the infectious PrP^{Sc} isomer, presumably in all prion diseases (Pan et al., 1993), which is essential in the progression of the prion disease (Prusiner, 1998). The conversion is thought to occur purely through protein-protein interactions. However, it has been suggested that there may be other factors, possibly proteins or short RNA molecules, which may participate in this conversion reaction; although none have been identified to date (Daude, 2004).

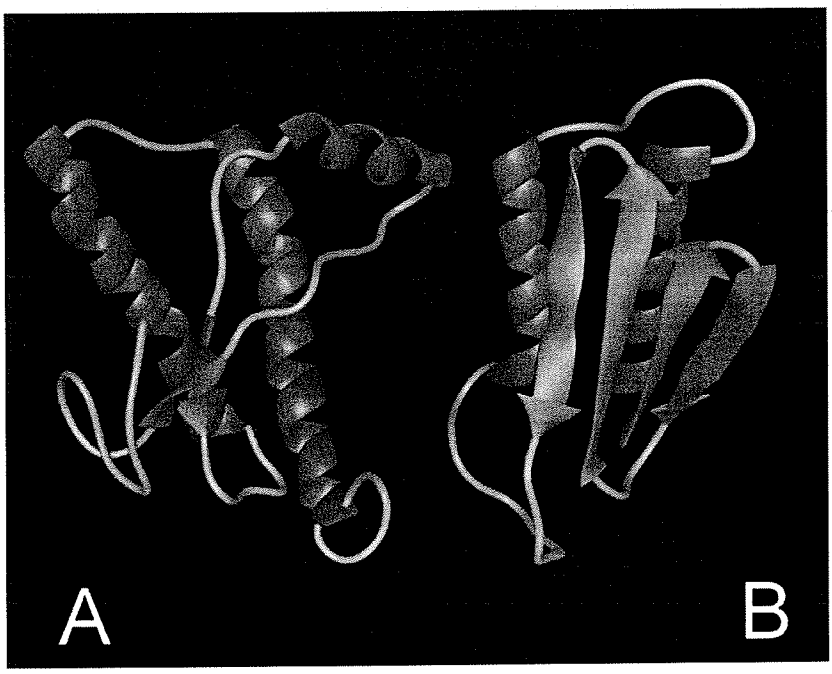

Figure 1: Ribbon diagrams showing the α-helix conformation of PrP^{C} isomer of the prion protein (A) and the β-sheet conformation of PrP^{Sc} isomer (B).
http://cloud.prohosting.com/lzambeni/prions/prpc-prpsc.jpg

1.4 Cellular trafficking of PrP^C

The biosynthetic pathway of PrP^C was elucidated using neuronal cell lines and was found to be similar to other secreted and membrane-bound proteins (**Figure 2**). Translation and post-translational modifications occur in the rough endoplasmic reticulum (RER). The modifications to the prion protein include cleavage of the N-terminal signal peptide, the formation of a disulphide bond, addition of two N-linked oligosaccharides and the attachment of the GPI anchor (Stahl et al., 1987; Haraguchi et al., 1989). After final modifications in the Golgi, the PrP^C is transported and anchored in the plasma membrane on the external cell surface.

PrP^C cycles between the cell surface and an endocytic compartment as demonstrated in neuronal cell culture by labelling PrP^C molecules on the cell surface with membrane-impermeant iodination or biotinylation reagents (Harris, 2003; Shyng et al., 1993). It seems likely that PrP^C to PrP^{Sc} conversion occurs either on the plasma membrane or following internalisation of PrP^C and PrP^{Sc} by endocytosis (Borchelt et al., 1992; Caughey and Raymond, 1991).

1.5 Strain characteristics of prions

A strain is a group of organisms of the same species, having distinctive characteristics but not usually considered a separate breed or variety. The characteristics of a strain are encoded by differences in the nucleic acid genome of the organism. Similarily, isolates of prion diseases have characteristics or variations that appear different enough to be considered strains. Although the term 'strain' is something of a misnomer when applied to TSEs since isolates of the infectious agent lack an apparent nucleic acid component.

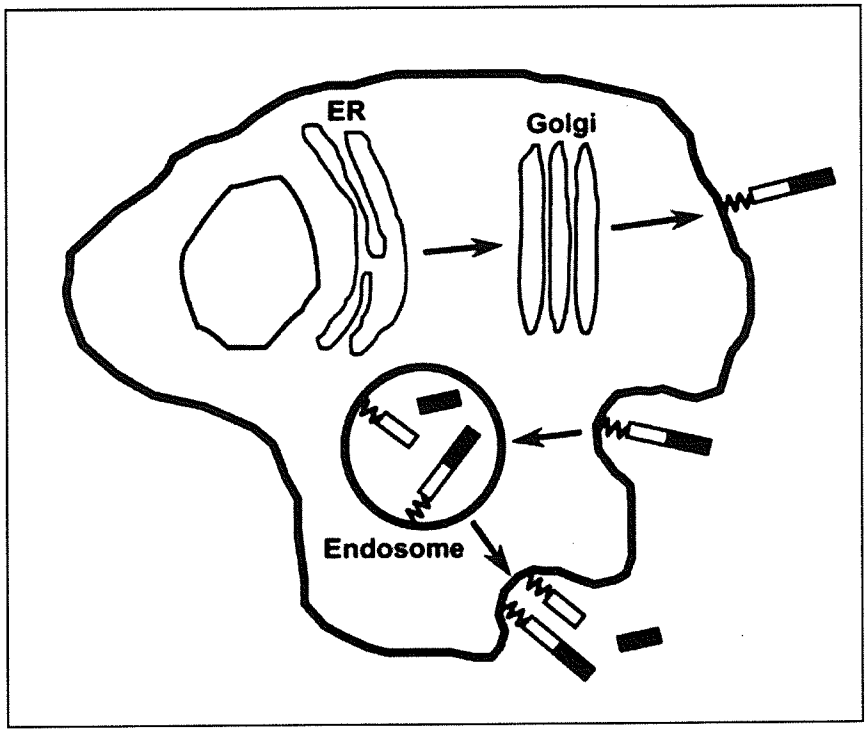

Figure 2: Cellular trafficking and cleavage of PrP. After reaching the cell surface, PrP^C is internalized into an endocytic compartment from which most of the molecules are recycled intact to the cell surface (Harris, 2003).

TSE strains are distinguished by the length of the incubation period from the initial infection to the onset of clinical disease, coupled with the pathological changes in the brain in a given host (Bruce et al., 1991; Bruce et al., 1994; Dickinson and Miekle, 1971; Fraser and Dickinson, 1968). Strain variations among prions are consistent and can be maintained through multiple serial passages in experimental animals (Dickinson and Meikle, 1971; Bruce et al., 1991), and often even after passage in alternate host species (Bruce, 2003). Strain characteristics appear to be caused by differences in PrP^{Sc} conformation (Bessen and Marsh, 1994; Bessen et al., 1995; Telling et al., 1996) and glycosylation state (Lawson et al., 2005).

The incubation period in mouse-adapted scrapie is affected not only by the prion agent strain but also by the genotype of the mouse (Bruce et al., 1991; Bruce, 2003; Dickinson and Miekle, 1971; Dickinson et al., 1975). The codons 108 (leucine or phenylalanine) and 189 (threonine or valine) of the prion protein appear to have a role in determining the length of the incubation period (Barron et al., 2005). The effects of the mouse genotype and scrapie strain agent on the mouse-adapted scrapie incubation period are summarized in Figure 3.

Characterization of TSE strains is extremely important for the epidemiology, diagnosis and surveillance of prion disease. Characterizing prion strains would allow the identification of the source of a TSE outbreak, as well as monitoring the incidence of cross-species transmissions (Booth et al., 2004b). The risk cross-species transmission has become more apparent, making research in TSE strain diagnostics an especially important, but difficult endeavor. For example, the use of strain diagnostics has shown

that BSE prions have characteristics identical to those of vCJD prions, concluding that vCJD has been directly derived from BSE (Collinge et al., 1996; Hill et al., 1997).

1.6 Mouse models and their applications in TSE research

The experimental transmission of sheep scrapie to mice occurred over forty years ago when it was found that the infectious scrapie agent in sheep could be adapted to mice through serial passaging (Zlotnik and Rennie, 1962; Zlotnik and Rennie, 1963). The successful adaptation of sheep scrapie to mice was an important development in prion research because it created a manageable working model system. Mouse-adapted scrapie is now one of the most widely studied TSE model systems.

Some TSEs could not be directly transmitted to mice, possibly due to differences in the prion protein structure between certain species, creating a species barrier. A species barrier in prion research describes the decrease in efficiency when attempting to passage a prion disease from one species to another (Pattinson, 1965). To overcome this barrier, transgenic mice were generated, where by researchers cloned the prion gene of the desired host animal into the mice thus creating mice susceptible to that TSE. For example, researchers replaced the mouse PrP gene with the bovine PrP gene thus creating transgenic or Tg(BoPrP) mice which are susceptible to BSE prions, as they express the bovine PrP protein (Scott et al., 1997).

The incubation periods of mouse-adapted scrapie can be influenced by the PRNP alleles (Bruce, 2003). There are two homozygous and one heterozygous allele combinations for the PRNP gene in mice (**Table 2**). The homozygous combinations include $PRNP^{a/a}$ (C57Blk mice; Genbank MI8070) and $PRNP^{b/b}$ (VM mice; Genbank

Table 2: Polymorphisms in the mouse PRNP alleles (based on Westaway et al, 1987)

Mouse Type	PRNP Allele	Incubation Period	Codon 108	Codon 189
C57Blk	$PRNP^{a/a}$	Short	Leu	Thr
VM	$PRNP^{b/b}$	Long	Phe	Val
F1 Cross (C57Blk x VM)	$PRNP^{a/b}$	Intermediate or extended	Leu	Val
PrP Null	$PRNP^{0/0}$	Resistant	N/A	N/A

MI8071). In both combinations the mRNA transcripts are 933nt and encode the PrP gene, although the former generally shortens the scrapie incubation period and is termed "short", while the latter lengthens the incubation periods and is termed "long" (Westaway et al., 1987). The heterozygous allele combination is an F1 cross of the $PRNP^{a/a}$ and $PRNP^{b/b}$, creating $PRNP^{a/b}$ mice. These $PRNP^{a/b}$ mice have incubation periods that are somewhere in between the short and long incubation periods (**Figure 3**), but can exhibit "overdominance", where the incubation period is longer than either of the parental strains (Somerville, 2002). It is also possible to create PrP knock out mice ($PRNP^{0/0}$), which appear to have a normal phenotype (Büeler et al, 1992; Manson et al., 1994), and these mice are completely resistant to prions (Büeler et al, 1993; Prusiner et al., 1993). These mice were useful model systems to explore the importance of PrP^{C} expression in the development of prion diseases.

Experimentally, prions can be delivered to model animals via oral, occular, intraperitoneal and most effectively, intracerebral inoculations (Aguzzi, 2003). The source of the inoculum in mouse model experiments is normally a 1% brain homogenate of a clinical mouse infected with a mouse-adapted prion strain (Zlotnik and Rennie, 1963).

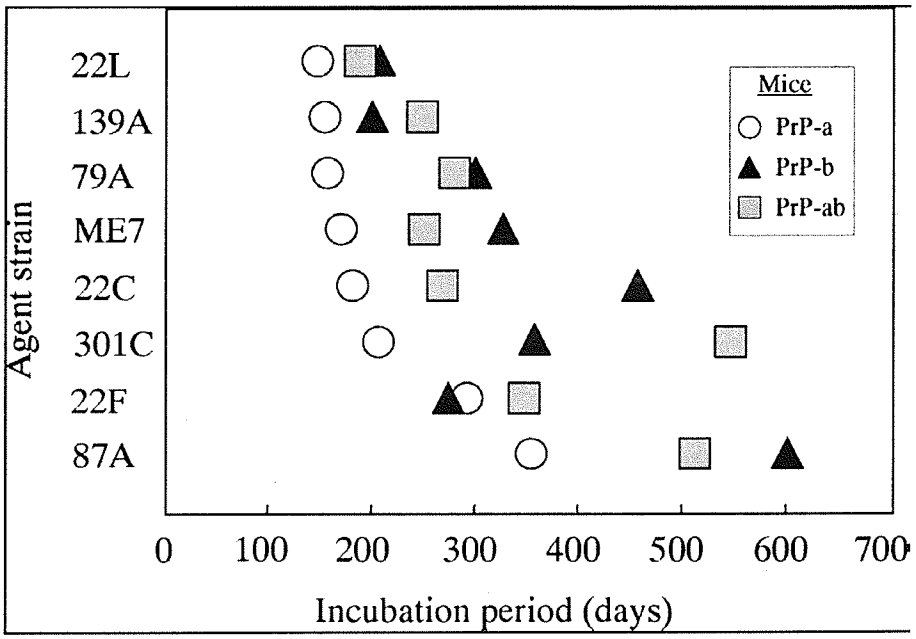

Figure 3: Effect of the mouse genome and prion strain on incubation periods from initial intracerebral injection to the development of clinical disease for eight TSE strains in the mice with three different PrP genotypes (Bruce, 2003).

1.7 Prion pathogenesis

The natural route of peripheral prion acquisition in sheep, goats, cattle and humans is considered to be oral (Anderson et al., 1996; Wilesmith et al., 1992). Other portals of entry include cutaneous transmission through accidental skin scarification (Taylor et al., 1996), surgical transmission of CJD via contaminated medical instruments (Flechsig et al., 2001) and blood transfusions (Hunter et al., 2002; Llewelyn et al., 2004; Peden et al., 2004). In mouse models orally innoculated with scrapie, prions cross the intestinal epithelium at the Peyer's patches before gaining access to the lymphoreticular system (Maignien et al., 1999). After the intestinal epithelium has been crossed, the infectivity is transported from the Peyer's patches to the distal components of the lymphoreticular system, including the spleen (Mabbot and Turner, 2005).

1.8 The lymphoreticular system and prions

Prion (PrP^{Sc}) accumulation has been shown to occur within spleen and other lymphoid tissues, with an absence of pathological effects (Aucouturier and Carnaud, 2002) and without a classical immune response (Kasper et al., 1982). The spleen and lymphoreticular system are a reservoir of infectivity (Clarke and Haig, 1971; Dickinson and Fraser, 1969; Dickinson and Miekle, 1969; Eklund et al., 1967; Kimberlin and Walker, 1979) and a site of prion replication (Eklund et al., 1967; Fraser and Dickinson, 1970; Kimberlin and Walker, 1989a) in mouse-adapted scrapie. The major exception to this rule is BSE, where the spleen was not found to contain prion infectivity (Mohri et al., 1992; Somerville et al., 1997b).

In mouse-adapted scrapie, the spleen is the first site where PrP^{Sc} infectivity can be detected, usually within two weeks (Race and Ernst, 1992; Farquhar et al., 1994; Blätter et al., 1997; Inoue et al., 2005). Early detection of infectivity in mice is independent of the route of inoculation, whether by intracerebral (i.c.), intraperitoneal (i.p.), or oral inoculation. Each route of inoculation showed accumulation of prion in the spleen long before infectivity could be detected in the brain (Büeler et al., 1993; Inoue et al. 2005). The i.p. and oral routes present obvious pathways to the accumulation of infectivity in the spleen, while accumulation of infectivity in the spleen after an i.c. inoculation is most likely due to an early uptake of the initial inoculums (Millson et al., 1979).

Accumulation of PrP^{Sc} occurs around the germinal centres and white pulp of the spleen, where follicular dendritic cells (FDCs) are localized (Cunnigham et al., 2005). In mouse-adapted scrapie the FDCs have a critical role in creating a reservoir of PrP^{Sc} infection (Kitamoto et al., 1991) and increasing their effectiveness in neuroinvasion (Brown et al., 1999; 2000; Jeffrey et al., 2000; Mabbott et al., 2000a; 2000b; Montrasio et al, 2000; Glatzel et al, 2001; Mohan et al, 2004). Despite the dogma that there is no pathological response during prion infection, recent evidence shows that during a murine scrapie infection an abnormal germinal centre reaction is observed in the spleen (McGovern et al., 2004). The FDCs in these regions showed functional abnormality, including hypertrophy of dendrites and increased PrP^{Sc} retention. These observations suggest there may be less obvious pathological changes in the spleen during the initial peripheral replication step that warrants further investigation.

In general it is thought that the accumulation of infectivity in mouse spleen reaches a steady state (plateau) and no further replication is observed (Kimberlin and

Walker, 1979), probably because the infectious PrP^{Sc} has exhausted the supply of PrP^{C} available for conversion (Yokoyama et al., 2001). The alternative model suggests a more dynamic state within the spleen tissues, where clearance of PrP^{Sc} is balanced by conversion of newly synthesized PrP^{C} into the PrP^{Sc} isomer (Kaeser et al., 2001). However, PrP^{Sc} deposits do not activate splenic macrophages (Cunningham et al., 2005), so removal of PrP^{Sc} by macrophages would not be efficient. The plateau of infectivity could also be the result of the host system being unable to clear the PrP^{Sc} deposits as quickly as they form (Cunningham et al., 2005). Recent evidence suggests that the PrP^{Sc} levels actually *decrease* after the plateau is reached (Inoue et al. 2005), but this has only been shown once.

Removal of the spleen (splenectomy) drastically increases the incubation period of mouse-adapted scrapie inoculated interperitoneally (Fraser and Dickinson, 1978; Kimberlin and Walker 1989b), highlighting its importance as a reservoir of infectivity. In this instance, it is likely that other components of the lymphoreticular system or a direct route to the nervous system exists and is being used for initial prion replication and the promotion of neuroinvasion (Beekes et al., 1996; Beekes et al., 1998; Kimberline and Walker, 1986; Kimberline and Walker, 1989a; Kimberline and Walker, 1989b; Lasmerzas et al., 1996).

1.9 The role of the spleen in neuroinvasion

The spleen contains follicular dendritic cells (FDCs) that accumulate infectivity and replicate the PrP^{Sc} to higher titres (Kitamoto et al., 1991). FDCs in spleen tissues are positioned close to sympathetic nerves (Prinz et al., 2003), which serve as a potential site of entry into the nervous system (Blättler et al., 1997; Glatzel and Aguzzi, 2000; Race et al., 2000). Reducing the number of sympathic nerves drastically increases the duration of the incubation period, and conversely, hyperinnervation decreases the duration (Glatzel et al., 2001). The proximity of the FDC cells to the sympathic nerves increases and decreases the rates of neuroinvasion, whether the cells are far from the nerves or closer, respectively (Prinz et al., 2003).

Exactly how the infectivity is delivered from the FDCs to the sympathetic nerves is not entirely clear, but likely involves vesicular (or exosomal) transport (Fevrier et al., 2004) or potentially a third mediator cell type such as dendritic cells (DCs) (Aucouturier et al., 2001; Defaweux et al., 2005), as FDCs have no physical contact with sympathetic nerves (Prinz et al., 2003).

Once the prion agent infects peripheral nervous system, it is believed that infectivity moves into the central nervous system using the autonomous nervous system (Beekes et al., 1998; Clarke and Kimberlin, 1984; Cole and Kimberlin, 1985; McBride and Beekes, 1999). Neurodegeneration occurs once the prion agent infects the brain tissues.

1.10 Diagnosing prion diseases

Prion diseases present a unique challenge for the development of markers that would be useful for antemortem clinical diagnosis. While most infectious diseases can be diagnosed using established methods, TSEs present a unique challenge. The prion cannot be visualized by microscopy, cultivated using media or cell culture, identified by detection with prion specific antibodies or detected by molecular methodologies (Kübler et al., 2003). The prion lacks an obvious nucleic acid component and so cannot be detected with the polymerase chain reaction (PCR), which eliminates the capacity to directly detect the prion agent. Furthermore, there is no antibody-mediated response against the misfolded PrP^{Sc} isomer of the normal host PrP^{C} protein (Porter et al., 1973). The identification of infected individuals is compounded by the fact that they may not show any clinical symptoms until well into the terminal disease state (Aguzzi and Sigurdson, 2004).

The development of markers for TSEs is critical for both diagnostics and intervention strategies. Early diagnosis of prion-infected invididuals or animals would allow appropriate strategies or treatments to be employed. This could affect human health as the detection of prion contamin7ated tissues (Aguzzi et al., 2004), surgical instruments (Flechsig et al., 2001) and blood supplies (Hunter et al., 2002; Llewelyn et al., 2004, Mabott and Turner, 2005, Peden et al., 2004) could prevent the entry of these diseases into the general population. In agriculture, early diagnosis of BSE infected cattle could prevent prion contaminated materials entering the food chain. The early identification of infected animals could prevent the unnecessary slaughter of entire herds,

as is currently done, because of one suspect animal as well as eliminating the risk of arising trade barriers.

1.10.1 Current diagnostic methods for prion diseases

Diagnostics currently available for prion diseases are limited and somewhat problematic. Prion diagnostic methods generally rely on the direct post-mortem detection of the disease-specific isomer of the prion protein. The two major methods to detect and confirm a prion infection include the antibody detection of Proteinase-K resistant PrP^{Sc} via Western blotting and histological or immunohistochemical examination of suspect brain tissues (Inoue et al., 2005). . However, these tests can be inaccurate due to cross-reactivity of experimentally generated α-PrP^{Sc} antibodies with PrP^{C} (Aguzzi et al., 2004). Furthermore, post-mortem examination of brain tissues only confirms the disease, but does not allow intervention.

The use of PrP^{Sc} as a pre-clinical marker or general marker for surveillance is limited the current methods are not sensitive enough to detected PrP^{Sc} in fluids such as blood, urine, saliva and cerebral spinal fluid. The need for the development of sensitive pre-clinical markers using accessible fluids or tissues for early detection of prion infection remains a important goal in averting the TSE risk to human and animal health.

1.10.2 Microarrays and surrogate markers

Molecular tests are useful in diagnosing diseases because they are both sensitive and specific (Kübler et al., 2003). Traditional molecular tests including PCR and variation of PCR (i.e. quantiative real-time PCR {qRT-PCR}) are rapid, but lack the capacity to

screen more than a few different targets simultaneously, and are thus limited in the development of diagnostic tests. One alternative is the use of microarray technology which can screen thousands of genetic elements simultaneously.

Microarrays, or gene chips, are libraries of segments of known genes and / or expressed sequence tags (ESTs) spotted onto glass slides that allow the monitoring of the spatial or temporal expression levels of thousands of genes simultaneously. Microarray chips can represent the entire gene complement of some organisms (such as bacteria) or just the genes expressed in one tissue type (such as mouse brain). Each chip can be spotted with over 100,000 individual gene elements. Microarrays generally require the use of RNA extracted from biological samples to allow the detection of transcript levels in the samples.

Microarray technology has been used elucidate the molecular mechanisms of infectious bacteria and viruses (Campbell and Ghazal, 2004) and even the host immune response to such infections (van der Pouw Kraan et al., 2004). Similarly, this technology can be applied to profiling the host response to the presence of different cancers, which has yielded distinguishing molecular profiles (Wadlow and Ramaswamy, 2005). Molecular profiling of cancers is especially important because prion diseases, although infectious, are often more reminiscent of a cancer than an infectious organism (Booth et al., 2004a).

Differential gene expression in prion diseases had been previously investigated using qRT-PCR, but only a few genes were examined (Dandoy-Dron et al., 1998; Duguid and Dinauer, 1990; Riemer et al., 2000; Miele et al., 2001). Microarray technology has been used by several groups for the exploration of host gene expression in prion infected

brain tissues (Booth et al., 2004a, 2004b; Brown et al., 2004; Riemer et al., 2004; Xiang et al., 2004). Screening thousands of transcripts simultaneously allowed the potential to develop a molecular signature for prion diseases, or even a particular prion strain (Booth et al., 2004b). These genes expressed in response to prion infection may represent surrogate markers of a prion infection. The differentially expressed transcripts could theoretically be adapted as markers useful in prion diagnostics using a high-throughput methodology such as qRT-PCR. These studies have not, to date, yielded defined diagnostic markers for prion infection.

1.11 Spleen gene expression profiling

Gene expression profiles from brain tissues of mice infected with a number of different prion strains have been obtained (Booth et al., 2004b). Their results provided insight into the pathological mechanisms of prion-induced neurodegeneration. However, the brain gene expression profiles may be shrouded by apoptotic signals and general responses to cell death, such as those not induced by the prion itself (Booth et al., 2004a). The brain and central nervous system are not practical candidates for the development of markers to prion infections due to the obvious difficulty of sampling this tissue from living individuals. The ideal sources of material for prion diagnostics would be easily accessible, and some examples include saliva, urine and blood.

The spleen is both a reservoir for infectivity and acts as a site of prion replication and is therefore a candidate tissue for investigating the molecular mechanisms of prion pathogenesis. The intimate association of the spleen with the blood and the lack of extensive tissue damage during prion infection means genes differentially expressed in

the spleen are more likely to be a direct response to the prion agent, and thus be more useful in the development of surrogate markers. Due to their small size, samples of blood from mice may not provide enough RNA to perform microarray experiments. However, differentially expressed genes in spleen tissues should provide insight into the signatures that may be present in blood samples. Thus, if a small number of surrogate markers could be identified by gene expression profiling of prion infected spleen tissues, these could then be adapted to a blood-based marker. An ideal pre-clinical marker candidate would be fast, sensitive, specific, cost-effective, and user-friendly.

To date no publications exist describing gene expression profiling of scrapie infected spleen or other lymphoid tissues. We hypothesized that there will be fewer differentially expressed genes found by microarray analysis in the spleen during scrapie infection when compared to the brain due to the neurological nature of the prion disease. These differentially expressed genes were more likely to reflect a direct response to the prion agent due to the lack of extensive tissue damage within the tissues. We expected differential gene expression profiles to parallel the accumulation of PrP^{Sc} deposits at the pre-clinical (100dpi) and clinical (148dpi) time points. The gene expression profiles from scrapie infected mouse spleen tissues with accumulated prion protein should allow further insight into the pathogenic mechanisms of TSEs, as well as potentially providing novel surrogate markers.

1.12 Project goals

The goals of this project were three fold:

1. Confirm the presence of accumulated PrP^{Sc} infectivity in the spleen during the disease progression, as well as the literature reported absence of pathology.
2. Determine the gene expression profile for prion infected spleen tissues during the progression of the disease, notably at the early, pre-clinical and clinical disease stages.
3. Investigate the potential of differentially expressed genes to be used as surrogate markers of pre-clinical scrapie infection in mice.

Materials and Methods

All procedures involving infectious materials were performed in Level3 containment.

2.1 Biological material

Prior to the beginning of this project, C57BL/6 mice (*Mus musculus*) were intracerebrally innoculated with 20µl 1% brain homogenate (obtained from the TSE Resource Centre, Institute for Animal Health, Compton, UK) prepared from clinically ill mice previously infected with scrapie strain ME7 or 79A. Additionally, a control group of mock-infected mice were innoculated intracerebrally with 20µl phosphate buffered saline (PBS). Mice were sacrificed when clinical symptoms of scrapie were being demonstrated (uncoordinated gait, flaccid paralysis of the hind limbs, rigidity, righting reflex abolished). This typically appeared between 148 and 153 days for 79A and between 153 and 160 days for ME7 scrapie. In addition to these mice, additional infected and control mice were sacrificed at 21 days post infection (dpi) and 100dpi. Brains and spleens were removed from all mice and stored in either RNA*later*™ (Ambion, Cat.7021) at –80°C for RNA extractions or 10% formalin for histology / immunohistochemistry. The formalin-fixed spleens and brains were imbedded in paraffin and sectioned for use in histological or immunohistochemical analysis. All procedures were approved by the Canadian Science Centre for Human and Animal Health Animal Care Committee.

2.1.1 RNA extractions from spleen tissues*

Whole mouse spleens were soaked in 2ml TRIzol® Reagent (Invitrogen, Cat.15596-018) for 20min to soften the tissues, and were then completely homogenized using an Omni

TH (Model: TH-115) tissue homogeniser and plastic disposable rotor stator generator probes (Omni Tips; Omni International, Cat.35750). The homogenate was then centrifuged** at 8800g for 10min at 4°C to separate cellular debris from the solution. The liquid phase was removed to a fresh tube and combined with 0.5ml chloroform, shaken vigorously for 15sec, and incubated at room temperature for 3min before being spun at 8800g for 15min at 4°C. The aqueous layer containing the RNA was transferred to a fresh tube and combined with 1ml of isopropyl alcohol and then incubated at room temperature for 10min. The precipitated RNA was then pelleted by centrifugation at 8800g for 10min at 4°C. The RNA pellet was washed once with 75% ethanol, pelleted by centrifugation at 7500g for 5min at 4°C, and was allowed to air dry.

2.1.2 RNA clean-up and DNase treatment

The RNA pellet was re-suspended in 0.5ml nuclease-free water (Ambion, Cat.9932) and clean up was performed using Qiagen RNAeasy Midi kits (Qiagen, Cat.75144), according to manufacturers instructions. This additional clean-up step ensured highly pure RNA in yields of 700-800ng/µl with $OD_{(260/280)}$ readings of 1.95-2.05.

Spleen tissues are notoriously high in nucleic acids (DNA and RNA) as well as nucleases. To ensure all contaminating genomic DNA (gDNA) was removed from purified RNA aliquots, a DNase step was employed. The TURBO DNA-*free*™ (Ambion, Cat.1907) was used according to the manufacturers instructions with some exceptions / additional steps. A rigorous DNase treatment was performed (uses 2x the DNase enzyme) and a ethanol-NaOAc precipitation step was done at the end to remove excess salt from the reaction mixture to prevent interfering with downstream reactions.

Finally, samples of the DNased RNA were randomly selected for gel analysis to confirm complete removal of genomic contamination. RNA was run on a denaturing agarose gel in 1X MOPS buffer containing 2.2M formamide. Total RNA was sized using an RNA ladder (Invitrogen, Cat.015620-016), and visualized by staining with ethidium bromide (0.5µg/ml).

*All surfaces decontaminated using RNaseZap (Ambion, Cat.9780) prior to beginning any RNA work.

**All centrifugation steps were performed using a refrigerated Allegra™ 21R centrifuge (Beckman).

2.2 Spleen and PrP^{Sc}

2.2.1 Haematoxylin and Eosin Staining

In order to visualize spleen structure during the course of prion infection, haematoxylin and eosin (H&E) staining was employed. Control (PBS) and infected (ME7 and 79A) spleens harvested at 21dpi, 100dpi and 148dpi were embedded in wax and 4µm sections were cut, then dried in a 60°C oven. The sections were dewaxed in two changes of xylene, then rehydrated through a progressive series of ethanol washes. To stain the nuclei the slides were transferred to haematoxylin (Surgipath, Cat.01542) for 3min and destained in 1% acid alcohol for 30sec, then counterstained in eosin (Surgipath, Cat.01600) for 3min. The slides were then dehydrated through alcohol, cleared in xylene, covered with polished coverslips and sealed with Micromount™ (Surgipath, 01732).

See Appendix 1 for complete procedural details.

2.2.2 Immunohistochemistry staining for PrP^{Sc}

Antibodies against PrP^{Sc} were used to visualize the accumulation of PrP^{Sc} over time in the scrapie infected mice spleens. As with H&E staining, control (PBS) and infected (ME7 and 79A) spleens harvested at the three aforementioned time points were embedded in paraffin and 4μm sections were cut, then dried in a 60°C oven. Procedures were identical to the H&E staining to get the slides free of wax and to running water. The sections were rinsed in TBS-Tween Buffer six times, transferred to 98% formic acid for 10min. Next, the slides were transferred to two successive 5min treatments in 3% H_2O_2.

To denature the PrP^{Sc} in preparation for antibody treatment, the slides were autoclaved for 10min at 121°C, 1.36atm and allowed to cool. Next, the slides were blocked with normal goat serum (1 drop in 10ml TBS buffer) at 45°C for 20min. The slides were then incubated with primary antibody (6H4, 1:1000; Prionics Switzerland, Cat.01-010) for 16hrs (overnight). The slides were then incubated for 20min with secondary antibody (goat-α-mouse, 1:500; Vector Laboratories, Cat.BA2000), and then 20min in Strept-ABC complex (Dako, Cat.K0377) at 45°C. To visualize the antibodies, the sections were incubated with DAB Substrate (Vector Laboratories, Cat.S3000) for 3min, then rinsed and transferred to haematoxylin for 3min for nuclei staining. The slides were then dehydrated through alcohol, cleared in xylene, covered with polished coverslips and sealed with Micromount™. Tissue section images were obtained using a Olympus Fluoview Confocal Microscope.

See Appendix 2 for complete procedural details.

2.3 Microarrays

2.3.1 Microarray construction

Prior to the beginning of this project, microarrays were prepared in house from two individual libraries, the Brain Molecular Anatomy Project (BMAP) library and the Mouse Sequence Verified (MSV) Unigene library. The two libraries and control elements make up a total of 17,644 individual spots on the microarrays. Each insert from the two libraries was amplified by PCR, then the amplicons were purified by using Millipore multiwell purification plates. Lyophilized PCR products were resuspended in 1x Micro-spotting Solution Plus (TeleChem) at a concentration of 0·25–0·75μg/μl. The DNA amplicons were spotted onto CMT–GAPS-coated glass slides (Corning) by using Stealth micro-spotting pins (TeleChem).

2.3.2 Labelled complementary DNA generation and purification

Samples of DNased and purified total RNA were used for oligo(dT)-primed reverse transcription and incorporation of aminoallyl-dUTP (Sigma, Cat.A0410) into complementary DNA (cDNA). Each reaction contained 10μg of RNA and 1μg of oligo(dT) primer (Invitrogen, Cat.18418012) brought to a total volume of 18.5μl with RNase-free water. This mixture was heated to 70°C for 10min to denature any secondary structure in the RNA and then placed on ice to prevent renaturing. To each reaction 9.6μl of master mix (6μl 5X 1st strand buffer, 3μl 0.1M DTT, 0.6μl 50X dNTP mix; Invitrogen, packaged with RT enzyme) and 2μl (200U/μl) Superscript II Reverse Transcriptase (Invitrogen, Cat.10342-020) were added. The reaction was incubated overnight (16hrs) at 42°C. In order to stop the reaction and hydrolyze the RNA, 10μl each and 0.5M

EDTA and 1M NaOH were added respectively, and the cDNA was heated to 65°C for 15min. The pH of the reaction was neutralized with 10µl of 1M HCl. The cDNA was purified using Microcon YM-30 filter devices (Millipore, Cat.42410) according to the manufacturers instructions. Elution volumes were adjusted to be equal across all samples before drying.

2.3.3 Microarray slide prehybridization

To prepare the microarray slides for hybridization, they were incubated at 42°C in prehybridization buffer (see Buffers in Appendix 3) for 45min to reduce background signal. After prehybridization the arrays were washed 5 times in dH_20 and once in isopropanol.

2.3.4 Microarray slide hybridization

The cDNA with aminoallyl-dUTP incorporation was dried to completeness and resuspended in freshly prepared 4.5µl 0.1M Na_2CO_3, pH 9.0. To each reaction either an Alexa Fluor^{555} (AF555) or Alexa Fluor^{647} (AF647) monofunctional reactive dye (Molecular Probes, Cat.A-20009/A-20006), made up in DMSO, was added. The labeling reaction was incubated in the dark before being purified using QIAquick PCR purification columns (Qiagen, Cat.28106) according to the manufacturers instructions and were dried to completion. The dried labelled cDNA was resuspended in 70µl DIG Easy Hyb hybridization buffer (Roche, Cat.1034946). To block non-specific hybridization, 1µl (20µg/µl) each Cot1-DNA (Invitrogen, Cat.18440016) and poly-A DNA (Invitrogen, Cat.polyA.gf) were added prior to hybridization. Before hybridizing

the labelled reaction mixture to the array, the mixture was heated to 95°C to denature any secondary structure and placed on ice. The mixture was added to each prehybridized array under a cleaned M-Series LifterSlip (Erie Scientific Company, Cat.M-5439-001-LS) and hybridized overnight (16hrs) at 42°C in a humid chamber.

2.3.5 Microarray slide washing and scanning

Following hybridization, lifter slips were removed and the arrays washed once each for 4min in Low Stringency Buffer, High Stringency Buffer and 0.1X SCC Buffer (see Appendix 3 for buffer compositions). After the last wash the arrays were dried via centrifugation. Slides were scanned immediately by using a VersArray scanner (Bio-Rad) at appropriate laser power and photomultiplier tube settings, so that high-intensity spots were not saturated.

2.3.6 Data analysis

Microarrays .TIFF images were uploaded into ArrayPro (MediaCybernetics) and spots were identified and grids constructed. The data obtained was stored in and analyzed using the GeneTraffic Microarray Database and Analysis System (Iobion Informatics, as well as the software package Significance Analysis for Microarrays (SAM; Tusher *et al.*, 2001). Normalization of raw intensities was achieved by using a linear regression smoothing algorithm (Loess best-fit) over individual array sub-grids. Finally, the $\log_2$ ratios for the resulting filtered and normalized intensity values were used for all further statistical analysis. Statistical analysis of the resulting gene list was performed using a one-class SAM analysis with a false discovery rate (FDR) of 10%. In order for a gene to

be considered significant, the spot intensity between the control PBS and scrapie infected mice, had to differ by a 1.3 fold change.

2.4 Validation

2.4.1 Spot Validation – Plasmid Sequencing

Positive clones were selected from library plates stored at -80°C and used to inoculate 5ml of LB broth containing 50μg/ml carbenicillin. Cultures were allowed to grow with shaking overnight 16hrs at 37°C or until turbidity was achieved. The cultures were pelleted by centrifugation at 9000g for 5min. Plasmids were purified from the clones using QIAprep Spin Miniprep kit (Qiagen, Cat.27104) according to the manufacturers instructions. Purified plasmids were restricted with 0.5μl (15U/μl) EcoRI (Invitrogen, Cat.15202-013) and Not I (Invitrogen, Cat.15441-025) in 10μl reaction volumes at 37°C overnight (16hrs). Fragments were resolved by gel electrophoresis through 1% agarose gel in 1X TBE buffer (Ambion, Cat.9863). DNA fragments were sized using the BRL 1-kb plus molecular weight ladder (Invitrogen, Cat.10787-018), and visualized by staining with ethidium bromide (0.5μg/ml). Validated plasmids were submitted for sequencing to the NML DNACore Facility (http://www.nml-dnacore.ca/) at a concentration of 150ng/μl. Sequences were aligned using the GeneDoc program v2.5.010 (Nicholas *et al.* 1997).

2.4.2 Semi-quantitative RT-PCR primer design

Primers were designed by manually examining target sequences looking for the following: fragments no larger than 400bp, GC rich 3' ends for primers, and unique

stretches of sequence approximately 20 nucleotides in length. Samples of RNA consisted of four pooled control (PBS) individual mouse spleens and four pooled individual infected (ME7) mouse spleens.

2.4.3 cDNA generation for semi- quantitative RT-PCR

Aliquots of 2μg of previously DNased and purified RNA were used to generate cDNA template for semi-quantitative RT-PCR (sqRT-PCR). To each tube 1μl of oligo(dT) and 1μl of 10mM dNTPs were added and brought to 10μl with water. This mixture was incubated at 65°C for 5min and then placed on ice for 1min. Master mix (4μl 5X first strand buffer, 2μl 0.1M DTT) and 1μl (200U/μl) Superscript II Reverse Transcriptase was added and the samples were incubated at 42°C for 50min, then heated to 70°C for 15min to denature the enzyme and cooled to 4°C. The samples were centrifuged and 1μl (4U/μl) RNaseH (Invitrogen, Cat.18021-014) was added and incubated at 37°C for 20min to remove any RNA left from the RT reaction. Lastly the cDNA was purified using Microcon YM-30 filter devices according to the manufacturers instructions. The final concentration of the cDNA was adjusted to 50ng/μl.

See Appendix 4 for complete protocol.

2.4.4 Semi-quantitative PCR conditions

The cDNA generated from the above RT reactions served as a template for semi-quantitative PCR. Reactions were performed in 52μl volumes under standard PCR conditions (see Appendix 5 for exact volumes and components). Primers varied according to the gene desired to be amplified and can be found in **Table 3**. Cycling

conditions were similar, except annealing temperatures and cycle numbers varied and can be found in **Table 4**. The reactions were removed during the last five cycles to ensure the PCR products were observed to be in the exponential range, and thus remaining useful for semi-quantitative RT-PCR. Amplicons were resolved by gel electrophoresis through 1% agarose gel in 1X TBE buffer. DNA fragments were sized using the BRL 100bp molecular weight ladder (Invitrogen, Cat.15628-050), and visualized by staining with ethidium bromide (0.5µl/ml).

PCR products intended for sequencing were pooled from four individual reactions and purified using the QIAquick PCR purification columns (Qiagen, Cat.28106) according to the manufacturers instructions. The purified amplicons were submitted to the NML DNACore Facility for sequencing at a concentration of 50ng/µl. The primers were provided individually at a concentration of 10ng/µl. Sequences were aligned using the GeneDoc program v2.5.010 (Nicholas *et al.* 1997).

Table 3: Gene target and primers for semi-quantiative RT-PCR

Gene Name, Accession and Primers		
Name	**Target**	**Primers (5'-3')**
45S RNA	45S preRNA	45SRNAF: GCCATGAATGTCCGTCCC 45SRNAR: CTCCTGTCTGTGGTGTCC
Unknown1	Unknown expressed sequence tag (EST)	Unknown1F: GAAGAATGCTTAGCATCC Unknown1R: GGGTGGAACCTATAATGG
Rgs2	Regulator of G-protein signalling	Rgs2F: GTGGTTCTAGGAATGTGG Rgs2R: TCATTGAACATTTGGAAG
Cpd	Carboxypeptidase D	CpdF: CAAGTTCATGTGACAGCC CpdR: AAGTCTTGTAGTCATGGG
Smyd5	SET and MYND containing domain 5	Smyd5F: TTATTGAGACCAGTGGGC Smyd5R: TACACACGAAGATGAGCC

Table 4: Cycling conditions for semi-quantiative RT-PCR

Gene	Denaturing	Annealing	Extension	Cycles Removed
45S RNA	93°C 45 secs	58°C 1 min	72°C 1 min	25, 26, 27, 28, 29, 30
Unknown1	93°C 45 secs	55°C 1 min	72°C 1 min	25, 26, 27, 28, 29, 30
Rgs2	93°C 45 secs	56°C 1 min	72°C 1 min	29, 30, 31, 32, 33, 35
Cpd	93°C 45 secs	58°C 1 min	72°C 1 min	25, 26, 27, 28, 29, 30
Smyd5	93°C 45 secs	55°C 1 min	72°C 1 min	29, 30, 31, 32, 33, 35

Results

3.1 Scrapie infection of mice

3.1.1 Confirmation of prion infection in scrapie inoculated mice

Groups of 15 mice (C57Bl/6) were inoculated intracerebrally with brain homogenate prepared from C57Bl/6 mice clinically infected with the scrapie strains ME7 or 79A. The scrapie strains ME7 and 79A were chosen for this study as they have very similar incubation periods but exhibit different neuropathology features. This feature allows an identical time course to be used for each strain. Mock-infected mice were inoculated in the same way with phosphate buffered saline solution (PBS). Scrapie infected mice were either sacrificed at 21dpi or 100dpi, or after the development of advanced signs of clinical scrapie (between 148 and 161 dpi for ME7 and at 148dpi for 79A) as shown in **Table 5**. The clinical symptoms of scrapie were scored for severity using the following criteria: uncoordinated gait, flaccid paralysis of the hind limbs, rigidity, and the righting reflex being abolished. When two or more of these symptoms were apparent, the mouse was sacrificed and tissues stored for RNA collection or histology and immunohistochemistry. All procedures involving mice were approved by the Canadian Science Centre for Human and Animal Health Animal Care Committee.

Prion infection was confirmed using histological and immunohistochemical examination of brain sections from mice showing clinical symptoms of scrapie. **Figure 4** shows the results of these analyses on mouse hippocampus infected with ME7, 79A or PBS. A similar pattern of vacuolation was found in hippocampus from both strains of

Table 5: Summary of mice used in this study. Number of C57Blk mice inoculated with each scrapie strain for microarrrays immunohistochemistry / histology, and the time of sacrifice or death.

	Microarray Sacrificed		Microarray ---------- Sacrificed or Death ----------					Immunohistochemistry and Histology (Sacrificed)			
Inoculum	**21dpi**	**100dpi**	**148dpi**	**153dpi**	**159dpi**	**160dpi**	**161dpi**	**21dpi**	**100dpi**	**148dpi**	**Total**
Strain ME7	10	10	5	4	0	0	2	5	5	5	
Strain 79A	10	10	10	0	0	0	0	5	5	5	
PBS Control	10	10	10	0	5	10	0	5	5	5	
Totals	30	30	25	4	5	10	2	15	15	15	196

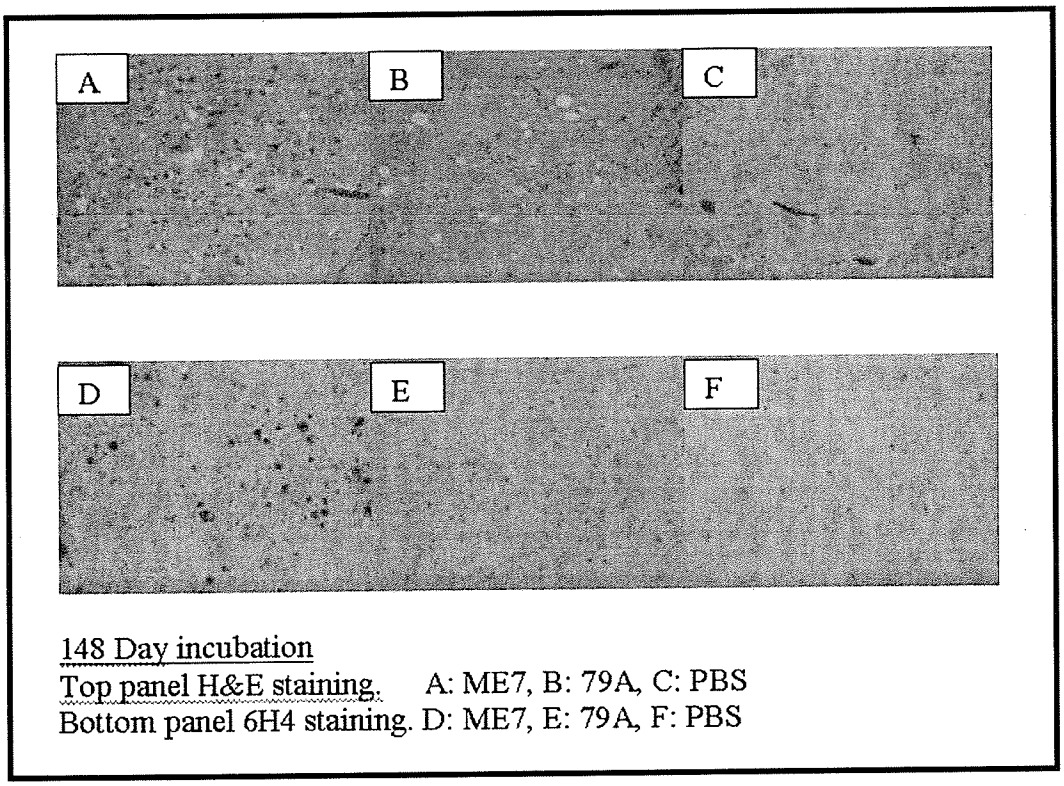

Figure 4: Histological and immunohistochemical sections of scrapie or PBS infected mouse hippocampus, showing typical pathological evidence including vacuolation and PrP^{Sc} deposition (6H4). Images kindly provided by Catherine Robertson.

scrapie-infected mice in comparison to the controls, with a slightly higher density observed in the ME7 infected mice. However, after immunohistochemical analysis using an antibody to prion protein an obvious difference between the two scrapie strains was that ME7 showed larger, punctate stained PrP^{Sc} deposits as compared to strain 79A, which demonstrated very fine diffuse staining. These observations were found consistently throughout the grey matter areas of the brain. Considerably more vacuolation was seen in the white matter of 79A-infected mice, than in those mice infected with ME7. These results are consistent with previously published studies and so confirmed the validity of the infection protocols employed (Fraser and Dickinson, 1973; Bruce et al., 1989; Bruce et al., 1991).

3.1.2 Spleens accumulate PrP^{Sc} without significant pathological changes

All spleens removed from mice at 21dpi, 100dpi, and 148dpi appeared normal i.e. no signs of physical trauma upon examination (i.e. swelling, shrinking, ruptures etc.); average weight of ~ 100mg, average length of ~ 15mm. Microscopic examination of histological spleen sections showed typical discrete white nodules (white pulp) embedded in a red matrix (dark pulp) (Burkitt et al., 1993). No obvious pathological changes or tissue damage was apparent at early, pre-clinical or clinical time points (**Figure 5; Figure 6**).

Immunohistochemistry was used to confirm the presence of PrP^{Sc} in spleen tissues during the disease time course. PrP^{Sc} deposits were not found in the 21dpi spleens as expected (**Figure 7**). At 100dpi PrP^{Sc} deposition was readily detectable, with larger amounts of deposition evident at 148dpi (**Figure 7**). Furthermore, at the clinical stage the

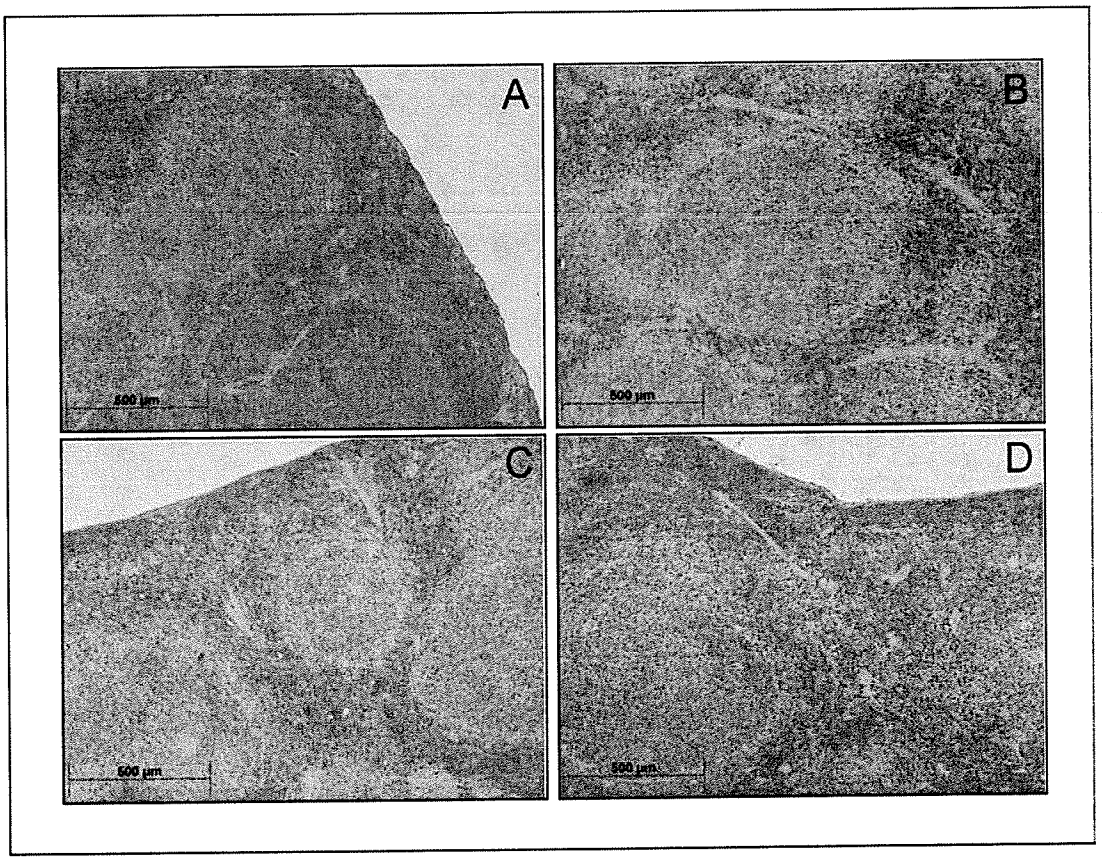

Figure 5: Histology sections of scrapie infected mice spleen (Strain 79A) at 21dpi (A), 100dpi (B), 148dpi (C) and a 148dpi PBS control (D). Haematoxylin and eosin staining of 4µm sections.

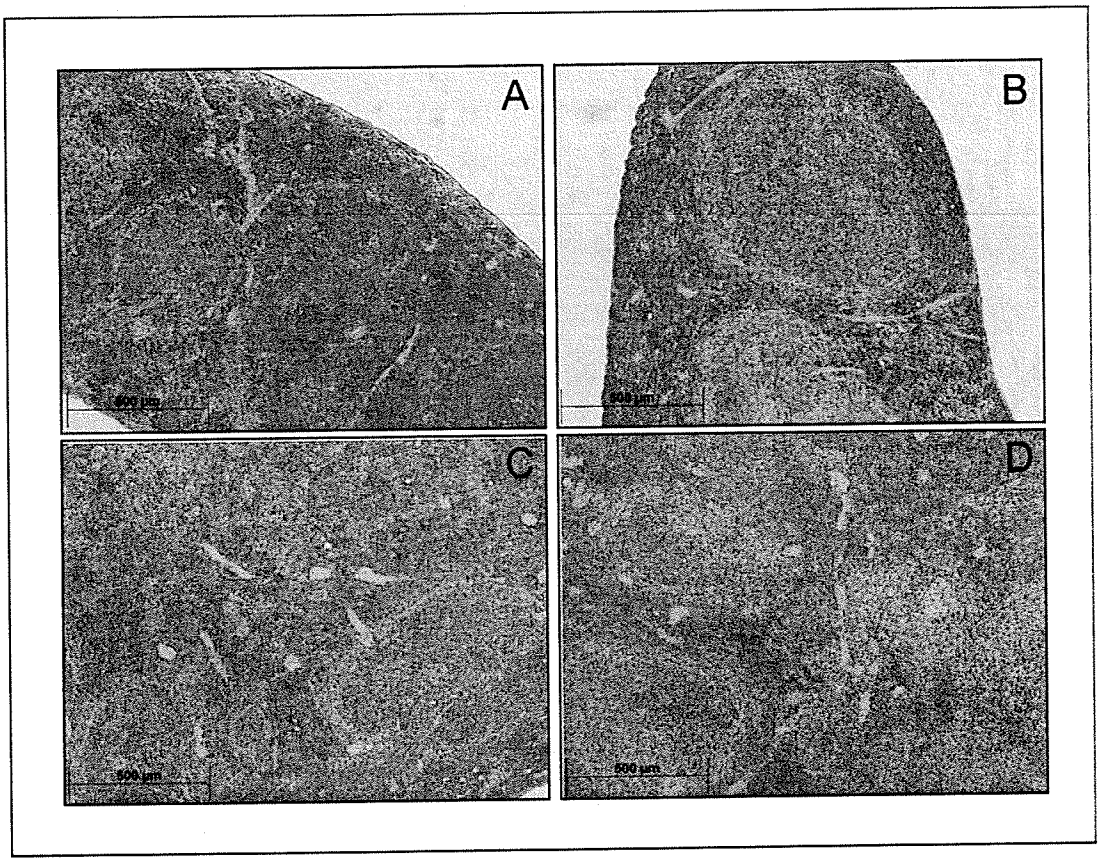

Figure 6: Histology sections of scrapie infected mice spleen (Strain ME7) at 21dpi (A), 100dpi (B), 148dpi (C) and a 148dpi PBS control (D). Haematoxylin and eosin staining of 4μm sections.

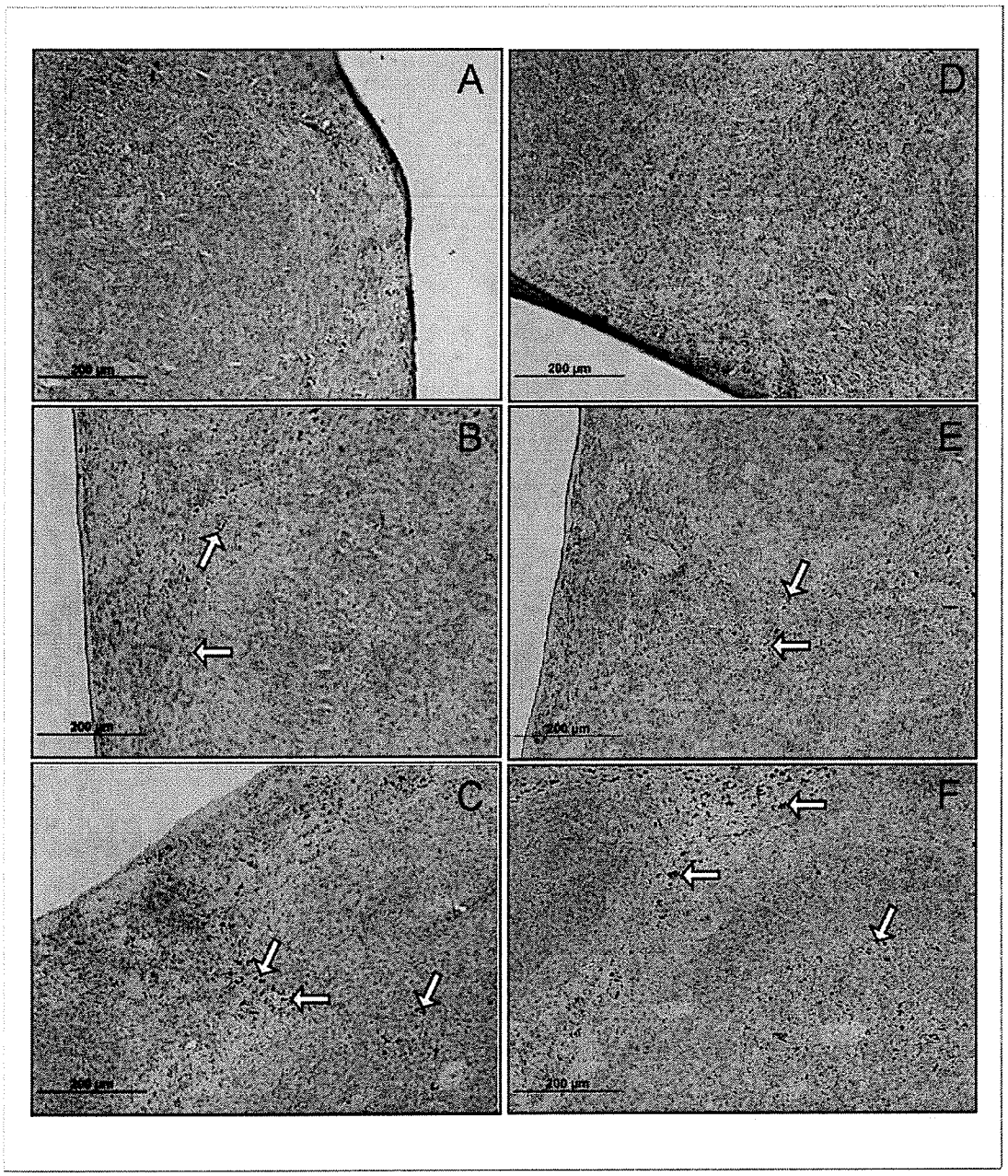

Figure 7: Immunohistochemical analysis of scrapie infected mice spleen; Strain 79A at 21dpi (A), 100dpi (B), 148dpi (C); Strain ME7 at 21dpi (D), 100dpi (E), 148dpi (F). Haematoxylin staining and 6H4 antibody with DAB substrate visualization of 4µm.

PrP^{Sc} appeared to accumulate most strongly around the regions of white pulp where FDCs are present, and to a lesser extent surrounding the central arteriole, which is partially consistent with literature reports (Cunnigham et al., 2005) and may reflect differences in staining procedures (**Figure 8**). No obvious or striking differences in deposition of PrP^{Sc} were observed at any of the three time points examined.

3.2 Gene expression profiling of mouse spleen in response to scrapie infection

3.2.1 Mouse microarray construction

The microarrays used in this work were prepared in house and were comprised of two independent cDNA libraries; the Brain Molecular Anatomy Project (BMAP) library and the Research Genetics Mouse 5K Cloneset library. The BMAP library is an 11,136 element cloneset composed of ESTs prepared from brain and associated tissues http://genome.uiowa.edu/projects/BMAP/index.html). The Research Genetics Mouse 5K Cloneset library is a 5184 element cloneset composed of the first 54 plates of the Research Genetics Sequence Verified library. The library was derived from mouse ESTs which have been 5' and 3' sequence verified (VMSR; http://array.mc.vanderbilt.edu/services/clonesetss.vmsr).

The BMAP cDNA library was originally selected by the Booth group for transcriptional analysis of scrapie infected brain tissues (Booth et al., 2004a, 2004b) because this library was prepared from mouse brain and associated tissues and scrapie is a neurological disease. This gave enormous potential for the discovery of genes expressed primarily in CNS tissue that have yet to be described as being associated with prion diseases. However, it is likely that only a very small minority of genes are

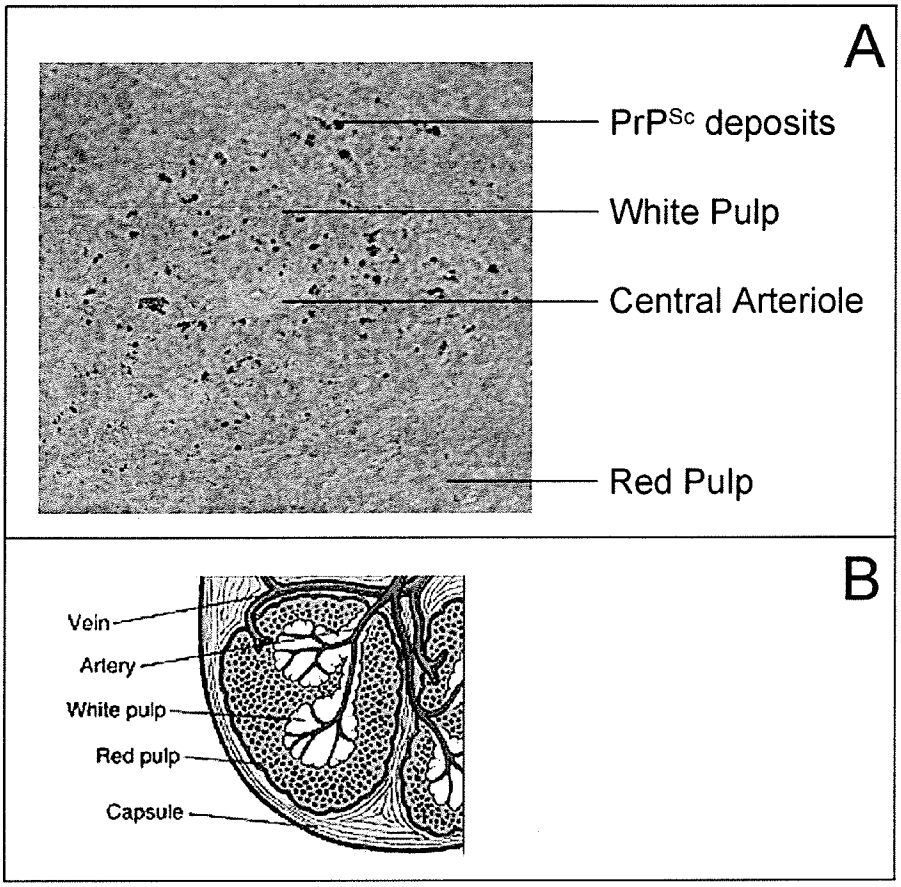

Figure 8: Spleen follicle showing PrP^{Sc} deposition (A) Scrapie infected mouse spleen follicle showing follicle morphology and PrP^{Sc} deposition. (B) Diagram of gross spleen morphology; red pulp - clusters of macrophages and erythrocytes, white pulp - lymphocytes suspended on arteriole.
www.merck.com/media/mmhe2/figures/fg179_1.gif

expressed in CNS alone, and this library is therefore a valid option for experiments involving tissues other than CNS, especially with the addition of the Mouse 5K cDNA library that comprises ESTs cloned from a number of mouse tissues. It has the added valuable advantage of providing a direct comparison with the Booth laboratories previous work on microarray analysis of scrapie infected CNS tissue (Booth et al., 2004a; 2004b).

Approximately 30% of the genes from the combined libraries on the array have been previously annotated. However, the majority of the genes spotted on the array are unannotated ESTs with no immediately definable biological function (**Table 6**). Using the online software package Onto-Express (OE), the 17,000 gene elements on the array were categorized according to biological function defined by the Gene Ontology Consortium (GO) (**Figure 9**). A broad spectrum of biological functions are represented by the genes on the array, including transcriptional regulation, signal transduction, cell cycling and signal cascades.

3.2.2 Extraction of total RNA from mouse spleens

Mouse spleens were stored in RNA*later*™ until the experimental time course (scrapie incubation period) was complete; storage of tissues in RNA*later*™, at -70°C, maintains RNA integrity for an extended period of time. This avoided the introduction of variation associated with differences in RNA quality that could be introduced during extractions performed at different times and with different batches of materials. Total RNA was then extracted from all of the mouse spleens under identical conditions.

The typical total RNA yield for an average mouse spleen was 202.6±55.6μg (n=10), with an $OD_{260/280}$ of 1.95-2.05. Denaturing agarose gels were used to visualize

Table 6: Number of annotated genes and unannotated EST sequences on BMAP/ msv arrays

cDNA Library	Annotated Genes	Unannotated EST Sequences	Total
BMAP	3957	7179	11136
Research Genetics	937	4247	5184
Combined Total	4894	11426	16320

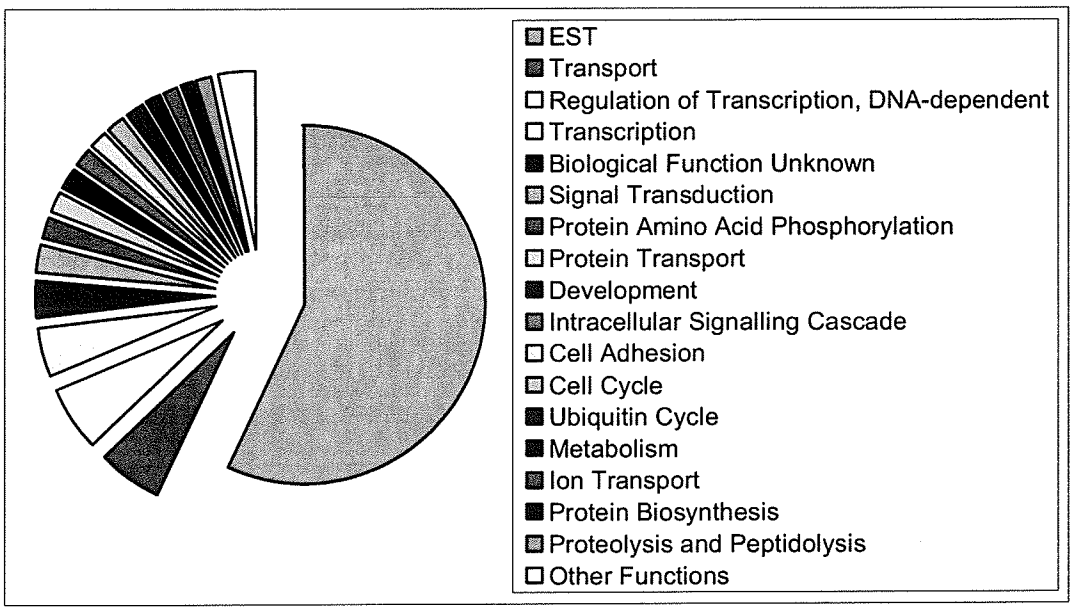

Figure 9: Gene ontology of the 16,320 accession numbers of BMAP and MSV cDNA libraries defined to their biological functions according to the Gene Ontology Consortium (GO).

the integrity of the 28S and 18S rRNA bands, where a genomic DNA (gDNA) band was evident (**Figure 10**). Spleen RNA extraction procedures are complicated by the fact that the spleen is rich in both nucleic acids and nucleases, which increases the potential for genomic DNA contamination (Ambion Inc., 2005a).

A DNase step was employed using a modified DNase enzyme (Ambion, Cat.1907) shown to dramatically reduce gDNA contamination (Ambion Inc., 2005b). Using this enzyme, gDNA was effectively removed from the RNA preparations as shown in (**Figure 10**). Subsequent RT reactions produced lower than expected yields, likely caused by the increased salt concentration in the reaction mixtures. To reduce salt concentration, an ethanol-NaOAc precipitation step was performed. After resuspension in pure water, the resulting RNA remained in good quality with an $OD_{260/280}$ of 1.95-2.05. Reverse transcriptase reactions were found to have an increased cDNA yield of approximately 50% after the ethanol-NaOAc treatment (**Table 7**). With the above considerations in mind, all further RNA extractions were subject to a DNase / ethanol precipitation step to minimize DNA contamination.

3.2.3 Microarray experimental design

Microarray experiments have intrinsic variability that can be divided into three major categories; biological variation, technical variation and measurement error (Churchill, 2002). In a microarray analysis we are in effect making 17,000 individual measurements at one time and selecting hundreds of genes that may change in expression in an experiment; in this case host gene expression changes in response to scrapie infection. Even small effects due to variation can produce significant numbers of false

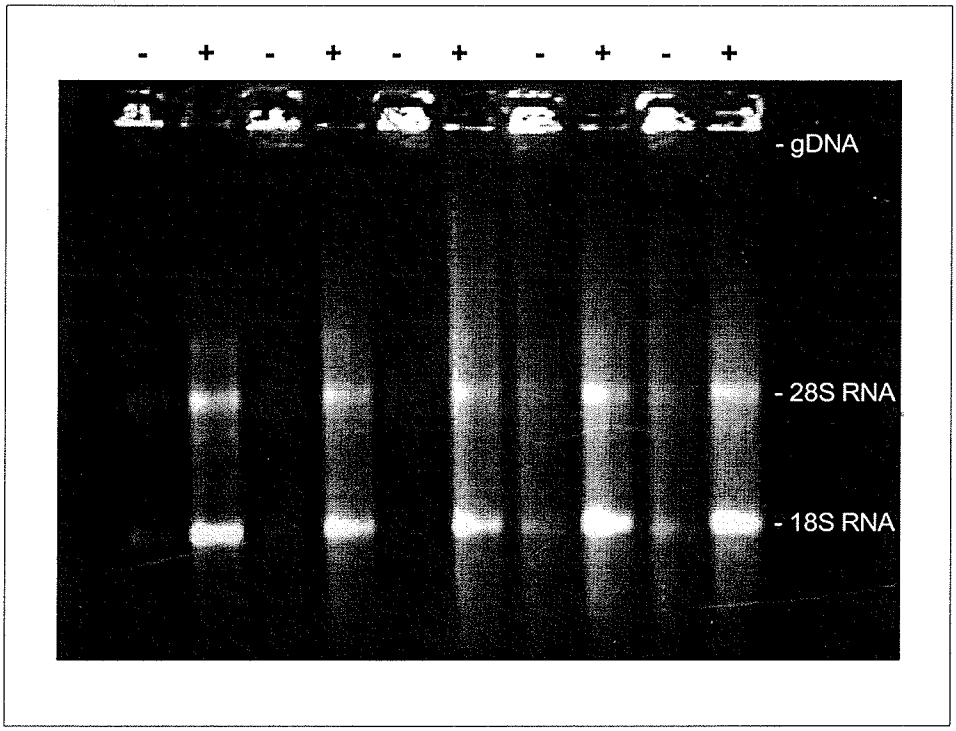

Figure 10: Total RNA extracted from uninfected spleen tissues, showing intact rRNA 28S and 18S bands in untreated (-) and DNased (+) samples. Genomic DNA (gDNA) contamination was treated with 2u Turbo DNase. 5µg total RNA loaded / lane.

Table 7: Differences in cDNA yields after ethanol precipitation.

Spleen cDNA	Ethanol Precipitation	ng/µl
1	No	4.08
2	No	6.19
3	Yes	13.21
4	Yes	14.4

positive and false negative results. We minimised the effects of experimental variation in the following ways.

The array experiments were arranged so that eight RNA samples from individual scrapie infected mice were hybridized against a pooled sample of RNA extracted from the mock-infected mice (the reference RNA). This is a standard design in two-colour microarray experiment and is shown in **Figure 11**. Eight replicates were used to strengthen the statistical significance of the results; a minimum of two mice is recommended for an array experiment (Churchill, 2002). Pooling the control RNA samples maintains what is expected to be a "normal" transcriptional profile for any mouse at the given time point, while maintaining the infected mouse samples independently allowed an estimation of variation in expression for each gene, between individual infected mice, so that only genes whose change in expression is consistent to prion infection are ranked highly.

The second category, technical variation, is introduced during the extraction, labelling and hybridization of the samples used for each array. All spleen RNA extractions were performed within a limited time interval and identical protocols and buffers were used to reduce variability between samples to reduce the technical variation. Fluorescent dyes exhibit a labelling bias for some genes, this was reduced by the use of a 'dye-swap' method; for four arrays the control RNA samples were labelled with Alexa555 (Cyanine 3; Cy3), and the RNA from infected samples was labelled with Alexa647 (Cyanine 5; Cy5), in the other four arrays the labels were reversed (**Figure 12**).

The last category, measurement error, is introduced during the scanning of the arrays. The fluorescent signal may be influenced by dust on the slide or the quality of the

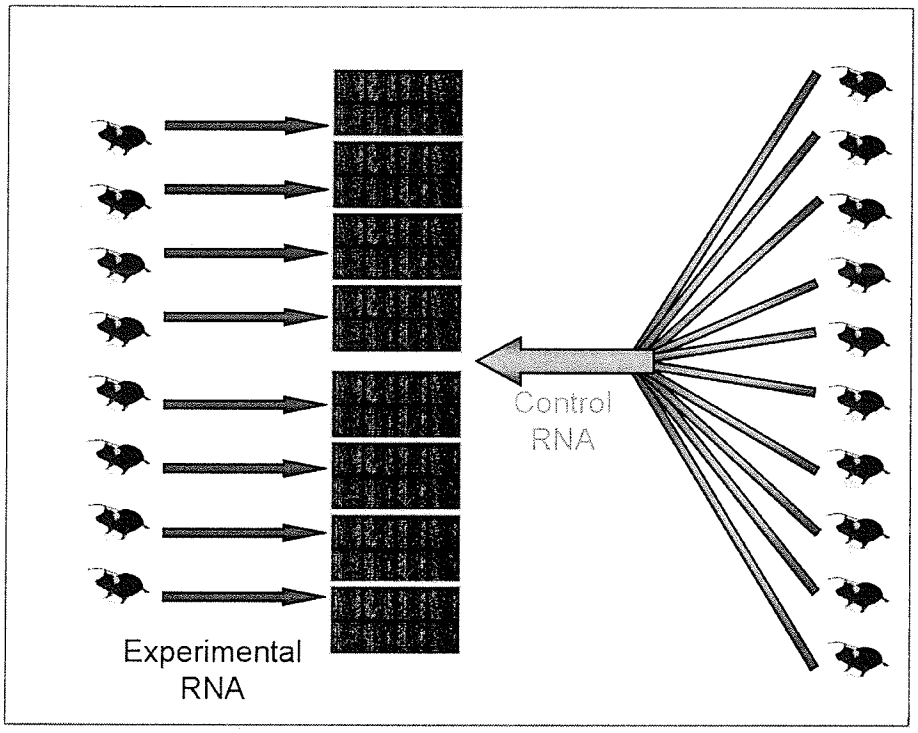

Figure 11: Microarray experimental design; RNA from eight prion infected mice versus pooled control of age-matched, mock-infected control mice hybridized to BMAP / MSV microarrays (Booth et al., 2004a, 2004b; Churchill 2002).

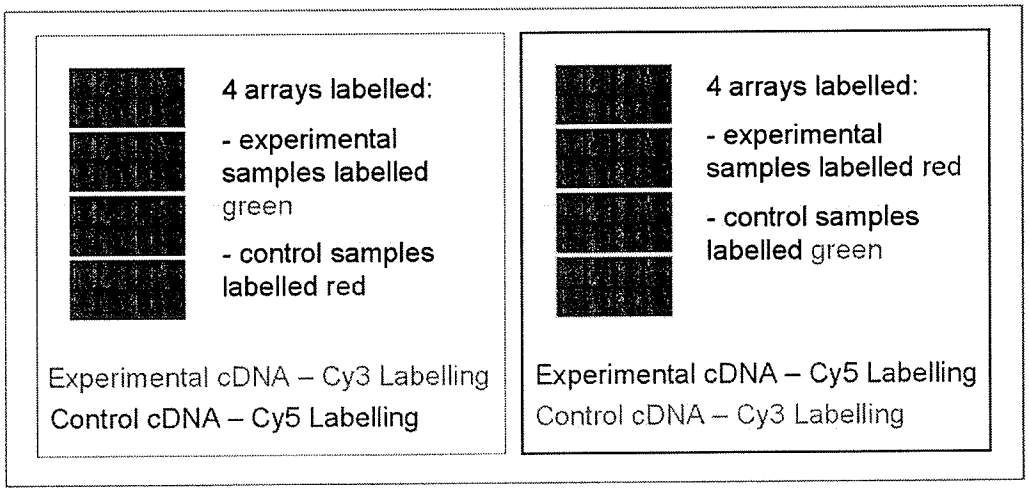

Figure 12: Dye-swapping methodology. Four infected cDNA samples labelled Cy3 on four microarrays and four infected samples labelled Cy5 on four microarrays. All experimental samples matched against age-matched, mock-infected control cDNA labelled opposite to infected.

lasers in the scanner. However, such variations in the fluorescent signal are easily accommodated by quality control to remove outlying signals and by normalizing the array images prior to analysis.

3.2.4 Microarray data collection

In total 48 arrays were performed, 8 for each time point for each strain. Slides were scanned and the spots quantified, local background intensity was determined for each spot and this was removed. Before the gene expression profiles of the RNA samples were analyzed and interpreted, the red and green intensities were normalized relative to one another so that the red/green ratios were as far as possible an unbiased representation of relative expression. A Loess (locally weighted scatterplot smoother) algorithm was used to normalize the raw microarray data. The Loess normalization procedure subtracts a Loess regression curve from the data to linearize it. The Loess function adjusts the signal intensity value for each dye on every spot in the array and equalizes the two based on regression curve calculated from each dye. The ratio of expression for each gene between scrapie infected samples and a pooled mock-infected control sample was then calculated for each array. The normal ratio constricts gene depression levels to values between 0 and 1, while an increase in expression can have any value between 1 and infinity. This causes the distribution of ratios to become skewed. Log ratios, however, have a normal-like distribution around zero, as seen in **Figure 13**. For this reason ratios were transformed into a $\log_2$ ratio to symmetrically represent relative changes in gene expression. A representative array from the experiment is shown in **Figure 14**. Signal intensity data from this array is shown in the box plots in **Figure 15,** the total red and

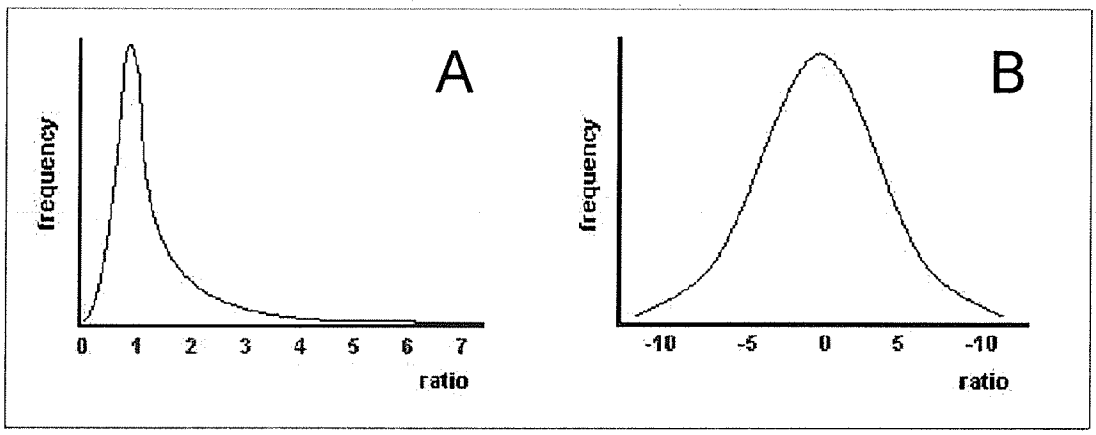

Figure 13: Normalization of microarray data. Graphs of normal (A) and logarithmic (B) gene ratios as applied to microarray data.
http://www.ucl.ac.uk/oncology/MicroCore/HTML_resource/images/norm_diffincurves.jpg

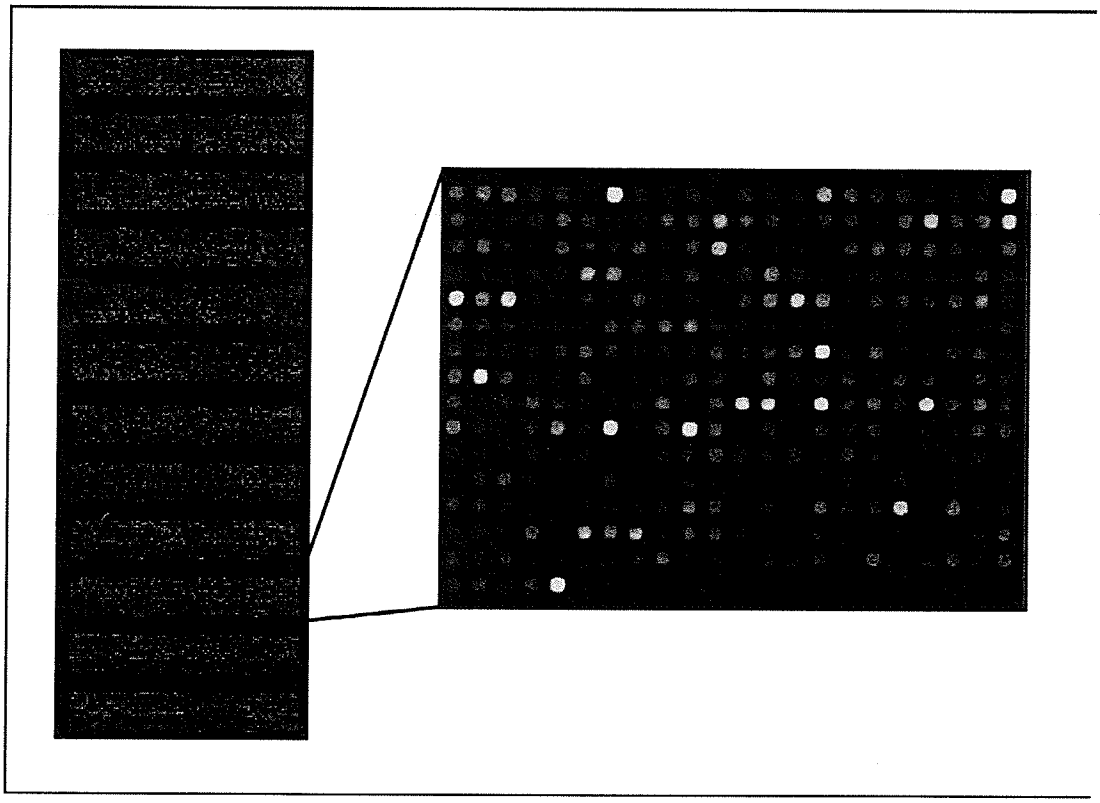

Figure 14: Representative hybridized array using RNA from ME7 infected mouse spleen taken at 148dpi against RNA from PBS inoculated control mouse spleen. Cy3 (green) control and Cy5 (red) infected.

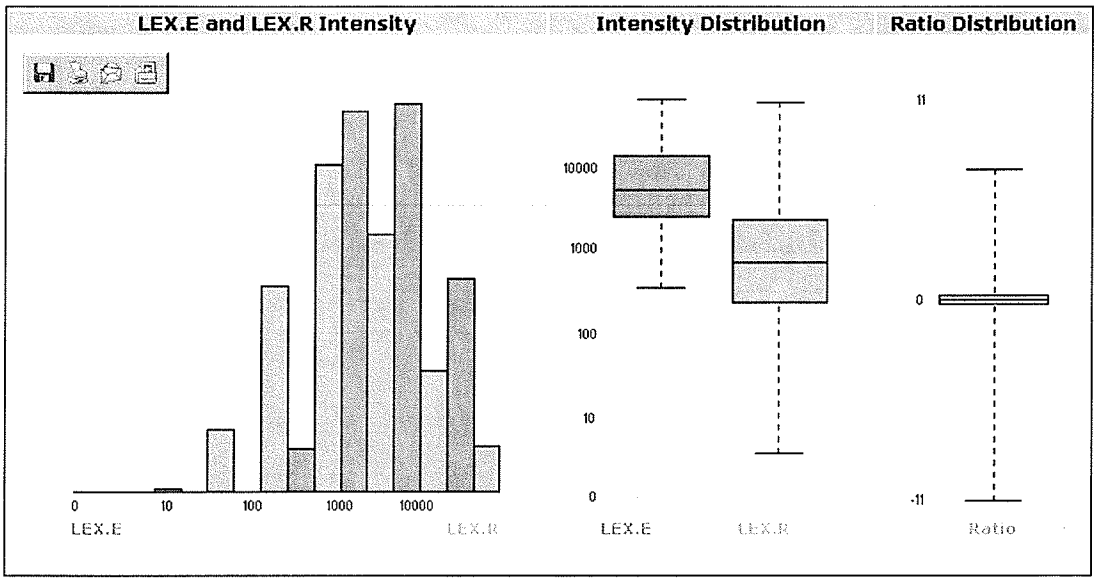

Figure 15: Box plots showing the raw signal intensity data before normalization. The total green signal (LEX.E) has an overall stronger intensity and smaller deviation than the red (LEX.R) signal. These differences were accounted for later with normalization.

green signals show some variation in this case. The effect of normalization is illustrated by the equalization seen in the average intensity levels and by the plots shown in **Figure 16**.

Using the signal intensity data for all the slides we were able to estimate the number of genes for which expression levels were significant in the spleen samples by counting those spots with signals greater than the average intensity for a number of control spots on the array. 11,507 genes could be scored as "present" in the spleen (68% of the genes on the array).

An initial exploratory data analysis step was performed using a Multidimensional Scaling technique. This method allows the visualization of the relationship between each of the samples in three-dimensional space using all of the gene expression data (**Figure 17**). From these visualizations, a clear differentiation between the samples labelled with the two different fluorescent dyes can be seen which is dye bias. This is illustrated in **Figure 17A** in which infected samples labelled with Alexa 647 are coloured red and those labelled with Alexa 555 are coloured green. This bias is accounted for in down-stream statistical analysis of the data, as there are equal numbers of replicas in each sample group labelled with each dye combination. In **Figure 17B** samples are coloured according to the incubation period. There was a limited relationship between the times of sampling on this plot, which suggested that there were no gross changes in gene expression during the course of prion disease in the spleen. However, in this case the plot was constructed using data from all 17K spots on the array and small groups of genes within the data that are differentially expressed over the course of infection must be selected by more stringent statistical methodologies.

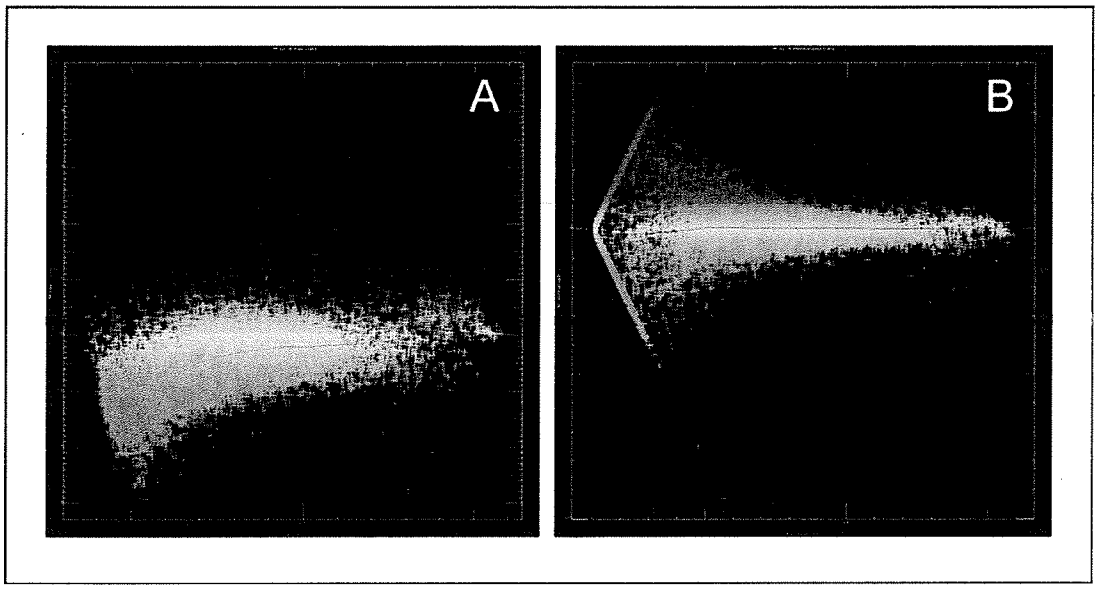

Figure 16: Scatterplots to show normalization of array data. (A) un-normalized array data (B) normalized array data, generated from microarray using RNA from ME7 infected mouse spleen taken at 148dpi against RNA from PBS inoculated control spleen. Cy3 (green) control and Cy5 (red) infected.

A

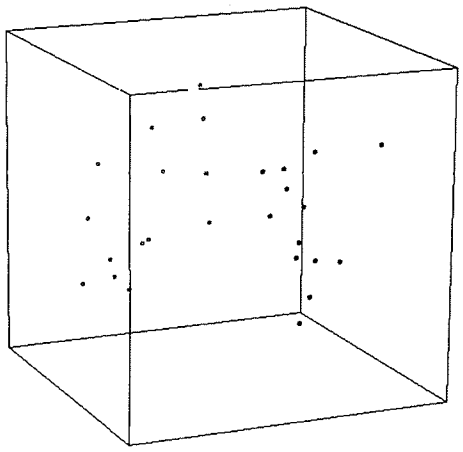

B

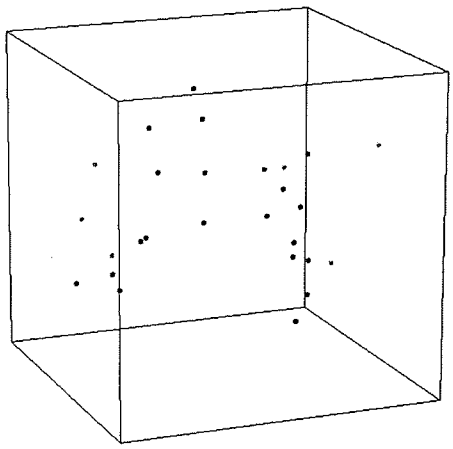

Figure 17: Multi-dimensional scaling plots of all gene expression data, **(A):** dye bias marked by the grouping of red and green points. Red and green points represent Alexa 647 and Alexa 555 dyes respectively. **(B):** Multi-dimensional scaling plot of all available gene expression data grouped according to the times of sampling. Colours represent times of sampling; blue - 21dpi, green - 100dpi, red - 148dpi.

3.2.5 Identification of differential gene expression profiles in scrapie-infected mouse spleen during clinical disease

The statistical microarray software package SAM was chosen to analyse the normalized microarray data. SAM identifies genes with statistically significant changes in expression by assimilating a set of gene specific t tests. SAM assigns each gene a modified *t* statistic (SAM score) based on its change in gene expression relative to the standard deviation (SD) of repeated measurements of that gene, which is why the microarray experiments were performed using biological replicates. The SAM scores are then collected and genes with scores greater than a user-determined threshold, the δ-value, are defined as been significant within the cut-off. The percentage of these genes identified as significant by chance is the false discovery rate (FDR). The FDR is estimated by collectively analysing permutations of the measurements for each gene. The user, to include smaller or larger sets of genes, can adjust the δ-value threshold and the FDR is recalculated accordingly.

Array data was filtered before analysis to remove genes with more than 10% missing data and those data that had intensity values below background threshold levels. This left 11,507 genes included in the analysis. A t-test analysis was performed using the SAM software to determine the differential gene expression profiles in scrapie-infected spleen from mice showing clinical symptoms of disease. The analysis was performed assuming that each array in the data set is equivalent and determines significant differences for the scrapie-infected mice (ME7 and 79A) in relation to the age-matched, mock-infected mice (PBS). The δ-value was set to have a resulting FDR of <10%. If a lower FDR was selected then the number of genes found to be significant would also change, but the list *order* remains the same, leaving only genes near the top of

the list as significant. Conversely, if the FDR is increased, the number of significant genes increases, but the number of false positives also increases (see **Table 8** for the number of significant genes selected for different δ values). An FDR close to 10% was chosen in this case because it gave the highest confidence that differentially expressed genes are not being excluded by excessive stringency, but also maintains the statistical significance in the data with a minimal number of false positives. In this case 100 genes were selected; 31 of the genes were up-regulated and the remaining 69 were down-regulated (**Figure 18**). Those genes that had fold changes of 1.4 or more when comparing age matched control mouse gene expression to infected mice are listed in **Table 9 and 10** (27 showing increased expression and 48 decreased expression).

We also performed multiple SAM two-class analysis of random groups of 4 microarrays within each class of arrays analysed (i.e. within the same time point). It was hypothesised that these random groupings would contain no genes that show significant gene expression, and is away to test the efficacy of the arrays and analysis. In each case we found less than 3 genes predicted as significant between the two groups; a representative two-class SAM plot is shown in **Figure 19**. This gives confidence that the technical variation among our arrays is small and the genes predicted to be significant by SAM are likely to have biological significance.

A number of highly up-regulated genes belonged to ribosomal RNAs and not to protein coding genes. Ribosomal RNAs are not expected to be present on the cDNA array due to the poly(A) labelling protocol which should exclude all non-polyadenylated (ie. non-mRNA) transcripts. However, recent evident shows that ribosomal RNAs can

Table 8: The effect of changing SAM delta values on the number of genes selected as significant and the FDR. An FDR of 10% (used for our analysis) is highlighted in **bold**.

delta (δ) value	Number of False Positives (median)	Number of genes called significant	False Discovery Rate (median)
0.00000	12412.40	14272	0.87
0.00025	12354.91	14210	0.87
0.00099	12299.59	14156	0.87
0.00223	12274.33	14133	0.87
0.00396	12147.14	14011	0.87
0.00618	11915.86	13775	0.87
0.00890	11697.64	13564	0.86
0.01212	11264.68	13121	0.86
0.01583	10908.82	12773	0.85
0.02003	10601.31	12489	0.85
0.05564	7602.85	9561	0.80
0.08012	5565.26	7443	0.75
0.09891	4505.96	6345	0.71
0.10905	3941.03	5718	0.69
0.11968	3395.69	5070	0.67
0.13081	2769.78	4346	0.64
0.14243	2261.04	3711	0.61
0.16716	1406.02	2566	0.55
0.18026	1085.87	2098	0.52
0.19386	890.74	1812	0.49
0.20796	627.22	1357	0.46
0.22255	476.95	1096	0.44
0.23763	385.04	935	0.41
0.26928	245.23	677	0.36
0.28585	201.23	590	0.34
0.33852	127.62	447	0.29
0.35707	111.51	416	0.27
0.37611	91.91	380	0.24
0.43619	54.01	273	0.20
0.50073	24.39	163	0.15
0.61819	**10.45**	**100**	**0.10**
0.64316	8.28	88	0.09
0.66863	6.97	82	0.08
0.69460	5.23	74	0.07
0.72106	5.23	68	0.08
0.74801	4.36	64	0.07
0.77546	3.48	55	0.06
0.80340	2.61	51	0.05
0.83184	2.61	48	0.05
0.86077	1.74	42	0.04
0.89019	1.74	41	0.04
0.95053	0.87	28	0.03
0.98144	0.87	23	0.04
1.013+	0.00	<19	0.00

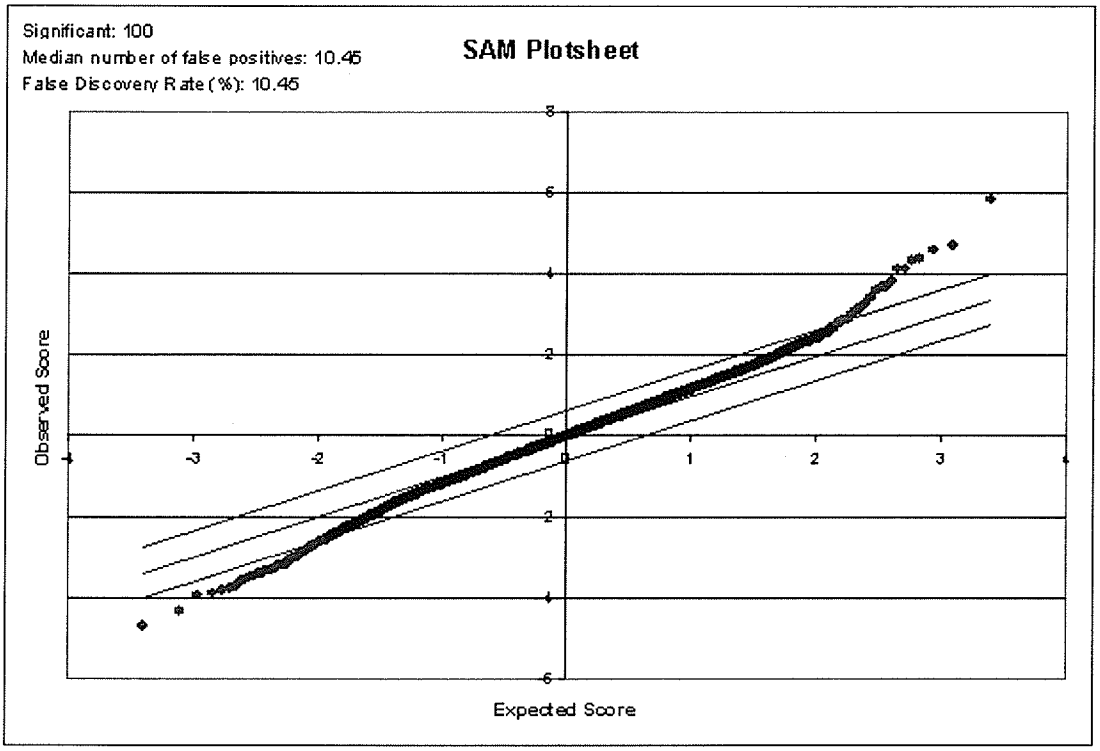

Figure 18: SAM plot of normalized microarray data obtained from 148dpi (endpoint) spleen arrays. One class test response showing differential gene expression of mice spleens infected with scrapie strain 79A and ME7. Red indicates genes that are up-regulated, green indicates genes that are down-regulated, while black indicates genes with no change.

Table 9: Complete list of genes up-regulated in spleen tissues during clinical scrapie

Accession Number	Gene Name	Description	GO Biological Function	SAM q-value	Fold Change
AI838717	RAB22A	RAB22A, member RAS oncogene family	Intracellular protein transport & small GTPase mediated signal transduction	0	2.50
AI846014	45S preRNA	Homology with *Mus musculus* 45s preRNA (by BLAST)	Ribosomal RNA precursor	0	2.46
AI841084	45S preRNA	Homology with *Mus musculus* 45s preRNA (by BLAST)	Ribosomal RNA precursor	0	2.29
AI843110	Unknown	EST	Unknown	0	2.0
AI449294	Unknown	EST	Unknown	0	1.85
AI846923	Foxd1	Forkhead box D1	Regulation of transcription & development	0	1.8
AI843077	Paqr8	Progestin and adipoQ receptor (by BLAST)	G-protein coupled signal transduction	0	1.68
AI837319	Tsc1	Tuberous sclerosis 1	Physiological process	0	1.7
AI843738	Smyd5	SET and MYND domain containing 5	Unknown function	0	1.78
AI844744	Rgs2	Regulator of G-protein signaling 2	Signalling	0	1.4
AI843740	Mtmr4	Myotubularin related protein 4	Protein and amino acid dephosphorylation	0	1.48
AI837652	Unknown	EST	Unknown function	2.0	1.5
AI837617	Unknown	EST	Unknown function	3.79	1.48
AI837049	Scamp1	Secreted membrane carrier protein 1	Protein transport & exocytosis	3.79	1.75
AI449359	Unknown	EST	Unknown function	3.79	1.43
AI851386	Unknown	EST	Unknown function	4.15	1.57
AI851523	Unknown	Similar to granulosa cell HMG-box protein-1	Unknown function	5.44	1.59
AI852426	Unknown	EST	Unknown function	5.44	1.6
AI844013	Cpd	Carboxypeptidase D	Proteolysis and peptidolysis	6.31	1.45
AI852380	Hspg2	Perlecan (heparan sulphate glycoprotein 2)	Cell adhesion & protein localization	6.34	2.80
AI854627	Unknown	EST	Unknown function	6.34	1.6
AI843131	Unknown	EST	Unknown function	6.34	1.47
AI844822	Atrx	Alpha thalassemia (homolog)	Transcriptional regulator & response to DNA damage	7.69	1.63
AI846647	Cpt1a	Carnitine palmitoyltransferase 1a	Lipid & fatty acid metabolism	7.69	1.43
AI839084	Unknown	EST	Unknown function	8.5	1.54
AI836470	Mtvr2	Mammary tumor virus receptor 2	Receptor activity	9.4	1.73

Table 10: Complete list of genes down-regulated in spleen tissues during clinical scrapie (148dpi).

Accession Number	Gene Name	Description	GO Biological Function	SAM q-value	Fold Change
AI429475	Xpo7	Exportin 7	Nucleocytoplasmic transport	0	-2.33
AI838815	Unknown	potassium channel tetramerisation domain containing 1	Unknown function	0	-1.57
AI852222	Tmcc2	Transmembrane and coiled-coil domains protein 2	Unknown function	0	-2.48
AI849600	Unknown	EST	Unknown function	0	-3.4
AI850079	Pib5pa	Phosphatidylinositol (4,5) bisphosphate 5-phosphatase	Inositol or phosphatidylinositol phosphatase activity	0	-1.61
AI844948	Unknown	EST	Unknown function	0	-1.47
AI844893	Plec1	Plectin 1	Cytoskeletal molecule	3.79	-1.55
AI449966	Unknown	EST	Unknown function	3.79	-1.51
AI844687	Ppp3cb	Protein phosphatase 3	Protein amino acid dephosphorylation	3.79	-1.57
AI845192	Prph1	Peripherin 1	intermediate filament & protein binding	3.79	1.47
AI836400	Max	Max protein	Regulation of transcription	3.79	-1.5
AI845325	Tex9	Testis expressed gene 9	muscle contraction	3.79	-1.5
AI844960	Unknown	EST	Unknown function	3.79	-1.44
AI843288	Unknown	EST	Unknown function	3.79	-1.43
AI449992	Unknown	EST	Unknown function	3.79	-1.5
AI848816	Gas1	Growth arrest specific 1	Cell cycle arrest protein	3.79	-1.43
AI849052	Sca1	Spinocerebellar ataxia 1 homolog (human)	Nuclear protein	3.79	-1.55
AI852996	Nrlh2	Nuclear receptor subfamily 1, group H, member 2	Regulation of transcription & cellular lipid metabolism	3.79	-1.63
AI838089	Ttc3	Tetratricopeptide repeat domain 3	Unknown function	3.79	-1.63
AI844703	Tm4sf17	Tetraspanin 17	Membrane spanning	3.79	-1.74
AI843911	Dsip1	TSC22 domain family 3	Regulation of transcription & anti-apoptosis	4.25	-1.59
AI850147	Ntng2	Netrin G2	Cell differentiation and development	4.25	-1.45
AI848258	Unknown	EST	Unknown function	4.25	-1.44
AI844927	0610042I15 Rik	RIKEN cDNA 0610042I15	Unknown function	5.44	-1.45
AI838253	Unknown	EST	Unknown function	5.44	-2.97
AI452348	Rnf34	Similar to human ring finger protein 34	apoptosis	5.44	-1.49

AI448873	Unknown	EST	Unknown function	5.44	-1.46
AI848990	Caml	Calcium modulating ligand	Receptor recycling & epidermal growth factor receptor signalling pathway	5.44	1.41
AI850097	Nrbp2	Nuclear receptor binding protein 2	Receptor activity	6.34	-1.43
AI845238	RIKEN cDNA 1700030G06 gene	Probable S-adenosylmethionine synthetase	Synthetase	6.8	-1.4
AI845078	Cdc42se1	CDC42 small effector 1	Negative regulation of JNK cascade & small GTPase mediated signal transduction	6.8	-1.71
AI847691	Prkwnk1	Protein kinase, lysine deficient	Protein amino acid phosphorylation	6.8	-1.42
AI840292	Rnf128	Ring finger 128	Proteolysis and peptidolysis & negative regulation of cytokine biosynthesis	6.8	-1.45
AI845273	Asph	Aspartate-beta-hydroxylase	Hydrolase	6.8	-1.46
AI834803	Ptprn	protein tyrosine phosphatase, receptor type, N	Protein amino acid dephosphorylation	6.8	-1.41
AI839176	Glul	glutamate-ammonia ligase (glutamine synthase)	Glutamine biosynthesis	6.8	-1.47
AI839707	Dullard	Dullard homolog	Unknown function	7.69	-1.54
AI428434	Slc43a1	Solute carrier family 43, member 1	Amino acid transport	7.69	-2.06
AI447583	Unknown	EST	Unknown function	7.69	-2.24
AI845070	Unknown	Putative zinc finger protein	Unknown function	7.69	-1.43
AI450259	Phtf2	Putative homeodomain transcription factor 2	Nuclear protein	7.69	-1.49
AI849629	Nedd4	Neuronally expressed, developmentally down-regulated gene 4	Protein modification & ubiquitin cycle	7.69	-1.46
AI844137	Brca2	Breast cancer 2	Response to DNA damage & repair	7.69	-1.43
AI836229	Hbxap	Neurofilament triplet H protein	Nuclear protein	7.69	-1.41
AI854089	Unknown	EST	Unknown function	8.5	-1.55
AI849328	9130401M01Rik	RIKEN cDNA 9130401M01 gene	Unknown function	9.4	-1.57
AI839342	Xabl	XPA binding protein 1	Small GTPase mediated signal transduction	9.4	-1.41
AI848905	Scrt1	Scratch homolog 1, zinc finger protein 37	Regulation of transcription	10.45	-1.53

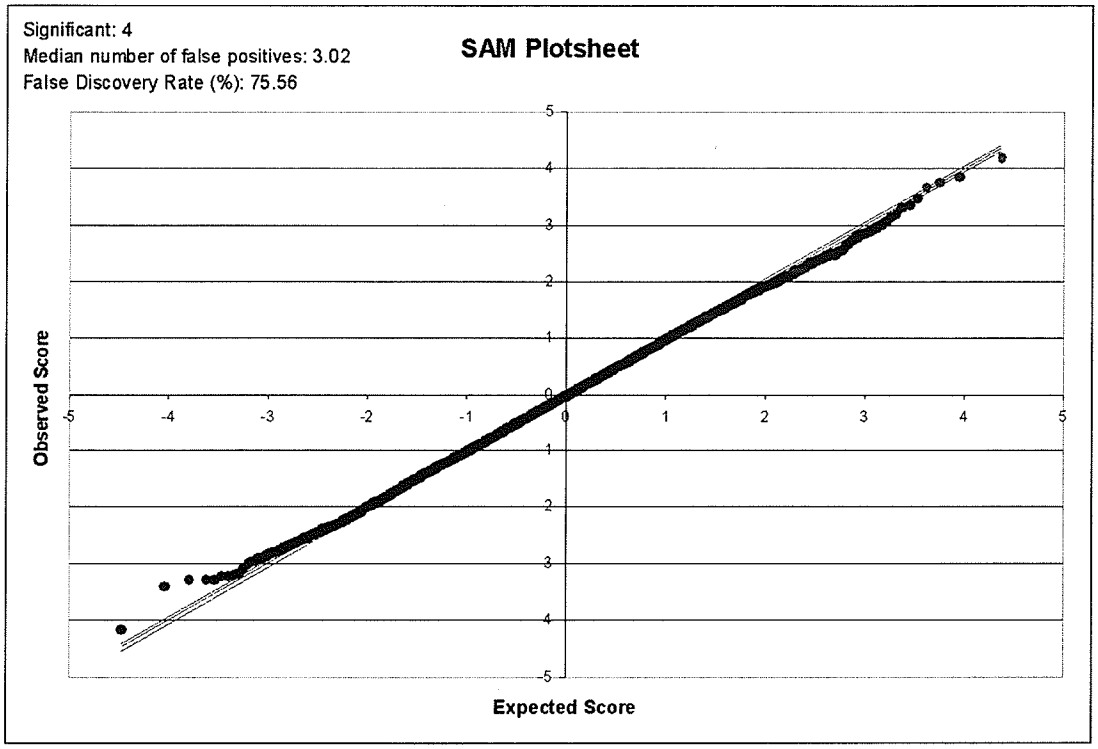

Figure 19: Two-class SAM analysis of random groups of microarrays (data obtained from 148dpi (endpoint) spleen arrays). Red indicates genes that are up-regulated, green indicates genes that are down-regulated, while black indicates genes with no change.

also be polyadenylated in many eukaryotes including the yeasts *Saccharomyces cervisiae* (Kuai et al., 2004) and *Candida albicans* (Fleischmann et al., 2004), the protozoan parasite *Leishmania* (Decuypere et al., 2005) and even humans (Slomovic et al, 2005). Although the evidence is circumstantial, it is entirely possible that polyadenylated rRNAs in the mouse transcriptisome are being reverse-transcribed into cDNA during the labelling process. The up-regulation of rRNAs during prion infection implies production of ribosomes, which would result in an increase in protein synthesis.

The up-regulated gene fold changes were found to range from 1.4x (Rgs2) to 2.80x (Hspg2), while the down-regulated gene fold changes ranged from –1.4x (RIKEN cDNA 1700030G06 gene) to –3.4 (EST). Of the total 27 genes found to have significant up-regulation, ten of these were unannotated ESTs. Five of the up-regulated genes were found to have fold changes greater than 2.0x including Hspg2 (↑2.80x), Rab22A (↑2.50x), two 45S preRNAs (↑2.46x, 2.29x) and an EST (AI843110; ↑2.46x). The remaining 22 up-regulated genes had fold changes lower than ↑2.0x.

The down-regulated gene list found 12 of the 42 genes to be ESTs with no known function. Six genes had fold changes greater than –2.0x including three ESTs (AI849600; ↓3.4x, AI838253; ↓2.97x, AI447583; ↓2.24x), Tmcc2 (↓2.48x), Xpo7 (↓2.33x) and Slc43a1 (↓2.06x). The remaining 36 genes had fold changes between -1.4x and -2.0x. Fold changes greater than 3.4x were not observed, while fold changes lower than 1.4x were excluded from the data analysis. These smaller gene fold changes (<1.4x) may be statistically significant, but would be difficult to validate using Northern analysis or quantiative real-time PCR (qRT-PCR).

Large fold changes were not expected for the spleen tissues during the scrapie disease course. Our observations of scrapie-infected mouse spleen by immunohistochemistry and histology showed a lack of tissue damage and no obvious pathological response (**Figure 5, 6, and 7**). Furthermore, passive replication (no obvious host response) of the scrapie agent in mouse spleen tissues has been a hallmark of prion infection for many years (Aucouturier and Carnaud, 2002). The largest factor, however, is that only small subsets of cells in the spleen are likely to be involved in prion pathogenesis and gene expression changes in this case would be masked by the much larger populations of non-affected cells. Thus it was expected that the gene expression changes in the spleen would be small and less numerous than the brain, but any genes found would be likely to have a direct involvement in scrapie pathogenesis.

3.2.6 EASE Functional analysis of genes differentially expressed in scrapie-infected mouse spleen during clinical disease

To further explore the functional groups of genes differentially expressed in scrapie-infected mouse spleen the EASE (Expression Analysis Systematic Explorer) software was used to examine the potential relationship between the biological functions of the genes and their expression patterns (Hosack et al., 2003).

EASE calculated EASE scores (Jacknife one-sided Fisher exact p-values) to identify over-represented gene categories with in the lists of genes. The Gene Ontology™ Consortium (GO) (http:/www.geneontology.org, Dragici et al, 2003) has defined the gene categories used for this analysis into groups called ontologies. A gene ontology is a structured, controlled vocabulary used to describe gene products in terms of their biological process, cellular component and molecular function. The structure of the

ontology allows a researcher to examine all the genes involved in a particular global process, or narrow the list down to a few specific classes of genes. The functional grouping of genes into ontologies allows insight into types of responses in the spleen to the scrapie agent. The selection criterion for differentially expressed genes was relaxed in this case to produce a more substantial list by reducing false negatives. An FDR of 20% gave 273 differentially expressed genes. The major biological processes in which the selected (and annotated) genes are involved are shown in **Table 11**.

The greatest numbers of genes were categorized into the functional categories of development and extracellular space, with 23 and 27 "list hits" (LH) respectively. List hits refer to the number of genes from the selected genes that fall into the biological category in question. Eleven genes were categorized into the functional category of DNA metabolism. The categories for prenyltransferase activity, one-carbon compound metabolism, and the regulation of mitotic cell cycle had the lowest numbers of list hits. Interestingly, pathogenesis and response to endogenous stimulus were two functional categories that occurred with some frequency. These groupings potentially represent the initial classification of scrapie-agent response genes in the spleen.

The significant genelist was further investigated using the software "Pathway Assist v3.0 (Ariadne Genomics)" which determines relationships between gene products based on databases (ResNet) built from common phrases extracted from Medline, for example, "protein A regulates protein B". ResNet contains over 500 000 functional links for more than 50 000 proteins, extracted from more than 5 000 000 Medline abstracts and

Table 11: EASE analysis of differentially expressed gene lists for clinical scrapie infected mice spleens for over-representation of functional categories using EASE.

Functional Category	LH	LT	PH	PT	Ease Score (p-value)
regulation of mitotic cell cycle	3	119	6	4764	8.55E-03
pathogenesis	4	119	21	4764	1.42E-02
DNA repair	6	119	65	4764	2.17E-02
DNA metabolism	11	119	202	4764	2.72E-02
one-carbon compound metabolism	3	119	11	4764	2.89E-02
response to endogenous stimulus	6	119	74	4764	3.56E-02
prenyltransferase activity	3	121	13	4976	3.78E-02
transferase activity, transferring alkyl or aryl (other than methyl) groups	4	121	32	4976	4.08E-02
phosphoric monoester hydrolase activity	7	121	107	4976	4.36E-02
extracellular matrix	7	114	114	4715	5.48E-02
protein amino acid dephosphorylation	5	119	60	4764	6.04E-02
dephosphorylation	5	119	61	4764	6.34E-02
extracellular space	27	114	820	4715	7.44E-02
development	23	119	658	4764	8.37E-02
mitotic cell cycle	7	119	128	4764	9.67E-02

LH – list hits, LT – list total, PH – population hits, PT- list total

full-length articles. PathwayAssist allows the visualization and exploration of biological pathways, gene regulation networks and protein-protein interactions.

A molecular network illustrating the direct interactions between some of the 100 genes selected is shown in **Figure 20**. Genes highlighted in green were down regulated in scrapie infected mouse-spleen are highlighted in green and those that were up regulated highlighted in blue.

At the centre of the network of molecular interactions is Col1A1 (procollagen, type I), which indirectly interacts with numerous proteins including the highly up-regulated Hspg2 (↑2.80x) and the cell cycle arrest protein Gas1 (↓1.43x), which indirectly interacted with the transcriptional regulator Max (↓1.5x). Col1A1 also interacted with BrcA2 (breast cancer 2), which had interactions with Tsc1 (↑2.80x) through Cdc2 (cell division cycle 2).

One cytokine was found to have direct interactions with four different down-regulated genes, including Prph (peripherin), Asl (adenylosuccinate lyase), Glul (glutamate-ammonia ligase) and Ikbke (inhibitor of kappaB kinase epsilon). The up-regulated Scamp1 (↑1.75x) was found to indirectly interact with Glul.

One of the key genes pinpointed by this method codes for the protein perlecan (heparan sulphate glycoprotein 2). This was found to be our most up-regulated gene by microarray analysis with an average of 2.8 fold increases indicated at the clinical stage of infection. Perlecan is implicated in many biological processes, including most significantly, amyloid production in amyloidogenic diseases such as Alzheimer's disease. As yet it has not been described in relation to prion diseases but given the similarity of the diseases in terms of deposition of amyloid it would not be surprising that this gene is

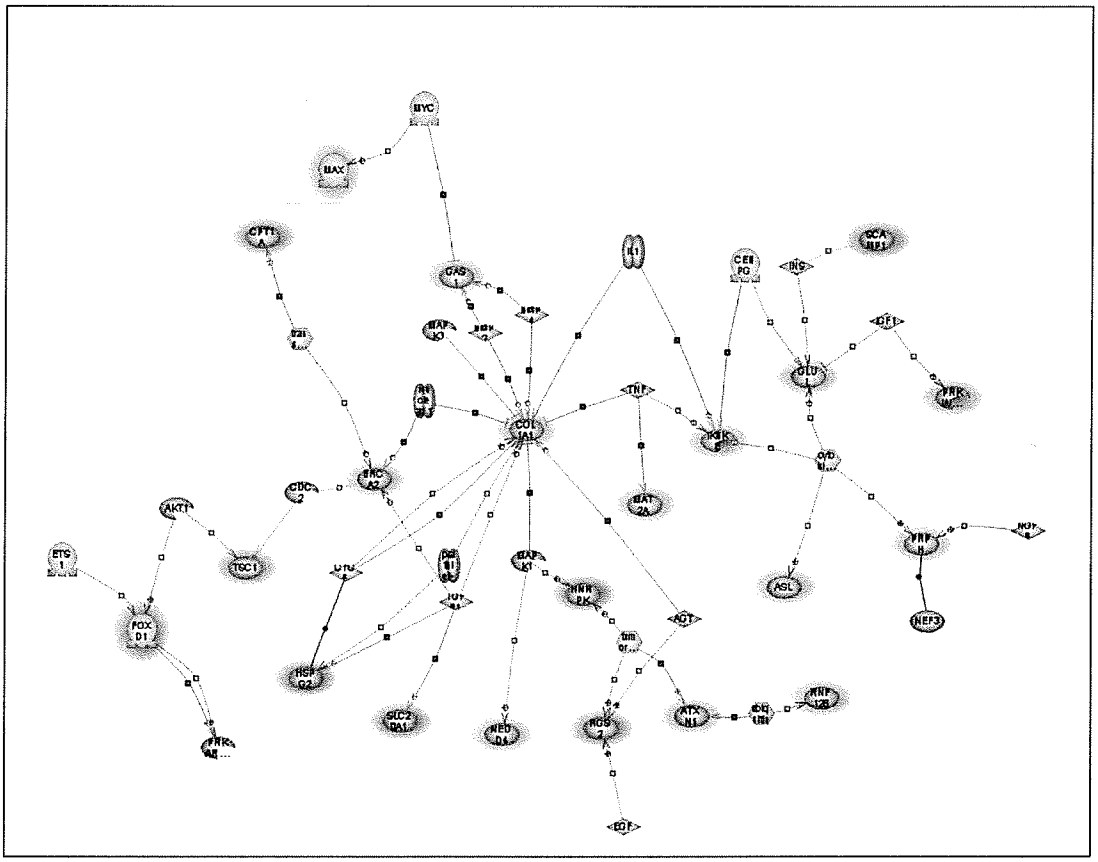

Figure 20: Molecular network generated by PathwayAssist showing the direct interactions between some of the 100 genes found to be differentially regulated in scrapie infected mouse spleen. Down-regulated genes are highlighted in green and up-regulated genes are highlighted in blue.

implicated in prion disease. A diagram showing the molecular interactions specifically associated with perlecan are shown in **Figure 21**.

Perlecan (Hspg2) interacts indirectly with two other up-regulated genes, Rgs2 which is a regulator of G-protein signalling, and Tsc1 (Tuberous sclerosis 1) to promote proliferation, differentiation, and maturation. Hspg2 and Tsc1 also have direct interactions with a growth factor activator, which is strong evidence strongly suggesting an increase in cell growth and division, possibly as a direct response to the infectious prion agent.

Perlecan is a basement membrane heparan sulphate proteoglycan with two or three heparan sulfphate molecules located in the N-terminal end of the molecule (Noonan et al., 2001). Glycosaminoglycans and in particular, heparan sulphate, are associated with prion disease pathology and metabolism proteins (Diaz_Nido et al., 2002). It has been shown in tissue culture that chronic cellular prion infections involve heparan sulphates in the continual formation of scrapie prion protein (PrP^{Sc}). More recently it has been demonstrated experimentally that heparan sulphate molecules are an essential component of prion protein binding at the cell surface and subsequent internalization (Horonchik et al., 2005). The up-regulation of a heparan sulphate proteoglycan, such as perlecan, in the spleens of clinical prion infected mice is especially noteworthy.

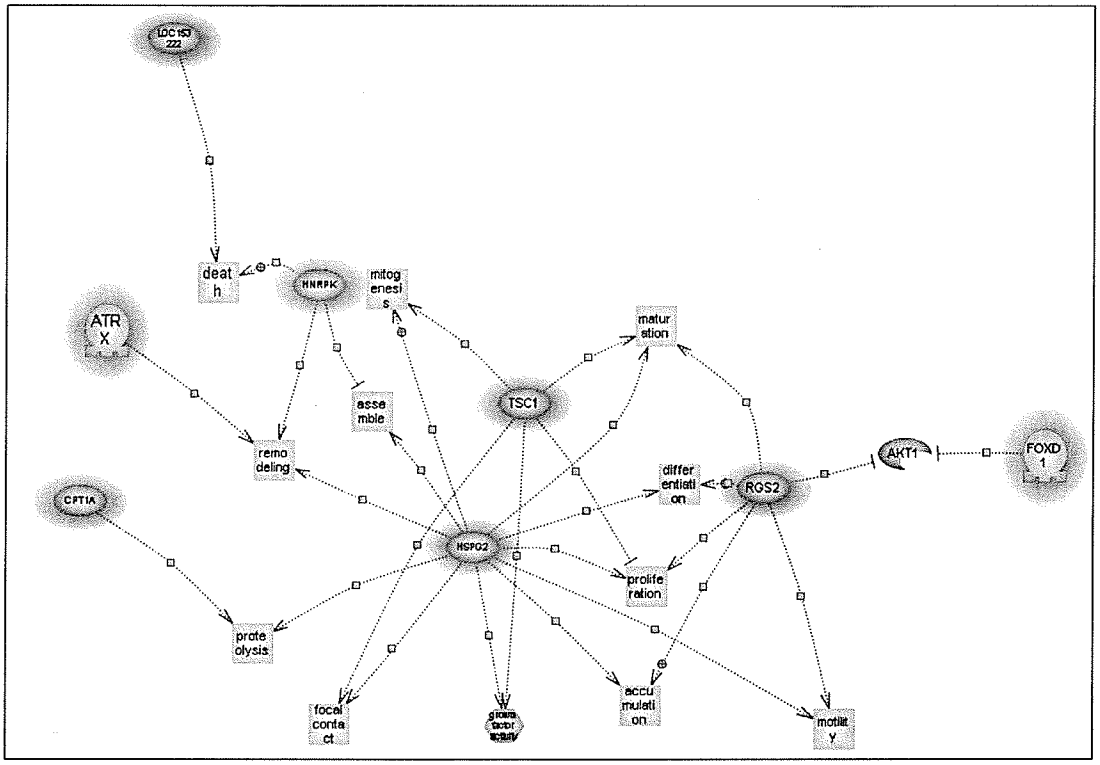

Figure 21: Molecular interactions specifically associated with perlecan (Hspg2) generated by PathwayAssist. Up-regulated genes are highlighted in blue.

3.2.7 Identification of differential gene expression profiles in scrapie-infected mouse spleen during pre-clinical disease

Microarrays were performed on RNA extracted from spleens from scrapie infected and mock-infected mice at 21 days post infection, prior to the appearance of PrP^{Sc} in the spleen, and at 100 days pos infection. A one-class SAM analysis of eight normalized arrays generated a plot that represented the gene expression profile (ME7 and 79A combined) for mouse spleen tissue at the 21dpi time point (**Figure 22A**). A total of 143 genes were selected as showing differential expression (FDR <10%) at the early time point, with only 1 of the genes up regulated and 142 down regulated (**Table 12**). A one-class SAM analysis was performed in the same fashion for the 100dpi time point, where no significant (FDR <10%) differential gene expression was discovered (**Figure 22B**). Analysis of the biological processes in which these genes are involved using the EASE program showed that the major groups of genes regulated at this stage of infection include immune function genes, response to biotic stimuli, cytokines, extracellular proteins and protein binding (**Table 13**).

3.3 Validation of microarray results

3.3.1 Confirmation of microarray spot IDs

The construction and management of data sets from large arrays, such as the ones used for these experiments, is a challenging task. A microarray slide is spotted with a large array of cDNA molecules or synthesized oligonucleotides in a specified order that is crucial for retrieving data from any experiments using the slides. The order of the printed

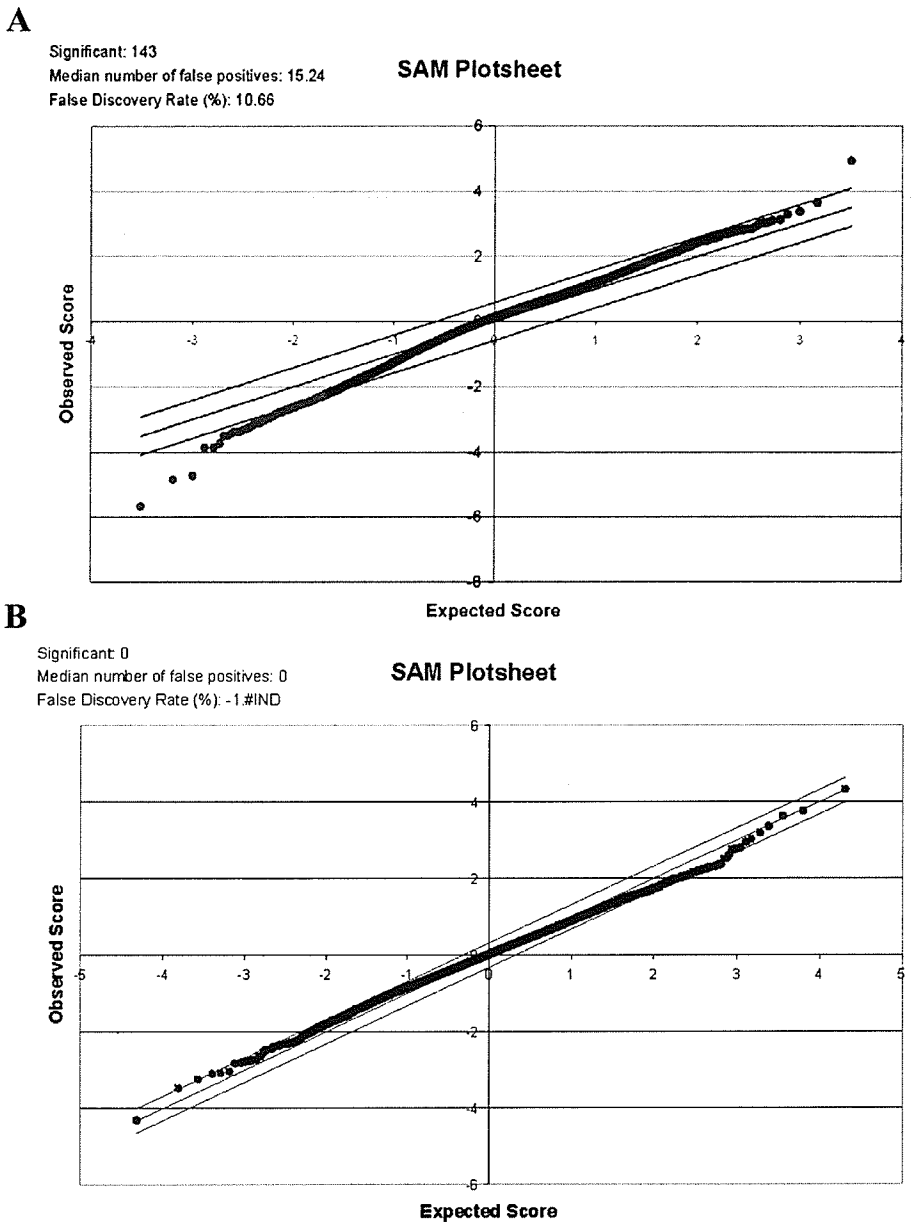

Figure 22: SAM plots of normalized microarray data obtained from 21dpi and 100dpi arrays. (A) One class test showing differential gene expression of mouse spleens infected with scrapie strain 79A or ME7 at 21dpi. (B) One class test response showing differential gene expression of mice spleens infected with scrapie strain 79A or ME7 at 100dpi. Red indicates genes that are up-regulated, green indicates genes that are down-regulated, while black indicates genes with no change.

Table 12: Complete list of functional genes found to be differentially expressed by microarray analysis in spleen tissues at the early time point (21dpi).

Accession Number	Gene Name	Description	Probable function	SAM q-value	Fold change
AI843896	Abl2	Tyrosine-protein kinase (related to human)	Tyrosine-protein kinase	0	3.1
AI324948	Slpi	Secretory leukocyte protease inhibitor	Endopeptidase inhibitor activity	0	-3.5
AI843944	Igh-4	Homologue to immunoglobulin heavy chain	Antibacterial humoral response	0	-3.55
AI324046	Igh-6	Homologue to immunoglobulin heavy chain	Antibacterial humoral response	0	-3.03
AI851769	EST	Expressed sequence tag	Unknown	0	-1.53
AI844421	Timp2	Tissue inhibitor of metalloproteinase 2	Metalloendopeptidase inhibitor activity	0	-1.51
AI840680	Pigs	Phosphatidylinositol glycan, class S	Endoplasmic reticulum, integral to membrane	0	-1.68
AI846398	Ifitm3	Interferon induced transmembrane protein 3	Negative regulation of proliferation	0	-1.68
AI849451	Tegt	Testis enhanced gene transcript	Apoptosis, endoplasmic reticulum	0	-1.65
AI841384	Ube2v1	Ubiquitin-conjugating enzyme E2 variant 1	Ubiquitin conjugating enzyme activity	0	-1.42
AI324646	Hmga1	high mobility group AT-hook 1	DNA binding, DNA packaging, chromatin	0	-1.77
AI842053	Lgals3bp	Lectin, galactoside-binding, soluble, 3 binding protein	Isomerase activity	0	-1.53
AI854794	Tenc1	Tensin like C1 domain-containing phosphatase	Potential tumor suppressor, phosphoinositide 3-phosphatase	0	-1.83
AI850047	Timp2	Tissue inhibitor of metalloproteinase 2	Metalloendopeptidase inhibitor activity	0	-1.53
AI528534	Eif4ebp2	Eukaryotic translation initiation factor 4E binding protein 2	cAMP-mediated signaling	5.06	-1.83
AI847886	Dpp3	Dipeptidylpeptidase 3	Aminopeptidase activity	5.06	-1.59
AI448908	Clic4	Chloride intracellular channel 4 (mitochondrial)	Chloride channel activity, chloride transport	5.06	-1.60
AI323873	Slc3a2	Solute carrier family 3	Alpha-amylase activity	5.06	-1.56
AI844529	Eif4ebp2	Eukaryotic translation initiation factor 4E binding protein 2	cAMP-mediated signaling	5.06	-1.45
AI448688	Slitl2	Slit-like 2	Platelet adhesion to blood vessels.	5.06	-1.64
AI450811	Unknown	Expressed sequence tag	Unknown function	5.06	-1.78

AI841464	Ptms	Parathymosin (Zinc-binding 11.5 kDa protein)	Immune response gene	5.06	-1.58
AI849649	Gpx3	Glutathione peroxidase 3	Lutathione peroxidase activity, response to oxidative stress	5.06	-1.54
AI846605	Grn	Granulin	Granulins have possible cytokine-like activity	5.06	-1.51
AI836908	Hmga1	High mobility group AT-hook 1	DNA binding, DNA packaging, chromatin	5.06	-1.76
AI844160	Tegt	Testis enhanced gene transcript	Apoptosis, endoplasmic reticulum	5.06	-1.57
AI426952	Zfp467	Zinc finger protein 467	DNA binding	5.06	-1.53
AI413641	Unknown	Expressed sequence tag	Unknown function	5.38	-1.55
AI841591	Minpp1	Multiple inositol polyphosphate histidine phosphatase 1	Acid phosphatase activity	5.38	-1.56
AI840232	Sparc	Secreted acidic cysteine rich glycoprotein	Calcium ion binding	5.38	-1.63
AI848443	Tnip1	TNFAIP3 interacting protein 1	Nef-associated factor 1	7.59	-1.42
AI841104	Shank3	SH3/ankyrin domain gene 3	MAPKKK cascade	7.59	-1.55
AI426775	Timp2	Tissue inhibitor of metalloproteinase 2	Metalloendopeptidase inhibitor activity	7.59	-1.72
AI849859	Fhl1	Four and a half LIM domains 1	Cell differentiation, cell growth	7.59	-1.50
AI426128	Tgfbr3	Similar to Ornithine decarboxylase (ODC)	Receptor activity	7.59	-1.49
AI838115	EST	Expressed sequence tag	Unknown function	7.59	-1.72
AI847606	Jundm2	Jun dimerization protein 2	DNA binding	7.59	-1.51
AI838336	Psap	Prosaposin	Sphingolipid metabolism	7.59	-1.62
AI851959	Cxcl12	Chemokine (C-X-C motif) ligand 12	T-cell proliferation	7.59	-1.74
AI844703	Tm4sf17	Tetraspanin 17	Integral to membrane.	7.59	-1.54
AI840080	Psarl	Presenilin associated, rhomboid-like	Hydrolase activity	7.59	-1.58
AI847027	Ptger1	Prostaglandin E receptor 1 (subtype EP1)	G-protein coupled receptor activity	7.59	-1.42
AI851001	Igfbp5	Insulin-like growth factor binding protein 5	Insulin-like growth factor binding	7.59	-1.84
AI844251	Sult4a1	Sulfotransferase family 4A, member 1	Sulfotransferase activity	7.59	-1.6
AI842934	Dag1	Dystroglycan 1	Cytoskeleton, dystroglycan complex	7.59	-1.7
AI840059	Usp10	Ubiquitin specific protease 10	Cysteine-type endopeptidase activity	8.07	-1.42
AI849104	Tceb1	Transcription elongation factor B (SIII), polypeptide	Regulation of transcription	8.07	-1.45

AI847447	Fscn1	Fascin homolog 1, actin bundling protein	Actin binding, actin filament binding	8.07	-1.46
AI327031	Hkr3	GLI-Kruppel family member HKR3	DNA-dependent, transcription factor activity	8.07	-1.41
AI842974	Mef2d	myocyte enhancer factor 2D	Regulation of transcription	8.07	-1.57
AI834914	Sepw1	Selenoprotein W	Selenium binding	8.07	-1.41
AI837587	Unknown	Expressed sequence tag	Unknown function	8.07	-1.72
AI451071	Prkar2b	Protein kinase, cAMP dependent regulatory	cAMP-dependent protein kinase complex	8.07	-1.65
AI851898	Ncstn	Nicastrin	Protein processing	8.07	-1.52
AI853301	Polr2a	Polymerase (RNA) II (DNA directed) polypeptide A	DNA binding	8.07	-1.92
AI843646	Rab11b	RAB11B, member RAS oncogene family	Protein transport; small GTPase mediated signal transduction	8.07	-1.45
AI448985	Unknown	Expressed sequence tag	Unknown function	8.07	-1.78
AI853284	Jemm2	Malignant mesothelioma-associated antigen	Unknown function	8.07	-1.46
AI849627	Unknown	Expressed sequence tag	Unknown function	8.07	-1.44
AI427475	Nav1	Neuron navigator 1	ATP binding, microtubule bundle formation	8.07	-2.04
AI847977	Psmd10	Proteosome (prosome, macropain) 26S subunit	DNA-dependent, transcription factor activity	8.07	-1.45
AI464509	Ifitm1	Interferon induced transmembrane protein 1	Response to biotic stimulus	8.07	-1.46
AI852824	Unknown	Expressed sequence tag	Unknown function	9.56	-3.41
AI448568	Unknown	Expressed sequence tag	Unknown function	9.56	-1.52
AI428436	Eef2k	Eukaryotic elongation factor-2 kinase	Protein amino acid phosphorylation	9.56	-1.44
AI841689	Cklfsf3	Chemokine-like factor super family 3	chemotaxis	9.56	-1.41
AI325229	Ucp2	Uncoupling protein 2 (mitochondrial, proton carrier)	Mitochondrial transport	9.56	-1.58
AI428010	Zbtb7b	T helper-inducing POZ/Krueppel factor	Cell differentiation; regulation of transcription	9.56	-1.48
AI850554	Dazap2	DAZ associated protein 2	Protein binding	9.56	-1.61
AI841117	Rapgef1	Rap guanine nucleotide exchange factor (GEF) 1	Cell-cell adhesion; platelet derived growth factor receptor signalling pathway	9.56	-1.52

AI854197	Bai2	G protein-coupled receptor brain-specific angiogenesis inhibitor 1	Peripheral nervous system development	9.56	-1.51
AI324158	Zbtb7a	POK erythroid myeloid ontogenic factor	Negative regulation of transcription	9.56	-1.7
AI849557	Unknown	Expressed sequence tag	Unknown function	9.56	-1.57
AI853821	Unknown	Expressed sequence tag	Unknown function	9.56	-1.43
AI848876	Fcer1g	Fc receptor, IgE, high affinity I, gamma polypeptide	Defense response; signal transduction; positive regulation of immune response and phogocytosis	9.56	-1.48
AI839014	Dlgap1	discs, large (Drosophila) homolog-associated protein 1	Cell-cell signalling; Synaptic transmission	9.56	-1.46
AI427746	Tex2	testis expressed gene 2	Unknown	9.56	-1.47
AI848817	Tnfsf9	tumor necrosis factor (ligand) superfamily, member 9	Immune response	9.56	-1.50
AI842613	Lnk	linker of T-cell receptor pathways	Cell differentiation; hemopoiesis	9.56	-1.51
AI452369	Nptxr	neuronal pentraxin receptor	Metal and calcium ion binding; receptor activity	9.56	-1.44
AI836234	Stmn4	stathmin-like 4	Intracellular signalling cascade	9.56	-1.57

Table 13: EASE analysis of differentially expressed gene lists for scrapie infected mouse spleens 21 days post infection for over-representation of functional categories.

Gene Category	List Hits	List Total	Population Hits	Population Total	EASE score
immune response	7	57	136	4764	4.87E-03
response to external stimuli	8	57	184	4764	5.34E-03
cytokine activity	4	60	48	4976	1.88E-02
organogenesis	10	57	367	4764	2.58E-02
extracellular space	16	55	820	4715	3.81E-02
signal transduction	14	57	801	4764	1.35E-01
cell adhesion	5	57	194	4764	1.93E-01
cell communication	16	57	1020	4764	2.02E-01

spots is maintained on large spreadsheet files that contain information such as the spot position, gene name, and accession number. The libraries from which are our arrays are constructed are known to contain errors introduced during manipulation of the library and also due to incomplete sequencing. Errors are estimated to occur at a frequency of approximately 4-5% of the clones. Ideally, therefore, the whole library should be re-sequenced prior to spotting. This is however time-consuming and expensive. The approach taken by our laboratory is to systematically sequence clones representing spots representing the genes found to be significant in a given experiment. Therefore spot sequencing was performed on the genes selected as interesting from the scrapie infected spleens.

The clones representing the twenty-two up-regulated ESTs in clinical scrapie were selected from the libraries and grown in LB broth for plasmid isolation. Plasmids were isolated from the bacteria at an average concentration of 200ng/µl and stored at -20°C until required. Each clone was subject to a restriction digest using EcoRI and NotI to free the insert from the vector and confirm the appropriate insert size (**Figure 23A**). However, two clones required a repeat digest, done in duplicate (**Figure 23B**) due to unexpected results.

Purified plasmids were prepared and used for sequence analysis. The resulting sequence alignments verified the identity of the majority of the clones (**Table 14**). However, despite repeats in triplicate, three clones did not sequence and no data could be obtained. A further twenty of the negatively regulated spots were plasmid isolated and sequenced, with eighteen of the spots being confirmed (data not shown). The sequencing data confirmed the accession numbers of the twenty most up and down-regulated genes.

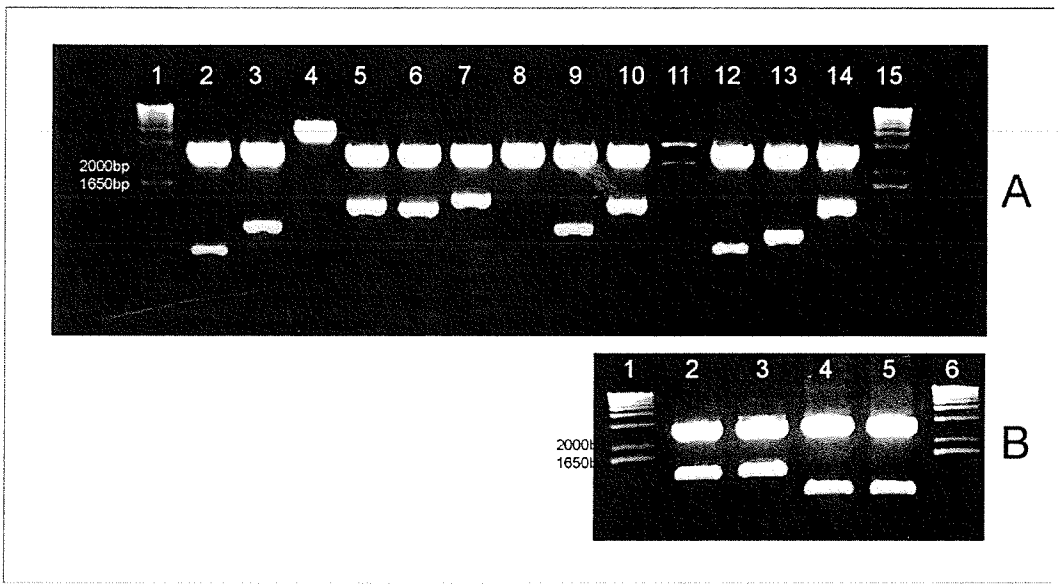

Figure 23: Plasmid digests, using EcoRI and Not I, of clones selected for spot validation. (A) Lane 1 and 15; 1kb-plus DNA ladder (Invitrogen). Lanes 2 – 14; P1-P13. (B) Lane 1 and 6; 1kb-plus DNA ladder (Invitrogen). Lanes 2 – 5; P3(×2) and P10(×2) repeats (see also **Table 14**).

Table 14: Sequence verification of twenty-two up-regulated genes determined by SAM analysis of clinical 79A and ME7 microarray data.

Plasmid Clone	Accession Number	Gene Name	Sequencing Status
P1	AI846014	45S preRNA	sequence verified
P2	AI841084	45S preRNA	sequence verified
P3	AI843110	EST	sequence verified
P4	AI843077	Paqr8	sequence verified
P5	AI837319	Tsc1	sequence verified
P6	AI843738	Smyd5	sequence verified
P7	AI851523	EST	sequence verified
P8	AI852426	EST	sequence verified
P9	AI837652	EST	sequence verified
P10	AI846647	Cpt1a	sequence verified
P11	AI851386	EST	sequence verified
P12	AI844744	Rgs2	sequence verified
P13	AI837617	EST	sequence verified
P14	AI844013	Cpd	sequence verified
P15	AI843131	EST	sequence verified
P16	AI848458	Srp19	sequence verified
P17	AI839203	EST	sequence unusable
P18	AI835930	45S preRNA	sequence unusable
P19	AI854421	Cpne6	sequence verified
P20	AI835752	EST	sequence unusable
P21	AI844822	Atrx	sequence verified
P22	AI843128	EST	sequence verified

3.3.2 Validation of genes found to be up-regulated in clinical scrapie spleen

The use of alternative methodologies in experimental validation of gene-expression levels obtained through microarray analysis is critical in confirming microarray data due to the inherent variation associated with this technology. Commonly used techniques to validate microarray data include semi-quantitative RT-PCR, real-time RT-PCR and Northern blots (Chuaqui et al., 2002).

Ten genes were selected for validation from the clinical up-regulated gene list and ten primer sets were developed to be used for initial screening using semi-quantitative RT-PCR (sqRT-PCR). This method was chosen to validate this work because it was specific, rapid, and easily implemented. Furthermore, semi-quantitative RT-PCR has previously been shown to be useful in validating microarray data (Marone et al., 2001; Ricciarelli et al., 2004).

Five of the ten primer sets were selected for optimization because discrete bands were initially obtained and required minimal optimization. Primers were optimized using gradient based PCR cycles and starting concentrations of 50ng/µl of uninfected spleen cDNA. Once a discrete band was obtained, the PCR reactions were purified and sent to the NML DNA Core for sequencing. Sequenced products were aligned against their respective accession numbers, thus confirming the identity of the genes examined.

Once the primer specificity had being confirmed, sqRT-PCR was performed using cDNA generated from a pool of either four infected (ME7) mice spleens or four PBS control mice spleens. The concentrations of both cDNA samples was 50ng/µl. All five genes examined had similar patterns, where both the control and infected samples showed bands appearing simultaneously for each cycle (**Figure 24**). This data was

quantified using the pixel intensity of each band as a measure of relative expression levels. Semi-quantitative RT-PCR assumed that in two RNA samples (a control and experimental) with a gene showing expression levels differing by at least 1.5 times that this difference would be sufficient to be visualized on a gel if taken during the exponential phase of a PCR reaction. If the PCR reaction proceeded to completion (i.e. 30 or more PCR cycles), a plateau of PCR product would be reached and the method would not be useful in quantitating transcript levels because the bands on the gel would appear to be equal. The band intensity was the same for both control and experimental samples, suggesting that there was no differential between the genes examined in the control and infected samples.

There are two possible explanations for the lack of validation of the genes examined. The first is that the methodology was not sensitive enough to show differential expression using strictly gel-based, visual methods. The alternative explanation is that the genes are in fact, not up-regulated, and the sqRT-PCR is valid.

3.3.3 Comparison of gene expression profiles in spleen from mice clinically infected with two different strains of mouse adapted scrapie

Previous results from the Booth lab had determined strain specific differences in gene expression in the brains of mice infected with 79A and ME7, likely related to the differences in pathology between the strains. Deposition of PrP^{Sc} in the spleen, however, occurs in similar pattern in each of these strains and so in this instance it was hypothesised that no differences in gene expression in the spleen between the two strains would be seen. In order to test this a two-class unpaired SAM analysis of clinical spleens

was performed and this showed no significant differences in the gene expression profiles between the two scrapie strains (**Figure 25**).

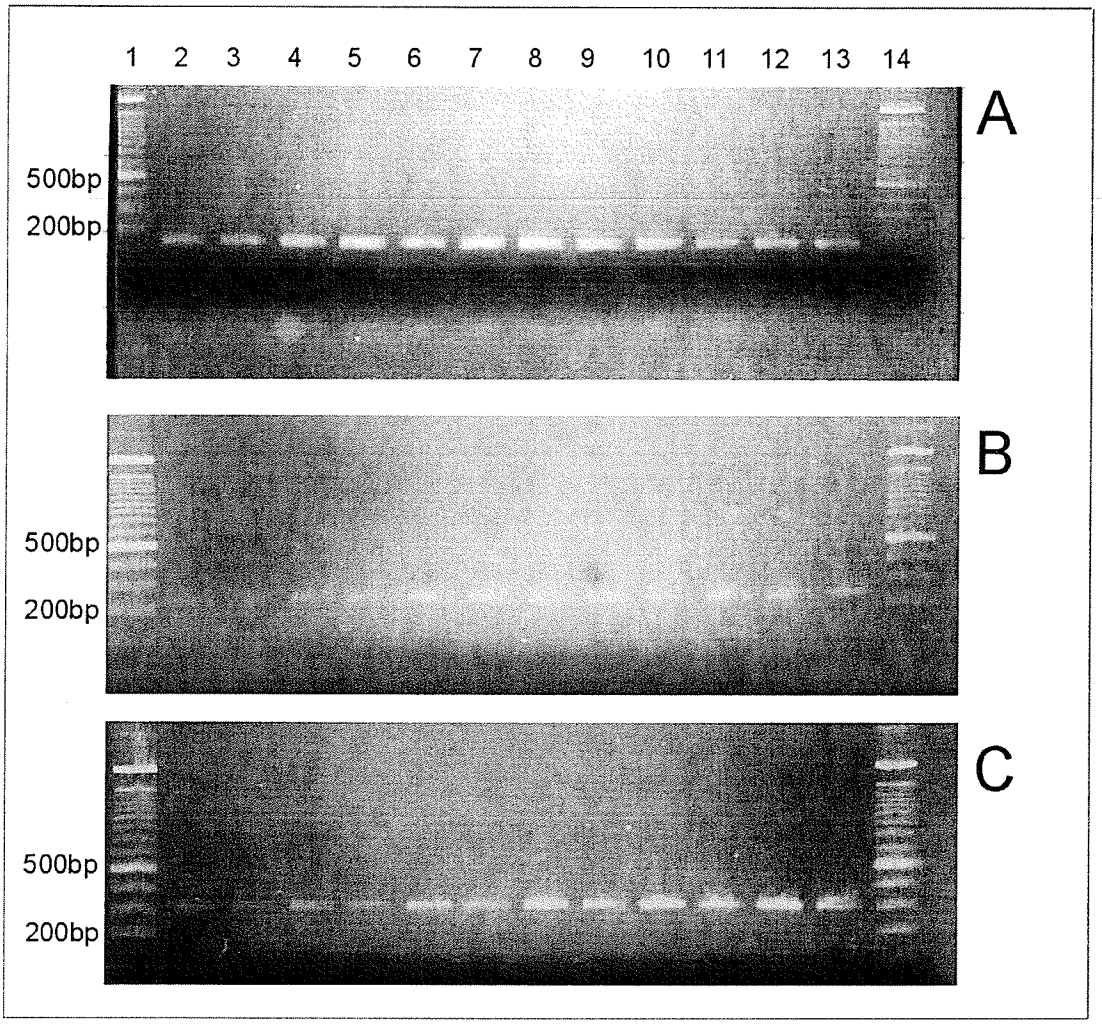

Figure 24: Examples of semi-quantitative RT-PCR gels. Lanes 1 and 14; 100bp DNA ladder (Invitrogen), Lanes 2, 4, 6, 7, 8, 10, and 12; control cDNA, Lanes 3, 5, 7, 9, 11, 13; ME7 cDNA; (A) 45S RNA sampled at 25, 26, 27, 28, 29 and 30 cycles. (B) Unknown1 sampled at 25, 26, 27, 28, 29 and 30 cycles. (C) Cpd sampled at, 25, 26, 27, 28, 29, and 30 cycles.

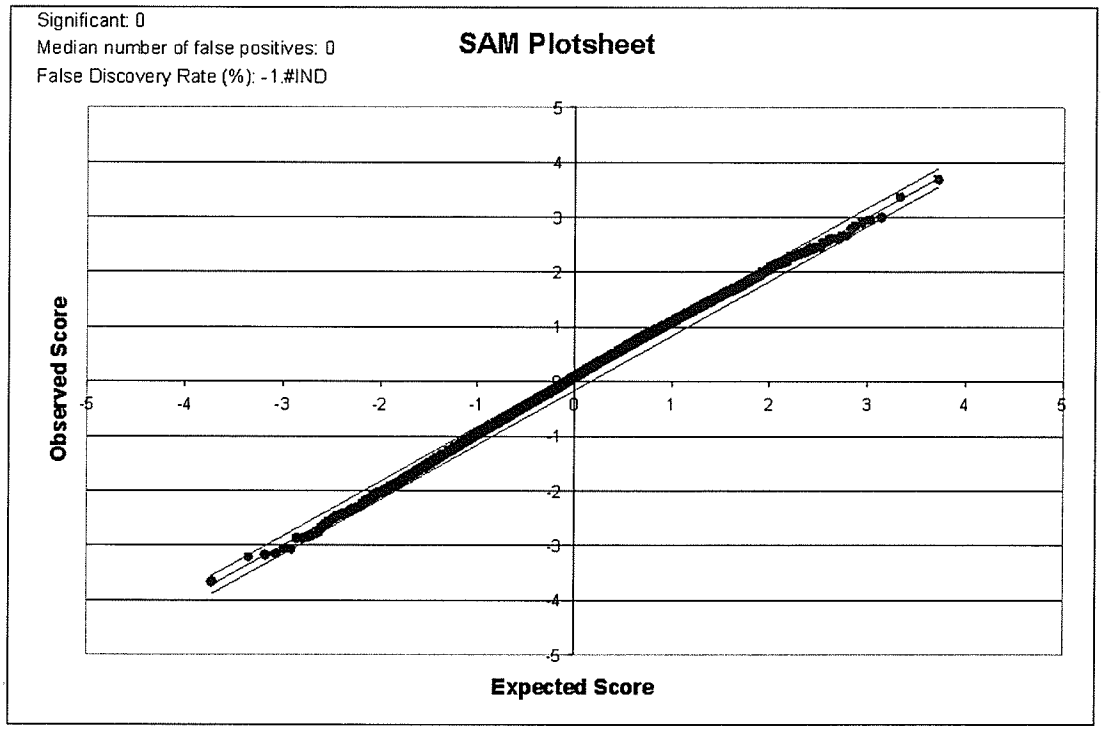

Figure 25: Two-class SAM analysis of ME7 versus 79A. SAM plot of normalized microarray data obtained from 148dpi (endpoint) spleen arrays. Red indicates genes that are up-regulated, green indicates genes that are down-regulated, while black indicates genes with no change.

Discussion

In a scrapie mouse model, we hypothesize that there will be fewer differentially expressed genes found by microarray analysis in the spleen during scrapie infection when compared to the brain due to the neurological nature of the prion disease. These differentially expressed genes are more likely to reflect a direct response to the prion agent due to the lack of extensive tissue damage within the tissues. This thesis represents a novel study of the global transcriptional response in mouse spleen to prion infection over time. The spleen was selected as an ideal candidate tissue for pre-clinical marker screening and also for exploring the molecular mechanisms of prion pathogenesis by global gene expression analysis for two major reasons:

Firstly, the spleen plays an important role in prion pathogenesis as a site of prion replication and as a reservoir of infectivity. Prion infection is associated with splenic but not to any great extent with circulating blood lymphocytes in scrapie infected animals (Raeber et al., 1999). Many spleen-associated cells have been implicated in prion pathogenesis, from replicating the infectious agent to transporting the infectivity to clearing PrP^{Sc} deposits. Macrophages play a role in clearing infectivity (Beringue et al. 2000), mature follicular dendritic cells support PrP^{Sc} replication (Brown et al. 1999, Montrasio et al. 2000, Mabbott et al. 2000a; 2000b), B-cells provide the appropriate signals to mature FDCs (Klein et al. 1997), and bone-marrow derived dendritic cells (DCs) may be involved in transporting infectivity (Huang et al., 2002; Rosicarelli et al., 2005).

Secondly, the spleen accumulates PrP^{Sc} deposits in the absense of a strong antibody mediated or inflammatory response. The gene expression changes in clinical

scrapie infected brain that may be a direct response to the prion agent are difficult to distinguish from the gross generalized response to tissue damage within the brain (Booth et al., 2000a). The spleen does not show extensive tissue damage during prion infection, which may allow the identification of a smaller number of genes more closely associated with a prion specific response and prion replication.

We measured gene expression changes in prion infected mouse spleen at three time points during the course of infection. The first was at 21 days post infection; a very early stage in infection when PrP^{Sc} deposits are not detectable in spleen tissues via immunohistochemistry using α-PrP^{Sc} antibodies (**Figure 7A, 7D**). Literature reports indicate infectivity is readily detectable in the spleen within two weeks of an intraperitoneal inoculation (Bruce, 1985; Büeler et al., 1993; Race and Ernst, 1992; Rubenstein et al., 1991), but PrP^{Sc} is only detectable in spleen tissues at 70 dpi after an intracerebral inoculation in mouse models (Inoue et al., 2005). The 21dpi time point was consequently intended as a control, since PrP^{Sc} accumulation would be extremely low at this time, however the mice would have had time to recover from the initial inoculation procedure. The Booth group has previously shown that mouse brain shows no differential gene expression by microarray analysis after an intracerebral inoculation using healthy mouse brain homogenate vs. PBS control (2004a) at 21 days post inoculation.

Surprisingly, the spleen showed some significant differential gene expression early in prion infection. Although the possibility existed that the gene expression changes were a direct response to PrP^{Sc}, this is unlikely due to a lack of immunohistochemical evidence of PrP^{Sc} accumulation (**Figure 7A, 7D**). In addition

none of the gene expression changes seen at this time were evident during later stages of prion infection when PrP^{Sc} was clearly evident in the spleen.

In clinical prion disease the mouse brain is undergoing neurodegeneration and there is a marked increase in the production of toxins, necrotic and apoptotic signals (Liberski et al. 2004). A diluted sample of clinical scrapie-infected mouse brain homogenate is typically used as the initial inoculum in prion disease research, and this approach was also used for this study. After an intracerebral inoculation the initial inoculum is thought to be removed by the spleen (Millson et al., 1979). The spleen and associated immune cells may have a reaction to the brain homogenate because of the presence of toxins and foreign antigens, such as cytokines, caspases, and endonculeases. Due to the immunological nature of the spleen, it would be difficult to tease out responses generated to the prion infection directly, as opposed to a more generalized response to the diseased brain inoculum.

PrP^{Sc} was readily detectable at the pre-clinical (100dpi) stage by immunohistochemistry, but there was a clear absence of tissue damage or pathology (**Figure 5B, Figure 6B**). Despite the evidence of PrP^{Sc} deposition, there were no significant gene expression changes from the intial early time point, which was unexpected. Studies on acute-phase responses in scrapie-infected mouse spleen have shown that the deposition of PrP^{Sc} is not proinflammatory and does not activate innate immunological pathways (Cunningham et al., 2005). Similarly, there was no activation of immune-associated genes at the pre-clinical time point in this study. These observations are unusual because the spleen and spleen-associated cells have been reported to have an active role replicating the prion agent and promoting neuroinvasion.

It is interesting to speculate how the prion agent might replicate within the spleen tissues without inducing an immune response and without any significant cellular response in the form of differential gene expression. The answer to this perplexing question of passive replication may lie with the follicular dendritic cells found within the spleen tissues.

Follicular dendritic cells (FDCs) are immune-associated cells thought to be important in the development of immunological memory (van Nierop and de Groot, 2002). These cells are strongly associated with primary follicle and B-cell secondary centres of lymphoid tissues where they sequester and present native antigens in the form of immune complexes to potential memory cells (Kosco-Vilbois, 2003; Monstrasio et al, 2000; van Nierop and de Groot, 2002). In mouse scrapie it is the FDCs that appear to have a critical role in creating a reservoir of PrP^{Sc} infection (Kitamoto et al., 1991) and increasing the effectiveness of neuroinvasion (Brown et al., 1999; 2000; Glatzel et al, 2001; Jeffrey et al., 2000; Mabbott et al., 2000a; 2000b; Mohan et al, 2004; Montrasio et al, 2000). Recent work has shown the physical proximity of FDCs to the sympathetic nerves in the spleen can affect the velocity of PrP^{Sc} transmission to the central nervous system (Prinz et al; 2003).

FDCs are ideal sites for prion replication in lymphoid tissues because they are long lived cells that express high levels of PrP^{C} (McBride et al., 1992) and are specialized to sequester and present unprocessed antigens (van Nierop and de Groot, 2002). The infectious PrP^{Sc} agent can be concentrated at the lymphoid follicles on FDCs (Ritchie et al., 1998), in the presence of an abundance of unchanged PrP^{C} 'template'. Once this template has been completely transformed into the infectious isoform a plateau of

infectivity is reached. It would appear from the lack of differential gene expression changes in the pre-clinical (100dpi) scrapie-infected mouse spleen that the prion can convert the PrP^{C} on the surface of the FDCs to the PrP^{Sc} isomer passively and without inducing a detectable host response. The passive conversion of PrP^{C} to PrP^{Sc} would be consistent with the protein-protein interactions expected from the protein only hypothesis.

The genes differentially expressed at the pre-clinical time point may be isolated to a few different cell types or even a limited subpopulation of a particular cell type. Transcripts differentially expressed in particular subpopulations of cells (i.e. FDCs) may be diluted by the sum of the gene expression in the entire organ. It is possible that the gene expression changes in response to the prion infection would be undetectable unless the cells with differential expression could be isolated.

Significant gene expression changes were found at the clinical time point in scrapie-infected spleen tissues, which was coupled with strong accumulation of PrP^{Sc} (**Figure 7C, 7F**) in an absense of obvious pathology (**Figure 5C, Figure 5C**). Thus, the gene expression profiles obtained for the clinical spleen may best represent a direct host response to prion infection. Alternatively, the gene expression changes may represent a general response to the neuropathology that was simultaneously occurring in the brain during the clinical disease state. In this case, the genes found to be differentially regulated at the clinical stage could thus be indirect markers of prion infection.

A number of genes were found to be up-regulated in mouse spleen during clinical prion disease, many of which are ESTs. Using the EASE software these genes were grouped into a number of functional categories, which included development, DNA

metabolism, and pathogenesis (**Table 11**). The online resource BLASTn (Altschul *et al.* 1990) was used to identify sequences related to the unknown ESTs and to retrieve any gene information therein (**Table 9**).

The most frequently up-regulated gene retrieved through BLASTn was the 45S preRNA gene, which was independently discovered two times. The 45S preRNA is the ribosomal rRNA precursor and is processed to produce the 18S, 5.8S, and 28S rRNAs. Finding this gene as being up-regulated during prion diseases would suggest an increase in ribosome production, due to the increase in ribosomal RNAs (rRNA). This would suggest that the spleen was more actively synthesizing a plethora of different proteins. This increase in protein production marks a generalized response to the prion infection.

Two genes *Tsc1* and *Rgs2* were found to be involved in signalling pathways. The first, tuberous sclerosis 1, or hamartin, is one of a pair of proteins (the other being *Tsc2* or tuberin) which make up the tuberous sclerosis complex (van Slegtenhorst et al. 1997). Combined, these gene products form a tumour suppressor complex involved in negatively controlling cell growth and proliferation (Hengstschlager et al. 2001, van Slegtenhorst et al. 1998; Yamamoto et al. 2002). The up regulation of a tumour response gene during clinical prion disease suggests that the pathology of the PrP^{Sc} may be more akin to cancers, than to bacteria or viral infections.

The second signalling gene, *Rgs2* is a regulator of G-protein signalling (RGS) involved in extracellular signalling pathways. G-protein linked receptors make up the largest known family of cell surface receptors, so the up-regulation of *Rgs2* is another general host response. RGS proteins act as α-subunit-specific GTPase activating proteins (GAPs) and are thought to play a role in shutting down G-protein mediated responses in

eukaryotes. Thus, even though this gene was up-regulated in the spleen at the clinical time point, its effect is a negative one.

The most highly up-regulated gene found differentially expressed was *Hspg2* or Perlecan, a heparan sulphate proteoglycan previously found to be associated with neurodegenerative disorders, but not yet reported in association with prion diseases. This finding is especially significant due to the recent discovery that heparan sulphate molecules are a mediator of PrP^{Sc} binding and internalization in tissue culture. How up regulation of this gene is achieved by the prion infection has yet to be determined.

Genes classically thought to be indirectly involved in prion pathogenesis in the spleen, such as the tumour necrosis factor (TNF) and lymphotoxins (LTs) α and β (Kitamoto et al., 1991; Brown et al., 1999; Prinz et al., 2003), were not found to be up-regulated. These genes are required for prion pathogenesis in the spleen tissues because they are produced by B-cells and mature FDCs. The results do not indicate that the prion infection induces or changes the transcript levels of either TNF or the LTα or LTβ. This evidence further supports that prions have a passive, non-inducing replication mechanism in spleen tissues.

Many pathological organisms produce proteins or chemicals which reduce or suppress the host immune response during infection. However, there is no conspicuous immune response to the prion agent, with no antibody production (Kasper et al., 1982) or conspicuous proinflammatory response (Cunningham et al., 2005). Similarly, at the clinical disease stage in spleen, there was no down regulation of transcripts coding for inflammatory cytokines, immunoglobulin subunits or other immune system components.

The lack of down-regulation of expected immune response genes supports the notion that prions can replication in the spleen without inducing a host immune response.

Gene expression analysis of scrapie infected mouse brains have yielded molecular profiles that were able to distinguish different prion strains (Booth et al., 2004b). These strain-discriminating profiles are a likely result of the different strain-induced neuropathologies occurring in the brain during clinical prion disease. Different neuropathologies may be a direct result the capacity of PrP^{Sc} to recognize and target specific neuronal populations (Bruce, 2003, Wadsworth et al., 1999). It has been suggested that degree and diversity of glycosylation of PrP may have a role in selectively targeting specific cell populations in the brain (Rudd et al., 2002). If different neurons are targeted differently in each prion strain, it may account for the differences in strain specific gene expression profiles obtained by the Booth group (Booth et al., 2004b).

The gene expression profiles obtained for clinical scrapie-infected mouse spleen do not indicate any strain specific gene expression changes. In scrapie infected mouse spleen, FDCs have been shown to be a major site of PrP^{Sc} accumulation (Brown et al., 1999; Ritchie et al., 1998). These cells represent a homogenous population for prion targeting, while prion-targeted brain cells are more diverse. It is possible that the prion agent targeting a single cell type results in gene expression profiles that are not strain discriminating. Regardless, the lack of strain specific gene changes at the clinical time point strengthens the hypothesis that the genes changing in the spleen are in response to the prion infection, as opposed to a generalized response to tissue damage.

The most useful gene expression profiles for pre-clinical diagnosis of scrapie infection would be obtained from the early and pre-clinical time points. However, the early gene expression changes in scrapie-infected spleen were unexpected and are difficult to distinguish from a gross generalized response to the initial inoculum. Profiles obtained from mice inoculated via an intraperitoneal or oral route may be more representative of a 'natural' route of prion infection. However, these methods have inconsistent incubation periods and are not as reliable for ensuring an appropriate and consistent infectious dose (I.D.) is delivered to the mouse. Microarray experiments and analysis requires high consistency and reproducibility between experiments to generate statistically significant results (Booth et al., 2004a). Although pre-clinical markers would present the most useful tools in prion diagnosis, the pre-clinical gene expression profiles obtained here would not be useful for diagnostics due to the lack of differential gene expression.

Clinical expression profiles are likely the most representative of a host response to prion infection and thus present the most useful subset of candidate marker genes. Genes such as the 45S preRNA gene, *Rgs2* and *Tsc1* are common and would normally be expressed at high levels, as such the potential of the genes to be detectable in small samples of blood is reasonable. Alternatively, genes showing a high level of differential expression such as *Hspg2*(up) or *Xpo7*(down) could be useful markers due to siginficant difference between infected and uninfected samples. The use of ESTs as diagnostic tools is also possible as the function of the gene does not have to be known or defined in order to use the gene as a marker of prion infeciton. Thus, it is not unreasonable to suggest that a handful of the genes found up-regulated in the clinical scrapie infected mouse spleen

could be adapted as blood based markers of prion infection using sensitive methodologies such as qRT-PCR.

Summary and Conclusions

In a scrapie mouse model, we hypothesized that there will be fewer differentially expressed genes found by microarray analysis in the spleen during scrapie infection when compared to the brain due to the neurological nature of the prion disease. We expected differential gene expression profiles to parallel the accumulation of PrP^{Sc} deposits at the pre-clinical (100dpi) and clinical (148dpi) time points. These differentially expressed genes are more likely to reflect a direct response to the prion agent due to the lack of extensive tissue damage within the tissues.

The prion agent, PrP^{Sc} accumulates in the spleen tissues prior to any other tissues (Inoue et al., 2005) and in the absence of any pathology (Aucouturier and Carnaud, 2002). This makes the spleen an ideal candidate tissue for the exploration of gene expression profiles which may be useful in prion diagnostics. Using microarraying technologies, the gene expression profiles for two prion strains, ME7 and 79A, were obtained for three time points.

The 21dpi time point was chosen as a control, since detectable PrP^{Sc} accumulation has not been reported until after 70dpi in mouse models (Inoue et al., 2005). We hypothesized that there would be no reaction to the scrapie agent at the 21dpi time point due to the lack of PrP^{Sc} deposits. The differentially expressed genes found here most likely represented reaction to the necrotic and apoptotic components of the scrapie inoculum, but not necessarily to the scrapie agent. The 100dpi time point was chosen because pathogical changes are evident in the brain tissues, but no clinical symptoms are present. Furthermore, the spleen shows detectable PrP^{Sc} accumulation by immunohistochemistry (**Figure 7**). The cells most likely to be involved are likely poorly

represented in the whole spleen, and thus may account for the limited differential gene expression obtained here. The 148dpi time point was chosen because it is the clinical stage of the prion disease using the strains selected, and the differential expression changes this stage may have represented the spleen reacting to the neurodegeneration occurring in the brain tissues.

Taken together, the gene expression profiles indicated that there is a general, but not strain-specific, response to PrP^{Sc} in the spleen during clinical prion disease. Whether this response is due to the accumulation of the PrP^{Sc} or an indirect measure of the effects of neurodegeneration on the brain remains to be elucidated.

Future Directions

Global analysis of spleen tissues offered insight into pathological mechanisms of prion diseases in peripheral tissues. However, it is likely that some of the genes found to be differentially regulated may be shrouded or diluted by other cells not intimately involved in prion diseases, such as structural cells. Ideally the cells thought to be intimately involved in prion pathogenesis in the spleen could be isolated and profiled for differential gene expression. Such cells could include follicular dendritic cells, bone-marrow derived dendritic cells, and macrophages, as these cells have been reported to either transport or support prion replication directly. Isolating these cells during a prion infection would remove the 'shrouding effect' of the other cells in the spleen that are not directly involved in prion pathogenesis. Methodologies such as laser-capture microdissection or fluorescent cell sorting would be ideal tools to separate these cells from the spleen tissues. Linear mRNA amplification strategies, such as the Eberwine method, would allow the small quantity of available RNA to be amplified for use in microarraying (Baugh et al., 2001; Gomes et al., 2003; Zhao et al., 2002) (**Figure 26**).

Further investigation of the early and pre-clinical time points would potentially generate novel genetic markers of prion infection. At these time points PrP^{Sc} is thought to be replicating and initiating neuroinvasion, and thus cellular response (if any) to the agent would be greatest at these times. Profiling the spleen tissues of another animal model system would also validate the genes as markers of pre-clinical indicators of prion infection. The selection of a number of genes from spleen tissues involved in prion pathogenesis would further the development of a blood-based prion marker useful in the diagnosis of TSEs in agriculture and human health.

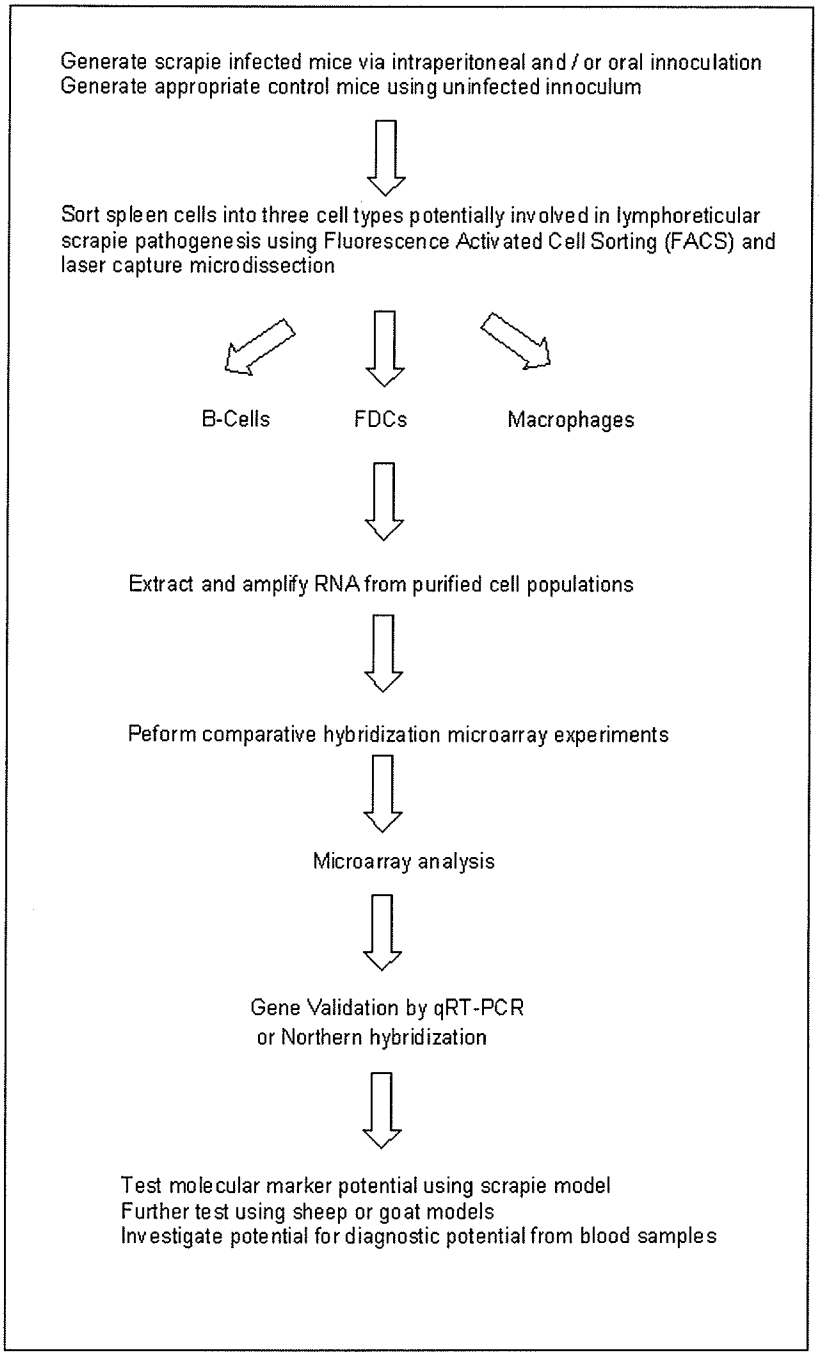

Figure 26: Future experimental procedures for development of scrapie-specific markers in the spleen and other lymphoreticular tissues based on results obtained.

Appendices

Appendix 1

Haematoxylin and Eosin Staining

1. Place slides to be stained in a slide rack, and leave them in the oven at 60°C for 30 minutes. This warms up the wax.

2. Remove slide rack from oven and place in two washes of xylene for 5 minutes each.

3. Take the slides to water: rinse successively in two washes of 100% EtOH, and one each of 90% EtOH and 70% EtOH. Then transfer into the bin in the sink with running water and rinse well.

4. Transfer from water to haematoxylin for 3 minutes, then rinse again in water. Empty during the wash to get rid of excess stain, then rinse some more.

5. Destain in 1% acid alcohol (around 30s) by dipping slides up and down, rinse again in water.

6. Rinse in STWS (Scott's Tap Water Substitute), rinse in water. Check a slide under the microscope to see if sufficient staining / destaining has occurred. Repeat if necessary.

7. Stain in eosin for 3 minutes, rinse in water and check again for sufficient staining.

8. Take back to xylene: rinse successively in one wash each 70% EtOH, 90% EtOH and two washes of 100% EtOH. Be sure no water gets into the 100% washes. Then rinse in two xylene baths, leaving the slides in the last one. If the slides do not rinse clear, take back to 100% EtOH and rinse, then go back to xylene. That should clean them up.

9. Polish coverslips that have been soaking in methanol with a clean cloth and lay them out.*Optional.

10. Place a drop of mounting medium on one edge of a coverslip. Remove a slide from xylene and dry the back partially with a kimwipe.

11. Place the edge of the slide on the side of the coverslip with the mounting medium, at an angle (~45°). Flatten the slide against the coverslip to seal it and dab the slide to remove any excess mounting medium. Allow the slides to dry at least overnight. If level 3 decontaminate before dunking out.

Appendix 2

Immunohistochemistry (α-PrP^{Sc})

1. Place slides to be stained in a slide rack, and leave them in the oven at 60°C for 30 minutes. This warms up the wax.

2. Remove slide rack from oven and place in two washes of xylene for 5 minutes each.

3. Take the slides to water: rinse successively in two washes of 100% EtOH, and one each of 90% EtOH and 70% EtOH. Then transfer into the bin in the sink with running water and rinse well.

4. Transfer slides to a 10-slot slide holder. Be sure to place the slides face to face before adding to the holder. Slot 10 should hold control and experimental samples to which no primary Ab will be added.

5. Rinse x6 in TBS-Tween Buffer (hereafter called 'Buffer'). To do this dip slides in buffer, then onto the paper toweling, then back into buffer. Repeat as many times as required, ensuring the buffer is being wicked up or down appropriately.

6. Transfer into 98% Formic acid for 10 minutes. To do this add formic acid to a slide box lid (the lids fresh slides come from work well) and dip the slides into the solution and leave them there for the duration required.

7. Rinse x6 in Buffer.

8. Transfer into 3% H2O2 for 5 minutes. Blot dry.

9. Transfer into 3% H2O2 (fresh) for 5 minutes.

10. Transfer slides to a slide rack and place in distilled water to rinse.

11. Submerge in a large metal canister with around in distilled water with the lid partially on. Autoclave for 10 minutes @ 121°C if using 6H4 as a primary Ab. Otherwise this step can be skipped. Let cool before handling.

12. Rinse x6 in Buffer.

13. Incubate with normal goat serum (1 drop in 10mL TBS buffer) at 45°C for 20 minutes.

14. Rinse x6 in Buffer.

15. Incubate overnight (18 hours) with primary Ab in fridge (4°C). Ab concentration is Ab specific, 6H4 is 1:1000. Make up 3mLs for 10 slots; dilute in TBS. Slot 10 (no

primary Ab) is incubated with 1x TBS. Slides are incubated with damp Kimwipes, to keep the slides from drying out. Moisten with TBS or water.

16. Rinse x6 in Buffer in the morning.

17. Incubate for 20 minutes at 45 with secondary AB (eg goat-anti-mouse) at 1:500 dilution. Make 200ul / slot used – typically 2-3mLs. Also think about preparing your Stept-ABC complex at this point. You'll need it in 30 minutes when you reach step #16.

18. Rinse x6 in Buffer.

19. Incubate for 20 minutes at 45°C with Stept-ABC complex (prepared 30 minutes in advance).

20. Rinse x6 in Buffer.

21. Incubate with DAB Substrated for ~3 minutes (until it turns a straw colour). This MUST have 3% H2O2 added. To check if its working properly add to Stept-ABC complex to see if you get a brown colour forming.

22. Rinse 6x in distilled water.

23. Transfer from water to haematoxylin for 3 minutes, then rinse again in water. Empty during the wash to get rid of excess stain, then rinse some more.

24. Destain in 1% acid alcohol (around 30s) by dipping slides up and down, rinse again in water.

25. Rinse in STWS (Scott's Tap Water Substitute), rinse in water. Check a slide under the microscope to see if sufficient staining / destaining has occurred. Repeat if necessary.

26. Take back to xylene: rinse successively in one wash each 70% EtOH, 90% EtOH and two washes of 100% EtOH. Be sure no water gets into the 100% washes. Then rinse in two xylene baths, leaving the slides in the last one. If the slides do not rinse clear, take back to 100% EtOH and rinse, then go back to xylene. That should clean them up.

27. Polish coverslips that have been soaking in methanol with a clean cloth and lay them out.*Optional.

28. Place a drop of mounting medium on one edge of a coverslip. Remove a slide from xylene and dry the back partially with a kimwipe.

29. Place the edge of the slide on the side of the coverslip with the mounting medium, at an angle (~45°). Flatten the slide against the coverslip to seal it and dab the slide to remove any excess mounting medium. Allow the slides to dry at least overnight. If level 3 decontaminate before dunking out.

Appendix 3

Buffer compositions

1. Prehybridzation buffer:

To make 250 ml prehybridization buffer:

62.5 ml 20X SSC
2.5 ml 10% SDS
2.5 g BSA
185 ml dH_20

Filter sterilize and store at 4°C until ready to use.

2. Low Stringency Wash Buffer (1X SSC and 0.2% SDS)

To make 1L low stringency wash buffer:

50 ml 20X SSC
20 ml 10% SDS
930 ml H_20

3. High Stringency Wash Buffer (0.1X SSC and 0.2% SDS)

To make 1L high stringency wash buffer:

5 ml 20X SSC
20 ml 10% SDS
975 ml H_20

4. 0.1X SSC

To make 1L 0.1X SSC:

5 ml 20X SSC
995 ml H_20

Appendix 4

First strand cDNA synthesis for RT-PCR

1. Use the SpeedVac and nuclease-free water to normalize 1-2μg RNA to 10μl final volume.
   a. Aliquot 2μg into thin-walled 0.5μl tubes
   b. Bring up to volume with water OR
   c. SpeedVac 5-10min to bring volume down to (or under) 10μl
   d. Check volumes with P10 and bring up to 10μ with water

2. Add 1μl oligo(dT) and 1μl 10mM dNTPs. Mix gently.

3. Incubate at 65°C for 5 min in PCR machine
   Ice for 1 min. Centrifuge to collect sample in bottom of tube

4. Add 4μl 5x first strand buffer, 2μl 0.1M DTT.
   Mix by centrifugation.
   Make master mix for multiple samples.

5. Incubate at 42°C for 50+ min.

6. Add 1μl Superscript (reverse transcriptase).
   Mix by flicking or brief centrifuge.

7. Incubate at 37°C for 20 min.

8. Heat to 70°C for 15 min to denature the enzyme. Cool to 4°C.

9. Centrifuge sample briefly and apply 1μl RNase H.

10. Incubate at 37 for 20 min.

11. Use the Microcon columns for PCR purification.
    a. Add 200μl to the 20μl RT rxn and 280μl to the column.
    b. Mix by pipette and apply to column.
    c. Spin 8 min at 12,000xg and discard flow through.
    d. Invert column into a fresh tube.
    e. Spin 3 min **at 1000 RPM**.
    f. Expect volumes to vary from 5μl to 50μl.

Final amounts (conc. by vol.) should be in the >1μg / 1 μg RNA used in the reaction.

Appendix 5
Semi-quantitative RT-PCR conditions

1. PCR Reaction Conditions

H_20	38.3µl
10X PCR Buffer (Invitrogen)	5µl
10mM dNTP Mix	4µl
50mM $MgCl_2$	1.5µl
40pmol Primer A	1µl
40pmol Primer B	1µl
Taq Polymerase (200u/µl)	0.5µl
cDNA	1µl [50ng / ul]

References

Aguzzi A. (2003) Prions and the immune system: a journey through gut, spleen, and nerves. *Adv Immunol.* **81:**123-71.

Aguzzi A, Heikenwalder M, Miele G. (2004) Progress and problems in the biology, diagnostics, and therapeutics of prion diseases. *J Clin Invest.* **114:**153-60.

Aguzzi A, Sigurdson CJ. (2004) Antiprion immunotherapy: to suppress or to stimulate? *Nat Rev Immunol.* **4:**725-36.

Alper T, Haig DA, Clarke MC. (1966) The exceptionally small size of the scrapie agent. *Biochem Biophys Res Commn.* **22:**278-84.

Altschul SF, Gish W, Miller W, Myers EW, Lipman DJ. (1990) Basic local alignment search tool. *J Mol Biol.* **215:**403-10.

Ambion Inc. (2005a) 177, Ambion Technical Bulletin: Isolation of total RNA from difficult tissues. [http://www.ambion.com/techlib/tb/tb_177.html]

Ambion Inc. (2005b) 11(4), TechNotes: The world's best DNase improved TURBO DNA-free™. [http://www.ambion.com/techlib/tn/114/10.html]

Anderson RM, Donnelly CA, Ferguson NM, Woolhouse ME, Watt CJ, Udy HJ, MaWhinney S, Dunstan SP, Southwood TR, Wilesmith JW, Ryan JB, Hoinville LJ, Hillerton JE, Austin AR, Wells GA. (1996) Transmission dynamics and epidemiology of BSE in British cattle. *Nature.* **382:**779-88.

Aucouturier P, Geissmann F, Damotte D, Saborio GP, Meeker HC, Kascsak R, Kascsak R, Carp RI, Wisniewski T. (2001) Infected splenic dendritic cells are sufficient for prion transmission to the CNS in mouse scrapie. *J Clin Invest.* **108:**703-8.

Aucouturier P, Carnaud C. (2002) The immune system and prion diseases: a relationship of complicity and blindness. *J Leukoc Biol.* **72:**1075-83.

Barron RM, Baybutt H, Tuzi NL, McCormack J, King D, Moore RC, Melton DW, Manson JC. (2005) Polymorphisms at codons 108 and 189 in murine PrP play distinct roles in the control of scrapie incubation time. *J Gen Virol.* **86:**859-68.

Baugh LR, Hill AA, Brown EL, Hunter CP. (2001) Quantitative analysis of mRNA amplification by in vitro transcription. *Nucleic Acids Res.* **29:**E29.

Beekes M, Baldauf E, Diringer H. (1996) Sequential appearance and accumulation of pathognomonic markers in the central nervous system of hamsters orally infected with scrapie. *J Gen Virol.* **77:**1925-34.

Beekes M., McBride PA, Baldauf E. (1998) Cerebral targeting indicates vagal spread of infection in hamsters fed with scrapie. *J Gen Virol.* **79:**601–7.

Bendheim PE, Brown HR, Rudelli RD, Scala LJ, Goller NL, Wen GY, Kascsak RJ, Cashman NR, Bolton DC. (1992) Nearly ubiquitous tissue distribution of the scrapie agent precursor protein. *Neurology* **42:**149-56.

Beringue V, Demoy M, Lasméza CI, Gouritin B, Weingarten C, Deslys JP, Andreux JP, Couvreur P, Dormont D. (2000) Role of spleen macrophages in the clearance of scrapie agent early in pathogenesis. *J Pathol.* **190:**495-502.

Bessen RA, Marsh RF. (1994) Distinct PrP properties suggest the molecular basis of strain variation in transmissible mink encephalopathy. *J Virol.* **68:**7859-68.

Bessen RA, Kocisko DA, Raymond GJ, Nandan S, Lansbury PT, Caughey B. (1995) Non-genetic propagation of strain-specific properties of scrapie prion protein. *Nature* **375:**698-700.

Blättler T, Brandner S, Raeber AJ, Klein MA, Voigtländer T, Weissmann C, Aguzzi A. (1997) PrP-expressing tissue required for transfer of scrapie infectivity from spleen to brain. *Nature* **389:**69–73.

Bolton DC, McKinley MP, Prusiner SB. (1982) Identification of a protein that purifies with the scrapie prion. *Science* **218:**1309-11.

Booth S, Bowman C, Baumgartner R, Sorensen G, Robertson C, Coulthart M, Phillipson C, Somorjai RL. (2004a) Identification of central nervous system genes involved in the host response to the scrapie agent during preclinical and clinical infection. *J Gen Virol.* **85:**3459-71.

Booth S, Bowman C, Baumgartner R, Dolenko B, Sorensen G, Robertson C, Coulthart M, Phillipson C, Somorjai R. (2004b) Molecular classification of scrapie strains in mice using gene expression profiling. *Biochem Biophys Res Commun.* **325:**1339-45.

Borchelt DR, Taraboulos A, Prusiner SB. (1992) Evidence for synthesis of scrapie prion proteins in the endocytic pathway. *J Biol Chem.* **267:**16188–99

Brown P. (1998) The clinical neurology and epidemiology of Creutzfeldt-Jakob disease, with special reference to iatrogenic cases. In: *Novel Infectious Agents and the Central Nervous System.* Chichester: Wiley; 2–23.

Brown KL, Stewart K, Ritchie DL, Mabbott NA, Williams A, Fraser H, Morrison WL, Bruce ME. (1999) Scrapie replication in lymphoid tissues depends on prion protein expressing follicular dendritic cells. *Nature Med.* **5:**1308-12

Brown KL, Stewart K, Ritchie DL, Fraser H, Morrison WL, Bruce ME. (2000) Follicular dendritic cells in scrapie pathogenesis. *Arch Virol.* **16:**13-21

Brown AR, Webb J, Rebus S, Williams A, Fazakerley JK. (2004) Identification of up-regulated genes by array analysis in scrapie-infected mouse brains. *Neuropathol Appl Neurobiol.* **30:**555-67.

Bruce, ME. (1985) Agent replication dynamics in a long incubation period model of mouse scrapie. *J Gen Virol.* **66:**2517-22.

Bruce ME, McBride PA, Farquhar CF. (1989) Precise targeting of the pathology of the sialoglycoprotein, PrP, and vacuolar degeneration in mouse scrapie. *Neurosci Lett.* **102:** 1–6

Bruce ME, McConnell I, Fraser H, Dickinson AG. (1991) The disease characteristics of different strains of scrapie in Sinc congenic mouse lines: implications for the nature of the agent and host control of pathogenesis. *J Gen Virol.* **72:**595-603.

Bruce M, Chree A, McConnell I, Foster J, Pearson G, Fraser H. (1994) Transmission of bovine spongiform encephalopathy and scrapie to mice: strain variation and the species barrier. *Philos Trans R Soc Lond B Biol Sci.* **343:**405-11.

Bruce ME. (2003) TSE strain variation. *Br Med Bull.* **66:**99-108.

Büeler H, Fischer M, Lang Y, Bluethmann H, Lipp HP, DeArmond SJ, Prusiner SB, Aguet M, Weissmann C. (1992) Normal development and behaviour of mice lacking the neuronal cell-surface PrP protein. *Nature.* **356:**577-82.

Büeler H, Aguzzi A, Sailer A, Greiner RA, Autenried P, Aguet M, Weissmann C. (1993) Mice devoid of PrP are resistant to scrapie. *Cell* **73:**1339-47.

Burkitt HG, Young B, Heath JW. (1993) *Wheaters' Functional Histology* Churchill Livingstone, New York, NY. 214-219.

Campbell CJ, Ghazal P. (2004) Molecular signatures for diagnosis of infection: application of microarray technology. *J Appl Microbiol.* **96:**18-23.

Caughey B, Raymond GJ. (1991) The scrapie-associated form of PrP is made from a cell surface precursor that is both protease- and phospholipase-sensitive. *J Biol Chem.* **266:** 18217–23.

Chesebro B, Race R, Wehrly K, Nishio J, Bloom M, Lechner D, Bergstrom S, Robbins K, Mayer L, Keith JM, Garon C, Haase A. (1985) Identification of scrapie prion protein-specific mRNA in scrapie-infected and uninfected brain. *Nature* **315:**331-3.

Chesebro, B. (2003) Introduction to the transmissible spongiform encephalopathies or prion diseases. *Br Med Bull.* **66:**1-20.

Chuaqui RF, Bonner RF, Best CJ, Gillespie JW, Flaig MJ, Hewitt SM, Phillips JL, Krizman DB, Tangrea MA, Ahram M, Linehan WM, Knezevic V, Emmert-Buck MR. (2002) Post-analysis follow-up and validation of microarray experiments. *Nat Genet.* **32 Suppl:**509-14.

Churchhill GA. (2002) Fundamentals of experimental design for cDNA microarrays. *Nat Genet.* **32 Suppl:**490-495

Clarke MC, Haig DA. (1971) Multiplication of scrapie agent in mouse spleen. *Res Vet Sci.* **12:**195-7.

Clarke MC, Kimberlin RH. (1984) Pathogenesis of mouse scrapie: distribution of agent in the pulp and stroma of infected spleens. *Vet Microbiol.* **9:**215–25.

Cole S, Kimberlin RH. (1985) Pathogenesis of mouse scrapie: dynamics of vacuolation in brain and spinal cord after intraperitoneal infection. *Neuropathol Appl Neurobiol.* **11:**213–27.

Collinge J, Sidle KC, Meads J, Ironside J, Hill AF. (1996) Molecular analysis of prion strain variation and the aetiology of 'new variant' CJD. *Nature* **383:**685-90.

Collinge J. (2001) Prion diseases of humans and animals: their causes and molecular basis. *Annu Rev Neurosci.* **24:**519-50.

Coustou V, Deleu C, Saupe S, Begueret J. (1997) The protein product of the het-s heterokaryon incompatibility gene of the fungus Podospora anserina behaves as a prion analog. *Proc Natl Acad Sci.* **94:**9773-8.

Cunningham C, Wilcockson DC, Boche D, Perry VH. (2005) Comparison of inflammatory and acute-phase responses in the brain and peripheral organs of the ME7 model of prion disease. *J Virol.* **79:**5174-84.

Dandoy-Dron F, Guillo F, Benboudjema L, Deslys JP, Lasmezas C, Dormont D, Tovey MG, Dron M. (1998) Gene expression in scrapie: Cloning of a new scrapie-responsive gene and the identification of increased levels of seven other mRNA transcripts. *J Biol Chem.* **273:**7691-7.

Daude, N. (2004) Prion diseases and the spleen. *Viral Immunol.* **17:**334-49.

DeArmond SJ, McKinley MP, Barry RA, Braunfeld MB, McColloch JR, Prusiner SB. (1985) Identification of prion amyloid filaments in scrapie-infected brain. *Cell* **41:**221-35.

Decuypere S, Vandesompele J, Yardley V, De Donckeri S, Laurent T, Rijal S, Llanos-Cuentas A, Chappuis F, Arevalo J, Dujardin JC. (2005) Differential polyadenylation of ribosomal RNA during post-transcriptional processing in Leishmania. *Parasitology.* **131(Pt 3):**321-9.

Defaweux V, Dorban G, Demonceau C, Piret J, Jolois O, Thellin O, Thielen C, Heinen E, Antoine N. (2005) Interfaces between dendritic cells, other immune cells, and nerve fibres in mouse Peyer's patches: Potential sites for neuroinvasion in prion diseases. *Microsc Res Tech.* **66:**1-9.

Derkatch IL, Bradley ME, Hong JY, Liebman SW. (2001) Prions affect the appearance of other prions: the story of [PIN(+)]. *Cell* **106:**171-82.

Diaz-Nido J, Wandosell F, Avila J. (2002) Glycosaminoglycans and beta-amyloid, prion and tau peptides in neurodegenerative diseases. *Peptides.* **23:**1323-32.

Dickinson AG, Fraser H. (1969) Genetical control of the concentration of ME7 scrapie agent in mouse spleen. *J Comp Pathol.* **79:**363-6.

Dickinson AG, Meikle VM. (1969) A comparison of some biological characteristics of the mouse-passaged scrapie agents, 22A and ME7. *Genet Res.* **13:**213-25.

Dickinson AG, Meikle VM. (1971) Host-genotype and agent effects in scrapie incubation: change in allelic interaction with different strains of agent. *Mol Gen Genet.* **112:**73-9.

Dickinson AG, Fraser H, Outram GW. (1975) Scrapie incubation time can exceed natural lifespan. *Nature* **256:**732-3.

Doh-ura K, Tateishi J, Sasaki H, Kitamoto T, Sakaki Y. (1989) Pro–leu change at position 102 of prion protein is the most common but not the sole mutation related to Gerstmann-Sträussler syndrome. *Biochem Biophys Res Commun.* **163:**974–9.

Draghici S, Khatri P, Bhavsar P, Shah A, Krawetz SA, Tainsky MA. (2003) Onto-Tools, the toolkit of the modern biologist: Onto-Express, Onto-Compare, Onto-Design and Onto-Translate. *Nucleic Acids Res.* **31:**3775-81.

Duguid JR, Dinauer MC. (1990) Library subtraction of in vitro cDNA libraries to identify differentially expressed genes in scrapie infection. *Nucleic Acids Res.* **18:**2789-92.

Eklund CM, Kennedy RC, Hadlow WJ. (1967) Pathogenesis of scrapie virus infection in the mouse. *J Infect Dis.* **117:**15-22.

Farquhar, C.F., Dornan, J., Somerville, R.A., Tunstall, A.M., Hope, J. (1994) Effect of *Sinc* genotype, agent isolate and route of infection on the accumulation of protease-

resistant PrP in non-central nervous system tissues during the development of murine scrapie. *J Gen Virol.* **75:** 495-504.

Fevrier B, Vilette D, Archer F, Loew D, Faigle W, Vidal M, Laude H, Raposo G. (2004) Cells release prions in association with exosomes. *Proc Natl Acad Sci.* **101:**9683-8.

Flechsig E, Hegyi I, Enari M, Schwarz P, Collinge J, Weissmann C. (2001) Transmission of scrapie by steel-surface-bound prions. *Mol Med.* **7:**679-84.

Fleischmann J, Liu H, Wu CP. (2004) Polyadenylation of ribosomal RNA by Candida albicans also involves the small subunit. *BMC Mol Biol.* **5:**17.

Ford MJ, Burton LJ, Morris RJ, Hall SM. (2002) Selective expression of prion protein in peripheral tissues of the adult mouse. *Neuroscience* **113:**177-92.

Fournier JG. 2001. Nonneuronal cellular prion protein. *Int Rev Cytol.* **208:**121-60.

Fraser H, Dickinson AG. (1968) The sequential development of the brain lesion of scrapie in three strains of mice. *J Comp Pathol.* **78:**301-11.

Fraser H, Dickinson AG. (1970) Pathogenesis of scrapie in the mouse: the role of the spleen. *Nature* **226:**462-3.

Fraser H, Dickinson AG. (1973). Scrapie in mice: Agent-strain differences in the distribution and intensity of grey matter vacuolation. *J Comp Pathol* **83:**29–40.

Fraser H, Dickinson AG. (1978) Studies of the lymphoreticular system in the pathogenesis of scrapie: the role of spleen and thymus. *J Comp Pathol.* **88:**563-73.

Glatzel M, Aguzzi A. (2000) Peripheral pathogenesis of prion diseases. *Microbes Infect.* **2:**613–19.

Glatzel M, Heppner FL, Albers KM, Aguzzi A. (2001) Sympathetic innervation of lymphoreticular organs is rate limiting for prion neuroinvasion. *Neuron* **31:**25-34

Gomes LI, Silva RL, Stolf BS, Cristo EB, Hirata R, Soares FA, Reis LF, Neves EJ, Carvalho AF. (2003) Comparative analysis of amplified and nonamplified RNA for hybridization in cDNA microarray. *Anal Biochem.* **321:**244-51.

Gordon, W. S. (1946) Louping-ill, tick-borne fever and scrapie. *Vet Rec.* **58:**516-20.

Guiroy DC, Yanagihara R, Gajdusek DC. (1991) Localization of amyloidogenic proteins and sulfated glycosaminoglycans in nontransmissible and transmissible cerebral amyloidoses. *Acta Neuropathol* **82:**87–92

Haraguchi T, Fisher S, Olofsson S, Endo T, Groth D, Tarentino A, Borchelt DR, Teplow D, Hood L, Burlingame A, Lyckef E, Kobatag A, Prusiner SB. (1989) Asparagine-linked glycosylation of the scrapie and cellular prion proteins. *Arch Biochem Biophys*; **274:**1–13

Harries-Jones R, Knight R, Will RG, Cousens S, Smith PG, Matthews WB. (1988) Creutzfeldt-Jakob disease in England and Wales, 1980–1984: a case-control study of potential risk factors. *J Neurol Neurosurg Psychiatry* **51:**1113–9

Harris DA. (2003) Trafficking, turnover and membrane topology of PrP: Protein function in prion disease. *Br Med Bull.* **66:**71-85.

Hengstschlager M, Rodman DM, Miloloza A, Hengstschlager-Ottnad E, Rosner M, Kubista M. (2001) Tuberous sclerosis gene products in proliferation control. *Mutat Res.* **488:**233-9.

Hill AF, Desbruslais M, Joiner S, Sidle KC, Gowland I, Collinge J, Doey LJ, Lantos P. (1997) The same prion strain causes vCJD and BSE. *Nature* **389:**448-50, 526.

Horiuchi M, Yamazaki N, Ikeda T, Ishiguro N, Shinagawa M. (1995) A cellular form of prion protein (PrP^C) exists in many non-neuronal tissues of sheep. *J Gen Virol.* **76:**2583-7.

Horonchik L, Tzaban S, Ben-Zaken O, Yedidia Y, Rouvinski A, Papy-Garcia D, Barritault D, Vlodavsky I, Taraboulos A. (2005) Heparan sulfate is a cellular receptor for purified infectious prions. *J Biol Chem.* **280:**17062-7.

Hosack DA, Dennis G Jr, Sherman BT, Lane HC, Lempicki RA. (2003) Identifying biological themes within lists of genes with EASE. *Genome Biol.* **4:**R70.

Hsiao K, Baker HF, Crow TJ, Poulter M, Owen F, Terwilliger JD, Westaway D, Ott J, Prusiner SB. (1989) Linkage of a prion protein missense variant to Gerstmann-Sträussler syndrome. *Nature* **338:**342–5.

Huang FP, Farquhar CF, Mabbott NA, Bruce ME, MacPherson GG. (2002) Migrating intestinal dendritic cells transport PrP(Sc) from the gut. *J Gen Virol.* **83:**267-71.

Hunter N, Foster J, Chong A, McCutcheon S, Parnham D, Eaton S, MacKenzie C, Houston F. (2002) Transmission of prion diseases by blood transfusion. *J Gen Virol.* **83:**2897-905.

Inoue Y, Yamakawa Y, Sakudo A, Kinumi T, Nakamura Y, Saeki K, Kamiyama T, Onodera T, Nishijima M. (2005) Infection route-independent accumulation of splenic abnormal prion protein. *Jpn J Infect Dis.* **58:**78-82.

Jeffrey M, McGovern G, Goodsir CM, Brown KL, Bruce ME. (2000) Sites of prion protein accumulation in scrapie-infected mouse spleen revealed by immuno-electron microscopy. *J Pathol.* **191:**323-32

Kaeser PS, Klein MA, Schwarz P, Aguzzi A. (2001) Efficient lymphoreticular prion propagation requires PrP(c) in stromal and hematopoietic cells. *J Virol.* **75:**7097-106.

Kascsak RJ, Rubenstein R, Merz PA, Carp RI, Wisniewski HM, Diringer H. (1985) Biochemical differences among scrapie-associated fibrils support the biological diversity of scrapie agents. *J Gen Virol.* **66:**1715-22.

Kasper KC, Stites DP, Bowman KA, Panitch H, Prusiner SB. (1982) Immunological studies of scrapie infection. *J Neuroimmunol.* **3:**187-201.

Kimberlin RH, Walker CA. (1979) Pathogenesis of mouse scrapie: dynamics of agent replication in spleen, spinal cord and brain after infection by different routes. *J Comp Pathol.* **89:**551-62.

Kimberlin RH, Walker CA. (1986) Pathogenesis of scrapie (strain 263K) in hamsters infected intracerebrally, intraperitoneally or intraocularly. *J Gen Virol.* **67:**255-63.

Kimberlin RH, Walker CA. (1989a) Pathogenesis of scrapie in mice after intragastric infection. *Virus Res.* **12:**213-20.

Kimberlin RH, Walker CA. (1989b) The role of the spleen in the neuroinvasion of scrapie in mice. *Virus Res.* **12:**201-11.

Kitamoto T, Muramoto T, Mohri S, Dohura K, Tateishi J. (1991) Abnormal isoform of prion protein accumulates in follicular dendritic cells in mice with Creutzfeldt-Jakob disease. *J Virol.* **65:**6292–95.

Klein MA, Frigg R, Flechsig E, Raeber AJ, Kalinke U, Bleuthmann H, Bootz F, Suter M, Zinkernagel RM, Aguzzi A. (1997) A crucial role for B cells in neuroinvasive scrapie. *Nature* **390:** 687-90.

Kosco-Vilbois MH. (2003) Are follicular dendritic cells really good for nothing? *Nat Immunol.* **3:**764-9.

Kuai L, Fang F, Butler JS, Sherman. (2004) Polyadenylation of rRNA in Saccharomyces cerevisiae. *Proc Natl Acad Sci.* **101:**8581-6.

Kübler E, Oesch B, Raeber AJ. (2003) Diagnosis of prion diseases. *Br Med Bull.* **66:**267-79.

Lasmezas CI, Cesbron JY, Deslys JP, Demaimay R, Adjou KT, Rioux R, Lemaire C, Locht C, Dormont D. (1996) Immune system-dependent and -independent replication of the scrapie agent. *J Virol.* **70:**1292-5.

Lawson VA, Collins SJ, Masters CL, Hill AF. (2005) Prion protein glycosylation. *J Neurochem.* **93:**793-801.

Llewelyn CA, Hewitt PE, Knight RS, Amar K, Cousens S, Mackenzie J, Will RG. (2004) Possible transmission of variant Creutzfeldt-Jakob disease by blood transfusion. *Lancet.* **363:**417-21.

Liberski PP, Sikorska B, Bratosiewicz-Wasik J, Gajdusek DC, Brown P. (2004) Neuronal cell death in transmissible spongiform encephalopathies (prion diseases) revisited: from apoptosis to autophagy. *Int J Biochem Cell Biol.* **36:**2473-90.

Mabbott NA, Mackay F, Minns F, Bruce ME. (2000a) Temporary inactivation of follicular dendritic cells delays neuroinvasion of scrapie. *Nat Med.* **6:**719-20.

Mabbott NA, Williams A, Farquhar CF, Pasparakis M, Kollias G, Bruce ME. (2000b) Tumor necrosis factor alpha-deficient, but not interleukin-6-deficient mice resist peripheral infection with scrapie. *J Virol.* **74:**3338-44.

Mabbott N, Turner M. (2005) Prions and the blood and immune systems. *Haematologica.* **90:**542-8

Maignien T, Lasmezas CI, Beringue V, Dormont D, Deslys JP. (1999) Pathogenesis of the oral route of infection of mice with scrapie and bovine spongiform encephalopathy agents. *J Gen Virol.* **80:**3035-42.

Manson JC, Clarke AR, Hooper ML, Aitchison L, McConnell I, Hope J. (1994) 129/Ola mice carrying a null mutation in PrP that abolishes mRNA production are developmentally normal. *Mol Neurobiol.* **8:**121-7.

Marone M, Mozzetti S, De Ritis D, Pierelli L, Scambia G. (2001) Semiquantitative RT-PCR analysis to assess the expression levels of multiple transcripts from the same sample. *Biol Proced Online.* **3:**19-25.

McBride PA, Eikelenboom P, Kraal G, Fraser H, Bruce ME. (1992) PrP protein is associated with follicular dendritic cells of spleens and lymph nodes in uninfected and scrapie-infected mice. *J Pathol.* **168:**413-8.

McBride PA, Beekes M. (1999) Pathological PrP is abundant in sympathetic and sensory ganglia of hamsters fed with scrapie. *Neurosci Lett.* **265:**135–8.

McGovern G, Brown KL, Bruce ME, Jeffrey M. (2004) Murine scrapie infection causes an abnormal germinal centre reaction in the spleen. *J Comp Pathol.* **130:**181-94.

Miele G, Manson J, Clinton M. (2001) A novel erythroid-specific marker of transmissible spongiform encephalopathies. *Nat Med.* **7:**361-4.

Millson GC, Kimberlin RH, Manning EJ, Collis SC. (1979) Early distribution of radioactive liposomes and scrapie infectivity in mouse tissues following administration. *Vet Microbiol.* **4:**88-99.

Mohan J, Brown KL, Farquhar CF, Bruce ME, Mabbot NA. (2004) Scrapie transmission following exposure through the skin is dependent on follicular dendritic cells in lymphoid tissues. *J Dermatol Sci.* **35:**101-11

Mohri S, Farquhar CF, Somerville RA, Jeffrey M, Foster J, Hope J. (1992) Immunodetection of a disease specific PrP fraction in scrapie-affected sheep and BSE-affected cattle. *Vet Rec.* **131:**537-9.

Montrasio F, Frigg R, Glatzel M, Klien MA, Mackay F, Aguzzi A, Weissmann C. (2000) Impaired prion replication in spleens of mice lacking functional follicular dendritic cells. *Science* **288:**1257-9

Moudjou M, Frobert Y, Grassi J, La Bonnardiere C. (2001) Cellular prion protein status in sheep: tissue-specific biochemical signatures. *J Gen Virol.* **82:**2017-24.

Naslavsky N, Stein R, Yanai A, Friedlander G, Taraboulos A. (1997) Characterization of detergent-insoluble complexes containing the cellular prion protein and its scrapie isoform. *J Biol Chem.* **272:**6324-31.

Nicholas KB, Nicholas HB Jr, Deerfield DW II. (1997) GeneDoc: Analysis and Visualization of Genetic Variation. *Embnew.News* **4:**14.

Noonan DM, Fulle A, Valente P, Cai S, Horigan E, Sasaki M, Yamada Y, Hassell JR. (2001) The complete sequence of perlecan, a basement membrane heparan sulfate proteoglycan, reveals extensive similarity with laminin A chain, low density lipoprotein-receptor, and the neural cell adhesion molecule. *J Biol Chem.* **266:**22939-47.

Oesch B, Westaway D, Walchli M, McKinley MP, Kent SB, Aebersold R, Barry RA, Tempst P, Teplow DB, Hood LE, Prusiner SB, Weissmann C. (1985). A cellular gene encodes scrapie PrP 27-30 protein. *Cell* 40:735-46.

Pan KM, Baldwin M, Nguyen J, Gasset M, Serban A, Groth D, Mehlhorn I, Huang Z, Fletterick RJ, Cohen FE, Prusiner SB. (1993) Conversion of alpha-helices into beta-sheets features in the formation of the scrapie prion proteins. *Proc Natl Acad Sci.* 90:10962-6.

Pattison IH. (1965) Experiments with scrapie with special reference to the nature of the agent and the pathology of the disease. In: Gajdusek CJ, Gibbs CJ, Alpers MP (eds) *Slow,*

Latent and Temperate Virus Infections, NINDB Monograph 2. Washington, DC: US Government Printing, 249–57

Peden AH, Head MW, Ritchie DL, Bell JE, Ironside JW. (2004) Preclinical vCJD after blood transfusion in a PRNP codon 129 heterozygous patient. *Lancet.* 364:527-**9.**

Porter DD, Porter HG, Cox NA. (1973) Failure to demonstrate a humoral immune response to scrapie infection in mice. *J Immunol.* 111:1407-10.

Prinz M, Helkenwalder M, Junt T, Schwarz P, Glatzel M, Heppner FL, Fu Y, Lipp M, Aguzzi A. (2003) Positioning of follicular dendritic cells within the spleen controls prion neuroinvasion. *Nature* 425:957-62.

Prusiner SB. (1982) Novel proteinaceous infectious particles cause scrapie. *Science.* 216:136-44.

Prusiner SB, Bolton DC, Groth DF, Bowman KA, Cochran SP, McKinley MP. (1982) Further purification and characterization of scrapie prions. *Biochemistry.* **21:**6942-50.

Prusiner SB, Groth D, Serban A, Koehler R, Foster D, Torchia M, Burton D, Yang SL, DeArmond SJ. (1993) Ablation of the prion protein (PrP) gene in mice prevents scrapie and facilitates production of anti-PrP antibodies. *Proc Natl Acad Sci.* 90:10608-12.

Prusiner SB. (1998) Prions. *Proc Natl Acad Sci.* 95:13363-83.

Race RE, Ernst D. (1992) Detection of proteinase K-resistant prion protein and infectivity in mouse spleen by 2 weeks after scrapie agent inoculation. *J Gen Virol.* **73:**3319-23.

Race R, Oldstone M, Chesebro B. (2000) Entry versus blockade of brain infection following oral or intraperitoneal scrapie administration: role of prion protein expression in peripheral nerves and spleen. *J Virol.* **74:**828–33.

Raeber AJ, Klein MA, Frigg R, Flechsig E, Aguzzi A, Weissmann C. (1999) PrP-dependent association of prions with splenic but not circulating lymphocytes of scrapie-infected mice. *EMBO J.* 18:2702-6

Ricciarelli R, d'Abramo C, Massone S, Marinari U, Pronzato M, Tabaton M. (2004) Microarray analysis in Alzheimer's disease and normal aging. *IUBMB Life.* 56:349-54.

Riek R, Hornemann S, Wider G, Billeter M, Glockshuber R, Wuthrich K. (1996) NMR structure of the mouse prion protein domain PrP(121-321). *Nature.* 382:180-2.

Riemer C, Queck I, Simon D, Kurth R, Baier M. (2000) Identification of upregulated genes in scrapie-infected brain tissue. *J Virol.* 74:10245-8.

Riemer C, Neidhold S, Burwinkel M, Schwarz A, Schultz J, Kratzschmar J, Monning U, Baier M. (2004) Gene expression profiling of scrapie-infected brain tissue. *Biochem Biophys Res Commun.* 323:556-64.

Riesner D. (2003) Biochemistry and structure of PrP^{C} and PrP^{Sc}. *Br Med Bull.* 66:21-33

Ritchie DL, Brown KL, Bruce M.E. (1998) Visualisation of PrP protein and follicular dendritic cells in uninfected and scrapie infected spleen. *J Cell Path.* 1:3-10.

Rivera-Milla E, Stuermer CA, Malaga-Trillo E. (2003) An evolutionary basis for scrapie disease: identification of a fish prion mRNA. *Trends Genet.* 19:72-5.

Rosicarelli B, Serafini B, Sbriccoli M, Lu M, Cardone F, Pocchiari M, Aloisi F. (2005) Migration of dendritic cells into the brain in a mouse model of prion disease. *J Neuroimmunol.* [Epub ahead of print]

Rubenstein R, Merz PA, Kascsak RJ, Scalici CL, Papini MC, Carp RI, Kimberlin RH. (1991) Scrapie-infected spleens: analysis of infectivity, scrapie-associated fibrils, and protease-resistant proteins. *J Infect Dis.* 164:29-35.

Rudd PM, Merry AH, Wormald MR, Dwek RA. (2002) Glycosylation and prion protein. *Curr Opin Struct Biol.* 12:578-86.

Scott, M. R., J. Safar, G. Telling, O. Nguyen, D. Groth, M. Torchia, R. Koehler, P. Tremblay, D. Walther, F. E. Cohen, S. J. DeArmond, and S. B. Prusiner. (1997) Identification of a prion protein epitope modulating transmission of bovine spongiform encephalopathy prions to transgenic mice. *Proc Natl Acad Sci.* 94:14279-14284.

Shyng SL, Huber MT, Harris DA. (1993) A prion protein cycles between the cell surface and an endocytic compartment in cultured neuroblastoma cells. *J Biol Chem.* 268: 15922–8

Slomovic S, Laufer D, Geiger D, Schuster G. (2005) Polyadenylation and degradation of human mitochondrial RNA: the prokaryotic past leaves its mark. *Mol Cell Biol.* **25:**6427-35.

Somerville RA, Chong A, Mulqueen OU, Birkett CR, Wood SC, Hope J. (1997a) Biochemical typing of scrapie strains. *Nature* 386:564.

Somerville RA, Birkett CR, Farquhar CF, Hunter N, Goldmann W, Dornan J, Grover D, Hennion RM, Percy C, Foster J, Jeffrey M. (1997b) Immunodetection of PrP^{Sc} in spleens of some scrapie-infected sheep but not BSE-infected cows. *J Gen Virol.* 78:2389-96.

Somerville RA. (2002) TSE agent strains and PrP: reconciling structure and function. *Trends Biochem Sci.* 27:606-12.

Stahl N, Borchelt DR, Hsiao K, Prusiner SB. (1987) Scrapie prion protein contains a phosphatidylinositol glycolipid. *Cell* 51:229-40.

Stahl N, Prusiner SB. (1991) Prions and prion proteins. *FASEB J.* 5:2799-807.

Taylor DM, McConnell I, Fraser H. (1996) Scrapie infection can be established readily through skin scarification in immunocompetent but not immunodeficient mice. *J Gen Virol.* 77:1595-9.

Telling GC, Parchi P, DeArmond SJ, Cortelli P, Montagna P, Gabizon R, Mastrianni J, Lugaresi E, Gambetti P, Prusiner SB. (1996) Evidence for the conformation of the pathologic isoform of the prion protein enciphering and propagating prion diversity. *Science* 274:2079-82.

Tusher VG, Tibshirani R, Chu G. (2001). Significance analysis of microarrays applied to the ionizing radiation response. *Proc Natl Acad Sci.* 98:5116–21.

van der Pouw Kraan TC, Kasperkovitz PV, Verbeet N, Verweij CL. (2004) Genomics in the immune system. *Clin Immunol.* 111:175-85.

van Nierop, K. and de Groot, C. (2002) Human follicular dendritic cells : function, origin and development. *Semin Immunol.* 14:251-7.

van Slegtenhorst M, de Hoogt R, Hermans C, Nellist M, Janssen B, Verhoef S, Lindhout D, van den Ouweland A, Halley D, Young J, Burley M, Jeremiah S, Woodward K, Nahmias J, Fox M, Ekong R, Osborne J, Wolfe J, Povey S, Snell RG, Cheadle JP, Jones AC, Tachataki M, Ravine D, Sampson JR, Reeve MP, Richardson P, Wilmer F, Munro C, Hawkins TL, Sepp T, Ali JB, Ward S, Green AJ, Yates JR, Kwiatkowska J, Henske EP, Short MP, Haines JH, Jozwiak S, Kwiatkowski DJ. (1997) Identification of the tuberous sclerosis gene TSC1 on chromosome 9q34. *Science* 277:805-8.

van Slegtenhorst M, Nellist M, Nagelkerken B, Cheadle J, Snell R, van den Ouweland A, Reuser A, Sampson J, Halley D, van der Sluijs P. (1998) Interaction between hamartin and tuberin, the TSC1 and TSC2 gene products. *Hum Mol Genet.* 7:1053-7

Wadlow R and Ramaswamy S. (2005) DNA microarrays in clinical cancer research. *Curr Mol Med.* 5:111-20.

Wadsworth JD, Jackson GS, Hill AF, Collinge J. (1999) Molecular biology of prion propagation. *Curr Opin Genet Dev.* 9:338-45.

Westaway D, Goodman PA, Mirenda CA, McKinley MP, Carlson GA, Prusiner SB. (1987) Distinct prion proteins in short and long scrapie incubation period mice. *Cell* 51:651-62.

Wickner RB, Edskes HK, Roberts BT, Baxa U, Pierce MM, Ross ED, Brachmann A. (2004) Prions: proteins as genes and infectious entities. *Genes Dev.* 18:470-85.

Wilesmith JW, Ryan JB, Hueston WD, Hoinville LJ. (1992) Bovine spongiform encephalopathy: epidemiological features 1985 to 1990. *Vet Rec.* 130:90-4.

Will RG. (1993) Epidemiology of Creutzfeldt-Jakob disease. *Br Med Bull.* 49:960–70

Will RG, Ironside JW, Zeidler M, Cousens SN, Estibeiro K, Alperovitch A, Poser S, Pocchiari M, Hofman A, Smith PG. (1996) A new variant of Creutzfeldt-Jakob disease in the UK. *Lancet* 347:921–5

Xiang W, Windl O, Wunsch G, Dugas M, Kohlmann A, Dierkes N, Westner IM, Kretzschmar HA. (2004) Identification of differentially expressed genes in scrapie-infected mouse brains by using global gene expression technology. *J Virol.* 78:11051-60.

Yamamoto Y, Jones KA, Mak BC, Muehlenbachs A, Yeung RS. (2002) Multicompartmental distribution of the tuberous sclerosis gene products, hamartin and tuberin. *Arch Biochem Biophys.* 404:210-17.

Yokoyama T, Kimura KM, Ushiki Y, Yamada S, Morooka A, Nakashiba T, Sassa T, Itohara S. (2001) In vivo conversion of cellular prion protein to pathogenic isoforms, as monitored by conformation-specific antibodies. *J Biol Chem.* 276:11265-71.

Zhao H, Hastie T, Whitfield ML, Borresen-Dale AL, Jeffrey SS. (2002) Optimization and evaluation of T7 based RNA linear amplification protocols for cDNA microarray analysis. *BMC Genomics.* 3:31.

Zlotnik I, Rennie JC. (1962) The pathology of the brain of mice inoculated with tissues from scrapie sheep. *J Comp Pathol.* 72:360-5.

Zlotnik I, Rennie JC. (1963) Further observations on the experimental transmission of scrapie from sheep and goats to laboratory mice. *J Comp Pathol.* 73:150-62.